Uncovering the complex cell wall of *Neochloris oleoabundans*, a promising green microalga

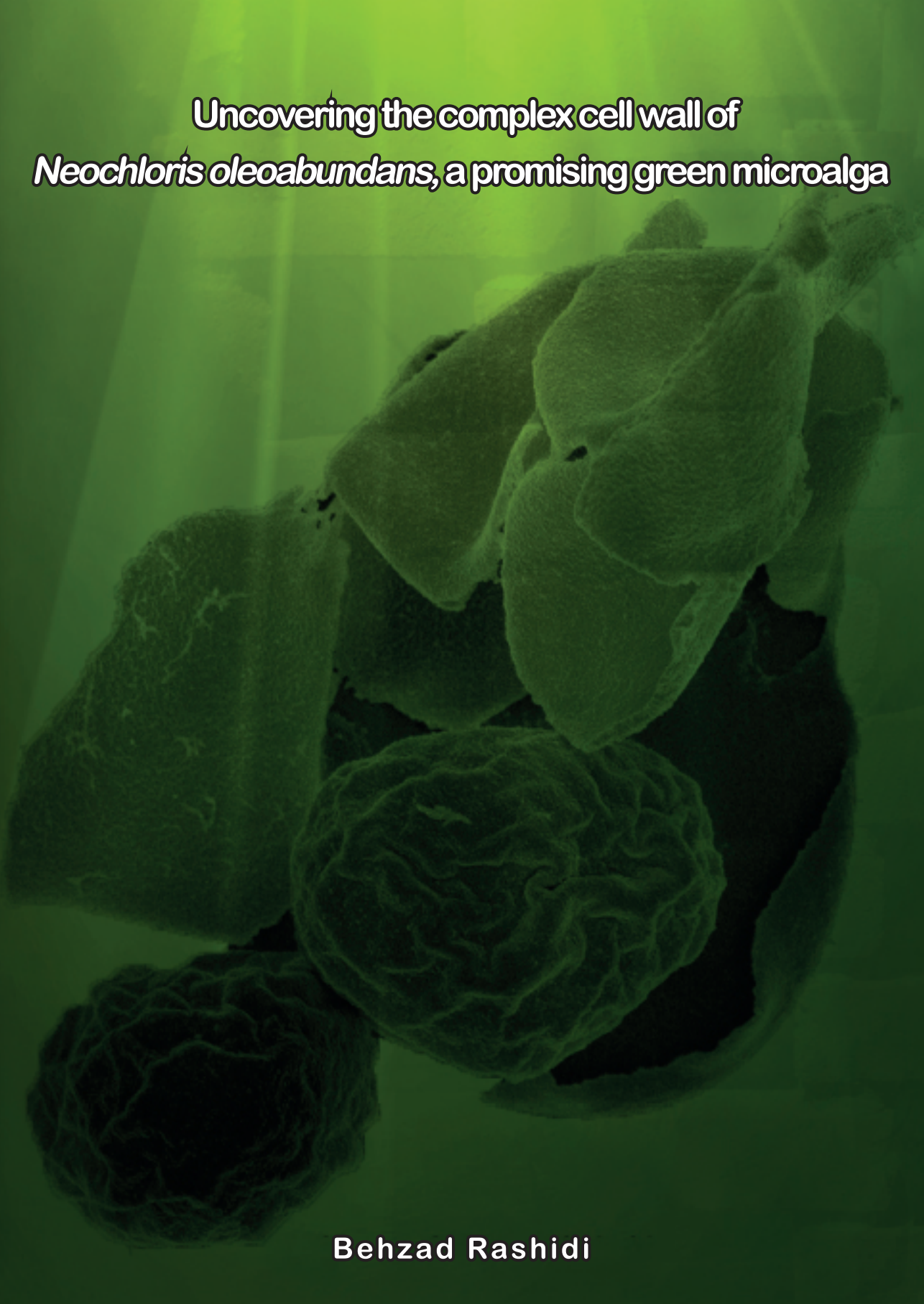

Behzad Rashidi

Propositions

1- Fundamental knowledge on algal cell walls is key to a successful biorefinery. (this thesis)

2- Carbohydrates are not the major component of all plant cell walls. (this thesis)

3- A biobased economy can make oil-rich countries a peaceful place to live.

4- Academic conferences should be held in countries without restrictive visa regulations.

5- Being pragmatic is a key for the successfulness of Dutch society.

6- Job insecurity hides burn-outs in many cultures.

Propositions belonging to the thesis, entitled "**Uncovering the complex cell wall of *Neochloris oleoabundans*, a promising green microalga**"

Behzad Rashidi

Wageningen, 29 May 2019

Uncovering the complex cell wall of *Neochloris oleoabundans*, a promising green microalga

Behzad Rashidi

Thesis committee

Promotor

Prof. Dr L.M. Trindade
Professor of Plant Breeding
Wageningen University & Research

Other members

Prof. Dr R.H. Wijffels, Wageningen University & Research
Prof. Dr M.H.M Eppink, Wageningen University & Research
Prof. Dr M.J.E.C van der Maarel, University of Groningen
Dr M.J Ketelaar, Wageningen University & Research

This research was conducted under the auspices of the Graduate School Experimental Plant Sciences

Uncovering the complex cell wall of *Neochloris oleoabundans,* a promising green microalga

Behzad Rashidi

Thesis

submitted in fulfilment of the requirements for the degree of doctor
at Wageningen University
by the authority of the Rector Magnificus,
Prof. Dr A.P.J. Mol,
in the presence of the
Thesis Committee appointed by the Academic Board
to be defended in public
on Wednesday 29 May 2019
at 11 a.m. in the Aula.

Behzad Rashidi
Uncovering the complex cell wall of *Neochloris oleoabundans*, a promising green microalga,
142 pages.
PhD thesis, Wageningen University, Wageningen, the Netherlands (2019)
With references, with summary in English
ISBN: 978-94-6343-929-9
DOI: 10.18174/474485

Table of Contents

CHAPTER 1

General introduction

1. The project: objectives embedded in this PhD thesis

The research outlined in this thesis was carried out within the framework of the AlgaePARC Biorefinery programme initiated by Wageningen University and Research Centre in cooperation with eleven industrial partners and the University of Twente. The overall objective of this project was to develop unique biorefinery strategies to extract and fractionate valuable cell components, such as lipids, proteins and carbohydrates, from the complex cytoplasmic matrix of green microalgae. The specific goal of my thesis was to understand and characterize algal cell walls in order to develop more effective and sustainable methods to extract cell components. *Neochloris oleoabundans* was considered to be the most suitable microalgae for this study, given its industrial potential and the tools available for this species. Zooming into the complexity and dynamic nature of the cell wall, this project aims to examine the remodelling of this structure when it is exposed to different environments. In order to enlarge the existent knowledge of algal cell walls, we studied the biosynthesis and modification of this complex matrix throughout the life cycle, and characterized the molecular determinants of those metabolic pathways. The results of the in-depth analysis of *Neochloris oleoabundans* cell wall have been compiled in this book.

2. World transition towards bio-based products

Over the years, several global research projects have focused on identifying alternative bio-resources to produce food, feed and fuel in the framework of carbon-neutral bio-economy. The driving forces behind the intensive exploration of promising feedstocks, an ever-increasing world population, the exponential industrialization of developing economies, a near depletion of fossil fuel and an alarming level of the surrounded atmospheric carbon dioxide, are noteworthy. Alongside the bio-resources available, lignocellulosic biomass adapted to the marginal areas together with aquatic biomass, as microalgae, are the feedstocks that better address the socio-economic concerns, in particular competition with food crops on fertile farmland. Nevertheless, numerous characteristics of microalgae outweigh the lignocellulosic biomass in various aspects, ranging from higher growth rate, less land required, independent of seasonal conditions and higher photo-conversion efficiency (utilization of solar radiation in terrestrial crops is generally below 1%, whereas it can reach up to 5% in microalgae) (Chen et al., 2018; Sajjadi et al., 2018). Sustainable bio-based component production in a green microalgae bio-factory can minimize the impact that humanity has been having on disrupting the carbon balance of Planet Earth.

3. Microalgae, as a promising renewable feedstock

Microalgae are a diverse group of plant-like organisms, which can capture photons from a light source and, together with water, essential nutrients and CO_2, produce biomolecules such as carbohydrates, lipids and proteins (Leu & Boussiba, 2014; Spolaore et al., 2006) (Figure 1).

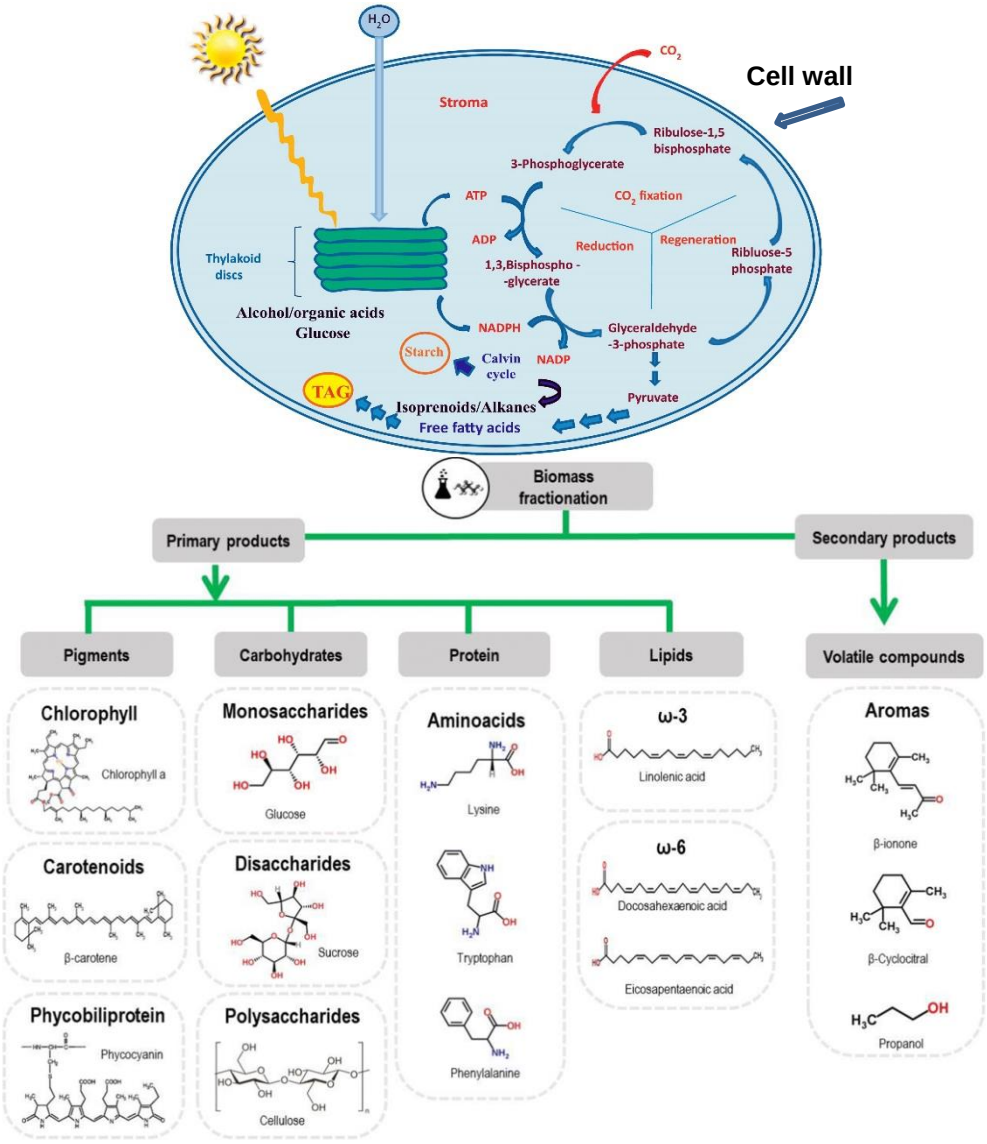

Figure 1. Microalgae green bio-based cell factory. Microalgae capture light and CO_2 and following the photosynthetic reactions produce macromolecules, which can be fractionated into several primary and secondary products. Figure adapted from (De Bhowmick et al., 2019; Deprá et al., 2018).

The term microalgae essentially refers to a microscopic single-cell organism, though it might encompass the colonial form of algae as well. Throughout this thesis, the terms of algae and microalgae are used equivalently and always allude to a single unicellular microscopic organism. Microalgae are widespread organisms residing in almost every niche in the environment. Their existence has been reported in diverse ecosystems including terrestrial, freshwater, saline water, alkaline and acidic habitats (Baudelet et al., 2017; Tirichine & Bowler, 2011). The enormous biodiversity among the green microalgae together with the broad spectrum of micro-habitats and cultivation conditions for more than 100 000 species of microalgae make these aquatic crops the first-rate resource of molecules for food, feed and bio-based products, such as biofuels and pharmaceuticals (Matos, 2017; Wijffels & Barbosa, 2010; Wijffels et al., 2013). On account of this, during recent years, there has been an increasing interest in the utilization of microalgae biomass as an alternative green feedstock. Despite the fact that microalgae are regarded as a potential candidate with highly sustainable biomass, techno-economical assessments revealed that bulk commodity production at this moment is not economically feasible and still suffers from a low return on investment (Liu et al., 2013; Ruiz et al., 2016). Amongst the potential strategies proposed to augment the commercial value of the algal feedstock is the generation of multiple (high-value) commodities instead of a single-centric product. However, and heading to the subject of this thesis, the first step to be taken after harvesting the biomass and prior to generating multiple products is to overcome the physical barrier of the cell in order to access its components. The intracellular components of microalgae are generally enclosed within the cell wall, which is considered as a rigid layer located on the outer part of the cell membrane. A successful valorisation of the multiple products depends on the kept integrity and functionalities of the cellular components upon disruption of the cell wall. Harsh disruption methods often imply the necessity for more effective and strong chemical or thermic treatments which can affect the quality and functionality of the valuable intracellular components. The development of cost-effective and mild methods for cell wall disruption has been a main, yet unsettled topic. For that, we need to have a better in-depth knowledge of microalgae cell walls.

4. Cell wall, as a physical barrier for extracting valuable intracellular constituents

Successful fractionation and isolation of microalgae intracellular components depends on the composition and structure of their cell walls. A microalgae cell wall is a complex 3D structure composed of polysaccharides, proteins, lipids and inorganic materials (Scholz et al., 2014). These building blocks configure a matrix of cross-linked molecules, nevertheless, many of these linkages and polymers still need to be identified and characterized. This dynamic matrix determines the cell

shape, enables it to expand, regulates its morphogenesis and protects it from abiotic and biotic stresses. Despite its biological functions, it is recognisable that such a complex physiochemical ultrastructure of the cell wall creates a barrier, which needs to be removed before the intracellular content can be reached (t Lam et al., 2017). Cell walls of microalgae are biochemically and morphologically diverse and in certain cases exhibit unique features (Baudelet et al., 2017; Fangel et al., 2012b). Species-specific cell wall characteristics cause a different level of susceptibility to the various disruption methods. To illustrate this, some of the microalgae cell walls are generally protein-based structures, while others mainly constituted by the combination of cellulose and hemicellulose. In practical terms, it is believed that protein-based cell walls are more prone to deconstruction compared to polysaccharide-rich ones (Mussgnug et al., 2010). Several studies have reported on development of methods for microalgae cell walls disruption. These methods consist mostly of harsh treatments that target cell wall as a whole, but the development of tailor-made mild and non-disruptive methods requires a better knowledge of the cell walls, including biochemical composition and morphological features. The fundamental knowledge to uncover the biochemical composition and configuration of the cell wall is a prerequisite to reveal its imperceptible rigidity and further design an applicable and selective disruption strategy.

5. Cell wall diversity across different life kingdoms

As a consequence of evolution and possibly different adaptive drives, cell walls across the life kingdoms are diverse (Baudelet et al., 2017; Bourmaud et al., 2018). Most of the eukaryote cell walls are fibrillar and polysaccharide-based, whereas the majority of prokaryote cell walls, such as bacteria, are peptidoglycan-based and non-fibrillar. Eukaryote cell walls are primarily composed of polysaccharides, though they might possess a significant amount of proteins and other components such as lignin and other phenolic compounds. The fungal cell wall is mainly composed of chitin or glucan. Chitin is a long chain polymer of N-acetylglucosamine, which is associated with cell wall rigidity. Together with polysaccharides, proteins can also be found in the fungal cell wall, though their biochemical and structural properties are more complex than in the plant cell wall. The primary cell wall of higher plants consists mainly of polysaccharides, in which cellulose is a major component. Cellulose is an unbranched polymer that contains several thousand β(1,4) linked glucose units assembled into long microfibrils. The cellulose polymers link through hemicellulose tethers to form a cellulose-hemicellulose network. These structures are embedded in a pectin matrix, which is a heteropolysaccharide rich in galacturonic acid(Sticklen, 2010). Besides polysaccharides, proteins such as arabinogalactan proteins, extensins, glycine-rich proteins, proline-rich proteins and enzymes are important cell wall constituents.

Algae cell walls, in general, display a greater biological diversity and metabolic plasticity compared to terrestrial plants (Bioenergy, 2017; Domozych et al., 2012). Taxonomically, the green microalgae are an immense group, consisting of two phyla, Chlorophyta and Charophyta / Streptophyta. Chlorophyta contains the majority of green algae, while the latter encompasses the group of algae from which land plants, embryophytes, are thought to have evolved. Each phylum displays a considerable degree of diversity in its cell wall structures and compositions. This dissertation aims to investigate the cell wall of a green alga belonging to Chlorophyta. In the following section, we provide a brief overview of the microalgae cell walls in this phylum.

6. Cell wall of Chlorophyta at a glance

Cell walls of species belonging to the Chlorophyta phylum comprise a diverse assortment of constituents; overall they display both unique features as well as components they share with (higher) plants and fungi (Baudelet et al., 2017; Domozych et al., 2012). Their cell wall building blocks are a combination of carbohydrates, frequently non-cellulosic, ranging from neutral to acidic and amino sugars, embedded in a nonfibrillar polysaccharide matrix. Additionally, Chlorophyta cell walls contain proteins, including different enzymes and hydroxyproline-rich glycoproteins, lipids and inorganic materials (Baudelet et al., 2017; Domozych et al., 2012). Furthermore, some of the algae belonging to Chlorophyta produce algaenan, an acetolysis-resistant-biopolymer which, due to its complexity it has become difficult to analyse its biochemical composition.

The phylum Chlorophyta is subdivided into two main distinct sub-phylums, Chlorophytina and Prasinophytina. The first sub-phylum contains four principal classes, Chlorophyceae, Trebouxiophyceae, Ulvophyceae and Chlorodendrophyceae. A recent study classified Chlorophyta into three main groups based on the different components of their cell walls (Baudelet et al., 2017). Group 1 has been composed by early diverging lineages belonging to Prasinophytina and Chlorodendrophyceae, in which cell walls are mainly composed of 2-keto-sugar acids 3-deoxy-manno-2-octolusonic acid (Kdo), 3-deoxy-5-O-Methyl-manno-2-octolusonic acid (5OMeKdo) and 3-deoxylyxo-2-heptulosaric acid (Dha). Group 2, combines unicellular algae related to Trebouxiophyceae and Chlorophyceae, in which the cell walls are mainly composed of mannans, glucans, arabinogalactans, algaenans and less frequently chitin-like polysaccharides. Group 3, comprises green macroalgae, chiefly marine lineages, in which cell walls, on the whole, contain sulphated polysaccharides, xylan, mannan and glucan. Group 2 includes algae which have great potential for industrial applications, and the majority are grown in freshwater. Group 2 can be further classified into two groups based on the plasticity of the cell wall during the cell cycle. The group which has plastic cell walls, namely those whose composition and structure vary throughout the different phases of the

cell cycle; and non-plastic, in which the cell wall remains almost unchanged during the cell cycle. Figure 2 summarizes the cell wall diversity in Chlorophyta phylum.

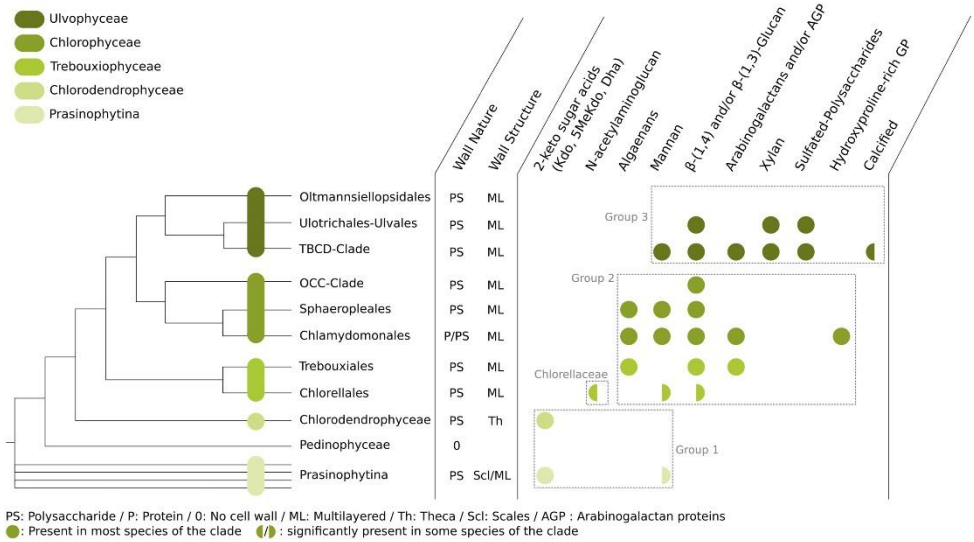

Figure 2. Summary of the cell wall structure and composition of Chlorophyta phylum. Figure adapted and slightly modified from (Baudelet et al., 2017).

7. *Neochloris oleoabundans*, a promising microalga from Chlorophyta phylum

Neochloris oleoabundans, also known as *Ettlia oleoabundans*, is a terrestrial freshwater microalga that belongs to the Chlorophyta phylum, class Chlorophyceae. It was originally isolated from the sand dunes in Saudi Arabia, an environment where the lack of water is a tenacious threat (S. Chantanachat & Bold, 1962). Owing to the flexibility of *N. oleoabundans* and its saline resistance mechanisms, this freshwater microalga can be also cultivated in saline medium with seawater salt concentration (1995). For many years, this microalga has been considered as one of the most credible candidates due to its high growth rate and biomass composition (Abu Hajar et al., 2017).

Cell division in this green microalga takes place by multiple fission, in which 2 to 8 daughter cells are released from the mother cell (de Winter et al., 2013). This mechanism, which is vital for evolution, enables the *N. oleoabundans* to grow during the light period (day) and undergo division during the dark period (night). By this means they make maximum use of the light for photosynthesis and growth. The cell shape of this microalga is generally spherical and its size varies depending on the phase in the cell cycle (Figure 3) (Abu Hajar et al., 2017; de Winter et al., 2013). Cell

size throughout the cell cycle varies from 2.5 to 4.5 µm with an average of 3-3.5 µm in diameter. Together with developmental phases, environmental factors also affect cell size, for example, it has been reported that nitrogen starvation can enlarge the *N. oleoabundans* cell diameter to about 5.2 µm (Davis et al., 2012).

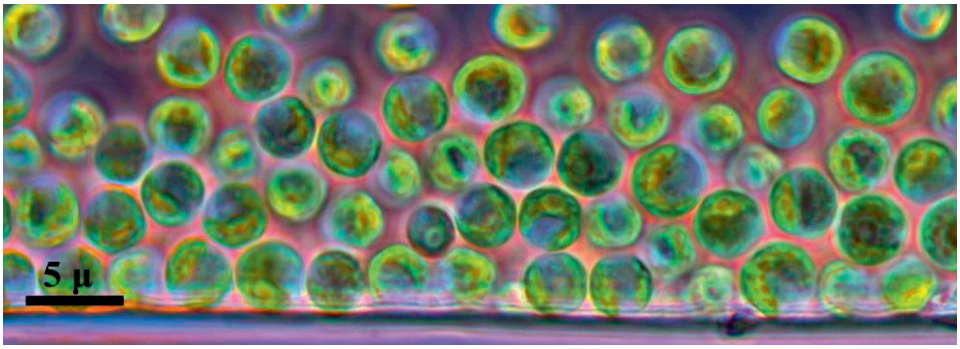

Figure 3. Microscopic observation of unicellular microalgae, *N. oleoabundans*.

Similar to other organisms, the major biomass components of *N. oleoabundans* are proteins, carbohydrates and lipids (Abu Hajar et al., 2017). Depending on the growth phase and environmental factors, the protein content of *N. oleoabundans* is between 30 to 45% of the total dry cell weight. *N. oleoabundans* tends to produce and accumulate increasing amounts of carbohydrates and lipids when undergoing stress conditions, such as nitrogen starvation, ranging from 20 to 38% and 35 to 54% (% dry cell weight), respectively.

In contrast to terrestrial plants, for which tools and methods to characterize cell wall properties have been developed over many decades, microalgae such as *N. oleoabundans* have a limited toolbox available. Hence, there is little information available on the type of cell wall monomers and their assembly to higher complex structures. Moreover, a specific function of the individual cell wall building blocks and their coordinated biosynthesis pathways still remain unidentified on the whole. Prior to engineering the cell wall constituents and structures, with different purposes for particular applications, it is considered vital to identify the biochemical composition, morphological structure and their underlying genetics as well as their biosynthetic pathways. Chemistry-based analytical techniques such as gas or liquid chromatography, high-resolution microscopy, and molecular tools are some of the approaches which could assist in characterizing and further mapping of the cell wall composition. Results from the comprehensive exploration of the cell wall might have significant implications: I, decreasing the cell wall disruption cost by means of a

targeted method, II, facilitating the biorefinery of microalgae to generate multi-functional products, III, exploiting the cell wall itself as a source of valuable molecules. In addition to the applied knowledge that could be gained from exploring the cell wall composition of *N. oleoabundands*, this information contributes significantly to the understanding of green microalgae (early-evolved plants) cell wall that has until now been given very little attention.

8. Aims and outline of this thesis

The overall aim of the study presented in this thesis is to gain new insights into cell wall building blocks of the early-evolved green microalgae, *N. oleoabundans*, and understand how they compare to cell walls of terrestrial plants.

In view of these prospects, the main objectives of this thesis are:

1- To develop a protocol for the isolation and comprehensive characterization of *N. oleoabundans* cell wall,
2- To visualize the cell wall ultrastructure by means of different microscopic techniques,
3- To monitor the cell wall remodelling and modification when cultivated under different growing conditions,
4- To uncover cell wall morphology throughout the cell cycle,
5- To identify the genes and underlying pathways involved in cell wall biosynthesis and modification.

These main objectives are addressed in the following chapters:

In **Chapter 2** we made a general characterization of the cell wall of the green microalgae, *N. oleoabundans*. We have tested different methods for the isolation of *N. oleoabundans* cell walls and the Neutral Detergent Fibre (NDF) proved to be the most suitable for this analysis. The NDF-cell wall extracted material was further subjected to different chemical analyses aiming to characterize the constituent carbohydrates, proteins, lipids and inorganic materials. This analysis was complemented by electron microscopic imaging, revealing the ultrastructure of the cell wall.

In **Chapter 3** we unveiled the impact of the environmental factors, salinity and nitrogen deficiency, on the *N. oleoabundans* cell wall components. Remodelling and modification of cell wall constituents from microalgae cultivated in nitrogen-deplete and nitrogen-replete freshwater and nitrogen-deplete and nitrogen-replete seawater are explained.

Chapter 4 describes the morphologic characteristics of cell wall development throughout the cell cycle. A library of microscopic-images of the cell wall ultrastructure, starting from the early growth-phase until the dividing phase were prepared. A model depicting the modification of the cell wall throughout the cell cycle is proposed.

Chapter 5 enlightens the molecular mechanisms underlying cell wall development throughout the cell cycle. In order to understand the molecular machinery involved in the cell wall carbohydrates biosynthesis, synchronized samples from different time points of the cell cycle were sequenced and their transcriptome profiles compared.

Chapter 6 discusses the major results and insights brought to light in this study. In this chapter, the implication of the results described in the previous chapters on the *N. oleoabundans* cell wall are discussed and an outlook on the steps to be taken in future in developing mild cell wall disruption has been proposed.

CHAPTER 2

Detailed biochemical and morphologic characteristics of the green microalga *Neochloris oleoabundans* cell wall

This chapter has been published as:

Behzad Rashidi, Luisa M. Trindade (2018) Detailed biochemical and morphologic characteristics of the green microalga *Neochloris oleoabundans* cell wall. Algal Res. 35: 152-159

Chlorophyta, the group of green algae of which there are more than 6000 species, manifests a great diversity of intercellular and extracellular components. Building blocks in the cell walls of Chlorophyta are very distinct and they may contain various components. Here, we characterize the cell walls of *Neochloris oleoabundans*, a Chlorophyte microalga, both in terms of biochemical composition and morphology. *N. oleoabundans* cell walls are composed of about 24.3% carbohydrates, 31.5% proteins, 22.2% lipids and 7.8% inorganic material, which contrasts to the cell walls of (higher) terrestrial plants in which carbohydrates are by far the main component. We also observed that cell wall carbohydrates are mainly non-cellulosic polysaccharides, essentially composed of rhamnose, galactose, glucuronic acid and glucosamine, of which glucose is only a minor component. The lipids comprising the *N. oleoabundans* cell walls are generally wax/cutin-like. Electron microscopic studies revealed that *N. oleoabundans* cell walls are approximately 200 nm thick and consist of two main layers: a thinner inner layer and a more electron-dense outer layer. On the outer layer are hair-like structures that are possibly rich in carbohydrates. These findings are an important contribution that enable us to understand the complexity of cell walls in green microalgae.

1. Introduction

Neochloris oleoabundans is a terrestrial microalga belonging to the Chlorophyta phylum. This species was first isolated from the sand dunes in Saudi Arabia, a very harsh environment where access to water is always a challenge (Chantanachat & Bold, 1962). Therefore, it must possess key properties to assure the viability of the cell. Depending on these specialized adaptations, *N. oleoabundans* can be cultivated in a freshwater medium as well as in saline water with seawater salt concentration (Arredondo-Vega et al., 1995; Popovich et al., 2012).

Green microalgae, such as *N. oleoabundans,* is outlined by its cell wall; a dynamic and rigid structure, that determines cell viability in a wide-range of environments, defends a cell from biotic and abiotic stresses, and provides plasticity, enabling cells to expand and assume different shapes.

Despite the significance of a cell wall in microalgae, only limited information is available on its composition and structure for most of the species (Baudelet et al., 2017). Chlorophyta, the largest group of green algae, displays a wide array of cell wall types regarding both chemical composition and morphology (Baudelet et al., 2017; Domozych et al., 2012; Fangel et al., 2012b). It is generally accepted that taxonomy can be a tool to speculate about the cell wall composition of algae and their related species (Baudelet et al., 2017; Domozych et al., 2012; Takeda, 1993). A recent review indicated that Chlorophyta can be taxonomically divided into three main groups depending on their cell wall composition and structure, which are distinctly different from those of terrestrial plants. Group 1, namely algae belonging to the Prasinophytina and Chlorodendrophyceae, in which cell walls are mainly composed of 2-keto-sugar acids 3-deoxy-manno-2-octolusonic acid (Kdo), 3-deoxy-5-O-Methyl-manno-2-octolusonic acid (5OMeKdo) and 3-deoxylyxo-2-heptulosaric acid (Dha); group 2, unicellular algae related to Trebouxiophyceae and Chlorophyceae, in which cell walls are mainly composed of mannans, glucans, arabinogalactans, algaenans and less frequently chitin-like polysaccharides; and group 3 comprises green macroalgae, chiefly marine lineages, in which cell walls on the whole contain sulphated polysaccharides, xylan, mannan and glucan (Baudelet et al., 2017). According to this taxonomical classification, *N. oleoabundans* belongs to “group 2” and is, therefore, expected to have a similar cell wall composition and structure as the other members.

On the basis of alkali extraction, algae cell walls could further be classified in accordance with the sugar composition of the alkali soluble part, hemicellulose, and the remaining residue, known as the “rigid cell wall”. To exemplify this classification, cell walls of the unicellular *Chlorella* strains, belonging to “group 2”, could be categorised into two distinct groups based on the presence or absence of

glucosamine in the “rigid cell wall” (Takeda, 1988a; Takeda, 1988b). For instance, *C. sorokiniana*, C*. vulgaris* and *C.kessleri* (currently known as *Parachlorella kessleri*, Trebouxiophyceae) belong to the glucosamine-rich rigid cell wall, whereas *C. fusca* (currently known as *Scenedesmus fuscus*, Chlorophyceae) lacks glucosamine and its “rigid cell wall” contains mannose and glucose (Loos & Meindl, 1982; Takeda, 1993). Rhamnose and galactose are the main sugars in the hemicellulose fraction of the glucosamine-rich rigid cell wall (Takeda, 1993).

Cell walls in the Chlorophyta phylum are very diverse and in addition to carbohydrates they comprise several other components. As far as protein is concerned, its abundance in the cell wall can differ substantially. This can be illustrated in *C. fusca* (currently known as *Scenedesmus fuscus*) which has approximately 7% protein content compared to *C. sorokiniana* with 17%. The amino acid profile of these two species appeared to be correspondingly different (Burczyk et al., 1999; Loos & Meindl, 1982; Russell, 1995). Alongside the aforementioned components, the presence or absence of algaenan, an acetolysis-resistant-biopolymer, in the cell wall, is yet another feature that creates diversity within the Chlorophyta species (Burczyk et al., 2014; Cheng et al., 2011). With few exceptions, such as species in the family Chlorellaceae, most of the microalgae belonging to “group 2” have an algaenanic layer, whereas this layer is absent in the cell wall of the other two groups of Chlorophyta (Baudelet et al., 2017).

Apart from their composition, Chlorophyta cell walls display different structures; some possess a single microfibrillar layer, referred to as the Inner layer (I-layer), while others have an additional layer, known as the Outer layer (O-layer). The O-layer, depending on the species, can be a mono-electron-dense layer or composed of three sub-layers, so called the trilaminar O-layer (Burczyk & Hesse, 1981; Burczyk et al., 2014; Gerken et al., 2013). *C. vulgaris* C-30*, C. sorokiniana* and *C. fusca* (currently known as *Scenedesmus fuscus*) are examples of microalgae that have a single microfibrillar I-layer, a mono O-layer and a trilaminar O-layer, respectively (Russell, 1995; Yamada & Sakaguchi, 1982).

In *N. oleoabundans,* research has generally focussed on studying the intercellular components. As far as we are aware this study is the first report on the detailed biochemical characterization and morphological appearance of the *N. oleoabundans* cell walls. The results provided herein will greatly contribute to advance our knowledge on the cell wall complexity in Chlorophyta.

2. Materials and Methods

2.1. *N. oleoabundans* cell culturing

Biomass was produced in a 280 L indoor tubular photobioreactor at AlgaePARC facilities (Wageningen, The Netherlands). Details of the reactor have already been described (Bosma et al., 2014). *N. oleoabundans* (UTEX 1185, University of Texas Culture Collection of Algae) was cultivated in a freshwater medium with the following components: 0.023 M $NaNO_3$, 0.017 M NaCl, 2.49 mM $MgSO_4$, 0.9 mM $CaCl_2$, 5.95 mM $NaHCO_3$, 282 µM $Na_2EDTA.H_2O$, 108 µM $FeSO_4.7H_2O$, 11 µM $MnCl_2.4H_2O$, 2.3 µM $ZnSO_4.7H_20$, 0.24 µM $Co(NO_3)_2.6H_2O$, 0.1 µM $CuSO_4.5H_2O$, 1.1 µM $Na_2MoO_4.2H_2O$. The culture was operated in a batch state without the use of artificial light, at a temperature of 25˚C and pH of 7.0. The reactor was monitored daily by measuring the optical density and dry weight as described earlier (Kliphuis et al., 2010). Additionally, quantum yield of the culture was monitored daily using portable AquaPen-P AP-P 100 (Photon Systems Instruments, Czech Republic) based on the manufacturer's protocol. Biomass was harvested several times at different points in time, centrifuged (80 Hz, ~3000g, 0.75 m^3 h^{-1}) using a spiral plate centrifuge (Evodos 10, Raamsdonksveer, The Netherlands), rinsed 3 times with water and lyophilized. The dry weight and quantum yield of the harvested biomass were approximately 0.5 g/L and 0.69, respectively. All the experiments were conducted with two biological replicates and four technical replicates. The lyophilized biomass from different harvest points of each biological replicate was pooled and used as material to commence the cell wall biochemical characterization.

2.2. Cell wall extraction

Figure 1 depicts the simplified schematic diagram of the cell wall extraction procedure used in this study. The extraction process began with 1 g lyophilized biomass that was mechanically disrupted for 1 min in a mill (Mixer Mill MM 200 - Retsch, Germany) at a frequency of 25 s^{-1}, followed by the removal of intercellular components including lipids, starch and soluble sugars. Cell wall disruption and the removal of intercellular components were carried out following a slightly modified version of the established protocol (Cheng et al., 2011). In brief, the biomass was incubated in 25 mL of chloroform: methanol (2:1) at 60°C for 30 min continuously shaking at 600 rpm. The samples were then centrifuged and the supernatant was discarded. All the centrifugal steps mentioned in this manuscript were conducted at 4200 g for 10 min unless stated otherwise. The intercellular lipids from the remaining pellets were extracted during two more cycles following the same process. Subsequent to a third extraction, the residual pellets were dried in an oven at 60°C until a constant weight was achieved. After removing the lipids, the biomass was then incubated in 25 mL of a maleate buffer at pH 6.5 (0.01 M $C_4H_4O_4$, 0.01 M NaCl,

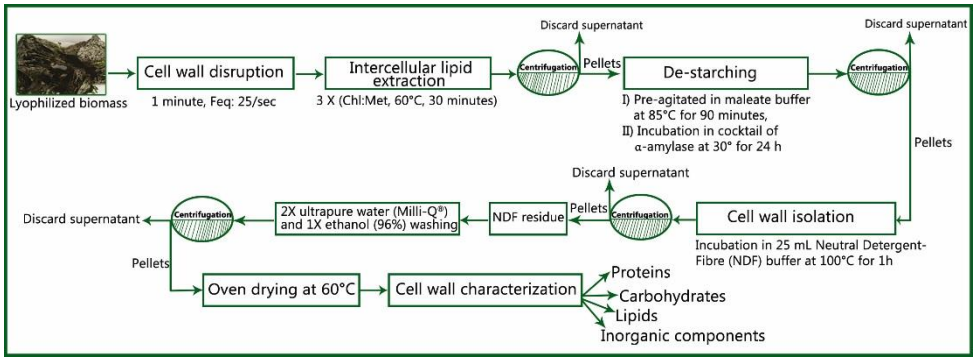

Figure 1. Schematic diagram of the cell wall extraction procedure.

0.001 M $CaCl_2$, and 0.05% w/v NaN_3) and agitated for 90 min at 85°C. Once the sample had cooled down to room temperature, a cocktail of alpha-amylase (50 µL/25 mL, ANKOM Technology Corporation, Fairpoint, NY) was added in which it was incubated for 24 h at 30°C. Following the centrifugal stage, the supernatant containing glucose derived from starch was discarded. During the next stage, cell walls were extracted from the oil-free de-starched biomass using a Neutral Detergent Fibre (NDF) buffer (104 mM sodium dodecyl sulphate, 50 mM ethylenediaminetetraacetic disodium salt (dihydrate), 17.8 mM sodium borate, 32 mM sodium phosphate dibasic (anhydrous), 79 mM sodium sulphite and 10 g/L triethylene glycol). Cell wall extraction is based on the protocol developed by Ankom Technology (ANKOM Technology Corporation, Fairpoint, NY), which is fundamentally based on the work of Van Soest (Goering HK, 1970; Van Soest, 1967). Cell wall extraction was performed manually without the Ankom apparatus. The biomass was incubated at 100°C for an hour in 25 mL of NDF buffer and stirred constantly at 600 rpm. Following the centrifugal stage, the remaining pellets were washed twice using ultrapure water (Milli-Q®) and once with ethanol (96%). The pellets were then dried in an oven (60°C) until constant weight was achieved. The final light brown coloured pellets correspond to the total cell wall and will be further referred to as NDF-cell walls.

2.3. Acid hydrolysis of cell walls and characterization of carbohydrates

Acid hydrolysis of the cell wall was carried out in line with the protocol “Determination of Total Carbohydrates in Algal Biomass” developed by the National Renewable Energy Laboratory with minor modifications for cell wall carbohydrates (Van Wychen, 2016). Concisely, 20 mg of dried NDF-cell walls were subjected to a two-stage H_2SO_4 hydrolysis, where at the first stage, 1 mL of 72% (V/V) H_2SO_4 was added to the sample and stirred for 1 h at 30°C. During the second stage, acid

concentration was diluted to 6% (V/V) and incubation continued for 1 h at 121°C (autoclave).

In parallel, 20 mg of NDF-cell walls were incubated with TFA for 2 or 3 h at 95°C at a concentration rate of 2 M and 6 M, respectively. These mild hydrolysis treatments were carried out in order to characterize the released monosaccharides that may have been degraded during the sulphuric acid hydrolysis process. Following hydrolysis the hydrolysate was cooled down, neutralized and after filtration using a 0.45 –µm filter, the content of each released monosaccharide was analysed. High Performance Anion Exchange Chromatography (HPAEC) was performed on a Dionex™ ICS5000+ DC (Detector/Chromatography Compartment) equipped with a Dionex™ CarboPac PA1 column (2 x 250 mm) preceded by a similar guard column (2 x 50mm) (Dionex/Thermo Fisher Scientific, Waltham, MA, USA). Separation was made at a flow rate of 0.25 mL/min at 30°C. The samples were cooled down to 5°C and a 2.5 µL sample was injected by means of a Dionex™ AS-AP (Autosampler Automated sample Preparation, Dionex/Thermo Fisher Scientific, Waltham, MA, USA). The elution programme involved an isocratic elution of 20 mM sodium hydroxide during 25 min followed by a linear gradient starting with 60 mM sodium acetate in 100 mM NaOH during 15 min and ending with 200 mM sodium acetate in 100 mM NaOH. The column was washed with 1 M sodium acetate in 100 mM NaOH for 5 min prior to re-equilibration in 20 mM sodium hydroxide for 30 min. The eluent was monitored by a 30°C thermostat Thermo Scientific ICS5000 and a pulsed electrochemical detector (PAD). The retention time (RT) was attained with a single injection of each sugar into the system which was used to characterize the monosaccharides of the cell wall. The amount of each sugar was quantified against a calibration curve, which was depicted by varying standard concentrations (0, 0.0005, 0.001, 0.0025, 0.005, 0.01, 0.025, 0.05, 0.1, 0.2 mg/mL).

2.4. Protein content and amino acid profile of the cell wall

A sample of 200 mg NDF-cell wall was dried in a convection oven for 1 h at 100°C and after cooling it down in a desiccator, the total nitrogen content was determined by combustion at 950˚C using a LECO analyser (LECO CN 628 Dumas analyser, LECO Corporation, USA). Amino acid characterization of *N. oleoabundans* was determined based on the EZ:faast™ method (Phenomenex Inc.) using the Gas Chromatography (GC) technique. Twenty mg of the cell walls were incubated in 6 N HCl for 24 h at 100°C. Later, following the manufacturer's instructions, the hydrolysate was cleaned and after derivatization, GC/FID (Agilent Technologies, Santa Clara, CA) was used to quantify and characterize the amino acids composing the NDF-cell walls proteins (Phenomenex). The protein content was then calculated by means of the nitrogen percentage and the conversion factor (NTP: Nitrogen to Protein), which was determined specifically for *N. oleoabundans* using an excel

sheet, ”Nitrogen-to-Protein Factor Calculator”, developed by the National Renewable Energy Laboratory (NREL, 2016). Three different NTP factors, including KA (N-factor of the maximum upper limit), KP (N-factor of the minimum lower limit) and K (mean N-factor) were calculated. Total protein content of the cell wall was assessed by multiplying the K value with the nitrogen content.

2.5. Lipids and inorganic components of the cell wall

The NDF-cell walls were analysed for potential lipid and inorganic constituents existent in the *N. oleoabundans* cell wall.

Lipid extraction was performed based on the procedure used by Jones et al. (Jones et al., 2012). One gram of the NDF-cell walls was incubated in 25 mL of chloroform: methanol (2:1) at 60°C for 30 min stirring continuously. The suspension was then centrifuged (4200 g, 5 min) and the isolated pellets were extracted for two more cycles following the same procedure. Subsequent to filtration (0.45 μm), the supernatants were bulked in a separatory funnel and by adding the right amount of distilled water, the proportion was altered to 8:4:3 chloroform: methanol: water (v/v/v). Subsequent to shaking, the lower phase containing the organic materials was transferred to pre-weighed Falcon tubes and after drying, the extracted lipids were weighed. The extracted lipids were then analysed by means of GC-MS (5975C inert MSD Agilent) equipped with a capillary column of Zebron ZB-5MS.

The inorganic content of the cell wall was assessed in accordance with the NREL protocol “Determination of Total Solids and Ash in Algal Biomass” (Wychen & Laurens, 2013). A pre-weighed dried glass tube containing 100 mg of the NDF-cell walls was put into a muffle furnace for 5 h at 575°C and the contents turned into ash. The samples were then cooled down to room temperature in a desiccator and the weight was recorded. For the characterization of ions, 3 mg of ash was mixed with 3 M formic acid at 99°C for 15 min and after being dissolved, the ions were analysed using the Ion Chromatography (IC) system 850 Professional (Metrohm Switzerland).

2.6. Imaging of the cell wall

For the microscopic analyses of *N. oleoabundans* cell walls, fresh biomass was produced in a Photobioreactor (PBR) (1.8 L Flat Panel, Labfors 5 Lux Flat Panel, Infors HT, Switzerland). The reactor was operated in a batch state on a daily basis using 16 h (light intensity of 500 μmol m^{-2} s^{-1}) and the temperature and pH were set at 30°C and 7.5±0.2, respectively. The growth medium was the same as the above-mentioned for the biomass that was used for biochemical characterization.

2.6.1. Transmission Electron Microscope (TEM)

The cells were collected, centrifuged (1000 g, 1 min) and re-suspended in 2% gelatine. Samples were placed in the specimen holder, after being soaked in hexadecene. Thereafter, pairs of holders were clamped together and instantly frozen by a high-pressure freezing instrument (HPM-010 Blazer, ABRA Fluid AG, Switzerland). Frozen cells were kept in liquid nitrogen and subsequently transferred to a homemade substitution apparatus containing a mixture of acetone, osmium tetroxide and uranyl acetate. Fast-substitution was performed between -90°C to 0°C which took about 5 h. The substituted sample was washed 3 times with acetone and later embedded in gradient concentrations of resin polymer (Lowicryl HM20) at 5°C for 3 days. Subsequently, the embedded cells were capsulated and polymerized for 3 days at 50°C. The polymerized samples were trimmed, sectioned (60 nm), post-stained by placing the grids in uranyl acetate and a citrate buffer. Samples were examined visually using a transmission electron microscope (JEOL JEM 1011, JEOL, MA, USA). Altogether approximately 200 electron microscopy images of multiple cells were captured and ImageJ 1.51f software (National institutes of Health, USA) was used to quantify the size of the cell wall.

2.6.2. Scanning Electron Microscope (SEM)

The cells collected were transferred to a poly-L-lysine coverslip and incubated in 3% glutaraldehyde solution in a PBS buffer. After 2 h, the slip was rinsed (3 times) in the PBS buffer and the sample post-fixed using 1% O_SO_4 for 1 h. After being affixed, cells were dehydrated using an ethanol gradient and dried by means of a critical point dryer. The coverslip was mounted on the carbon pad and coated with 15 nm Tungsten using a sputter-coater. The cells were visualized using FEI Magellan 400 at accelerating voltage of 2 kV (Magellan 400, FEI, Eindhoven, The Netherlands).

3. Results

3.1. Rhamnose is the most abundant monosaccharide of *N. oleoabundans* cell wall polysaccharides

Two different methods, concentrated H_2SO_4, a harsher treatment, and TFA hydrolysis, a milder treatment, were used to analyse the chemical composition of carbohydrates in the *N. oleoabundans* cell walls. Collectively, results from both acid hydrolysis revealed that *N. oleoabundans* cell walls contain as much as 24.3% carbohydrates (Figure 2). Cell wall carbohydrates were composed of rhamnose, arabinose, glucosamine, galactose, xylose, mannose, glucose, galacturonic acid and glucuronic acid (Figure 3). Rhamnose was by far the most abundant monosaccharide, corresponding to 33% of the total amount of released sugars, and together with galactose and glucuronic acid they comprise the largest proportion of

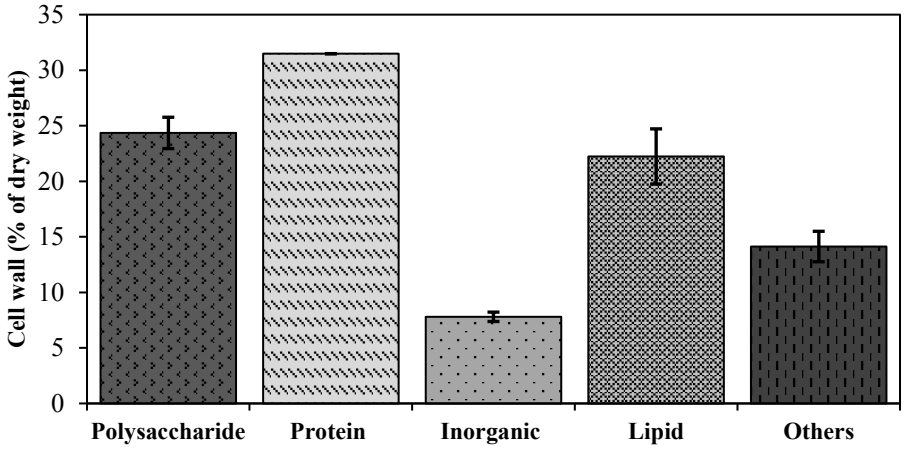

Figure 2. Percentage of components in the cell wall of *N. oleoabundans*. Values are the average of four replicates (two biological replicates, each measured in two technical replicates) and error bars represent the standard deviation (SD). "Others" fraction (~14%) stand for the portion of the cell wall composition that remained uncharacterized, most likely due to losses during the chemical analysis procedure. Acid-treatment is an essential step for the characterization of the cell wall, but inevitably destroys some components.

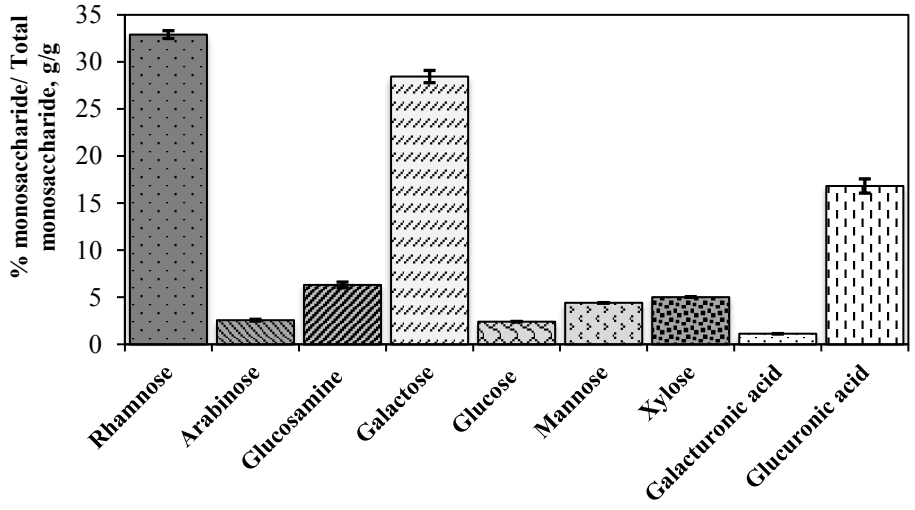

Figure 3. Monosaccharides composition of *N. oleoabundans* cell wall polysaccharides. Bars represent the amount of xylose, mannose, glucose and galacturonic acid are corrected based on TFA hydrolysis, while quantification of the other sugars is based on H_2SO_4 hydrolysis. Values are the average of four replicates (two biological replicates, each measured in two technical replicates) and error bars represent the standard deviation (SD).

the entire cell wall carbohydrates (78%). Our results indicated the presence of low amounts of glucose and galacturonic acid (<1% of NDF-cell wall), which were only detected in the TFA hydrolysate. Additionally, hydrolysing the cell wall mildly with TFA enabled a better separation of mannose and xylose and consequently the TFA chromatogram was also used to quantify these sugars.

3.2. Large amount of proteins in the *N. oleoabundans* cell walls

The first step in quantifying the cell wall protein was to determine the total nitrogen content, using the combustion method, which together with the results of the amino acids profile were used to calculate the Nitrogen-to-Protein (NTP) factors. The *N. oleoabundans* cell wall has NTP values of 6.5, 2.9 and 4.7 for KA (N-factor of the maximum upper limit), KP (N-factor of the minimum lower limit) and K (mean N-factor), respectively. Considering the amount of nitrogen (6.7% DW) and a Nitrogen-to-Protein factor of 4.7, we calculated that the *N. oleoabundans* cell wall contains 31.5% proteins (Figure 2). The amino acid profile of the NDF-cell wall proteins was characterized using the EZ:faast™ method and can be seen in Figure 4. The amino acid ratio and their entire content proved to be similar in all the replications. According to the amino acid classification based on the side chain structure, the *N. oleoabundans* cell wall is mainly composed of non-polar amino acids (> 67%).

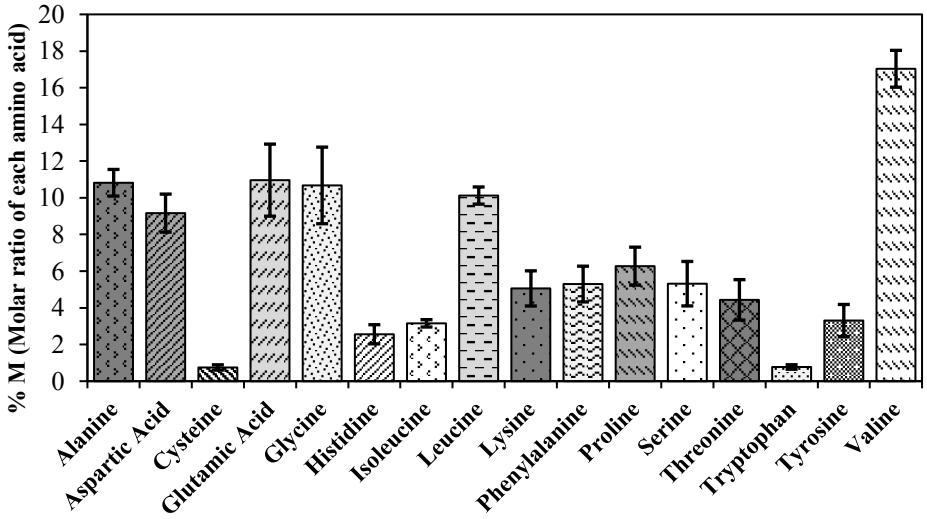

Figure 4. Detected amino acids composition of *N. oleoabundans* cell walls using EZ:faast™ method. Bars represent the percentage of molarity (%M) of each amino acid to the total identified amino acid content. Values are the average of four replicates (two biological replicates, each measured in two technical replicates) and error bars represent the standard deviation (SD). Using the EZ:faast™ method, we were able to disclose 16 amino acids in the cell wall. Due to the intrinsic limitation of the method we were unable to detect asparagine, glutamine and arginine. Asparagine and glutamine are quantitatively converted to

aspartic acid and glutamic acid during acid hydrolysis. Therefore, the absolute value of these two amino acids might be overrepresented. Methionine was not detected in the cell wall, which is most probably due to degradation during the HCl hydrolysis.

Amongst the polar amino acids, those with acidic residue are more abundant. Valine, alanine, leucine, glutamic acid, glycine and aspartic acid are the most abundant amino acids in *N. oleoabundans* cell walls.

3.3. Lipid and inorganic content of *N. oleoabundans* cell walls

Approximately 22% of the *N. oleoabundans* cell wall dry weight was extracted by means of chloroform: methanol, corresponding to the total cell wall lipids (Figure 2). Identification of the lipids obtained was further examined by GC analysis, and the mass spectra of the constituents was compared with a NIST library (National Institute of Standards and Technology). The lipids that were identified as having a predictability higher than 15% are summarized in Table 1. Furthermore, the lipid profile of the cell wall was compared to the lipids released after cell disruption (intercellular lipid) and the results indicated that some of the lipids are unique in the cell wall, while others are common between the cell wall and intercellular portion (Supplementary file 1). The intercellular fatty acid composition of *N. oleoabundans* includes: C16:0, C16:3, C18:0, C18:1, C18:2 and C18:3. Palmitic acid (C16:0) and stearic acid (C18:0) were the two lipids presented in both intercellular and cell wall fraction.

Table 1. GC-MS analysis of selected lipids in the cell wall (with a higher prediction level than 15%).

Component name	Molecular formula	MW (m/z)	MF	RMF	Prob.
Tetrahydro-2,5-dimethyl-2H-pyranmethanol[a]	$C_8H_{16}O_2$	144	706	722	16.6
5-methyl-3-Hexanol	$C_7H_{16}O$	116	666	788	15.1
1,3-di-tert-butylbenzene	$C_{14}H_{22}$	190	927	941	77.9
2,4-di-tert-butylphenol	$C_{14}H_{22}O$	206	946	948	62
Palmitic acid	$C_{16}H_{32}O_2$	256	934	936	82.9
Stearic acid	$C_{18}H_{36}O_2$	284	906	910	76.3
Cis-10-Nonadecenoic acid	$C_{19}H_{36}O_2$	296	666	679	29.2
9,19-Cyclolanost-6-en-3-ol, acetate	$C_{32}H_{52}O_2$	468	643	652	16.3
10,13-Octadecadiynoic acid, methyl ester	$C_{19}H_{30}O_2$	290	636	661	15.6

MW= Molecular weight; MF=Match factor (direct match); RMF= Reverse match factor; Prob.= Probability

[a] The underlined components correspond to unique lipids identified in the cell wall of *N. oleoabundans*

The total inorganic content of the cell wall was estimated in accordance with the NREL protocol developed for the algal biomass. Results of the inorganic analysis revealed that the NDF-cell wall of the *N. oleoabundans* contains 7.8% (DW) inorganic material (Figure 2). Characterization of the ash content by means of IC indicates that the inorganic fraction of the cell wall is composed of sulphate, sodium, phosphate, potassium, magnesium and calcium (Figure 5). Sulphate and sodium were the dominant ions, adding up to almost 80% of the total ash profile.

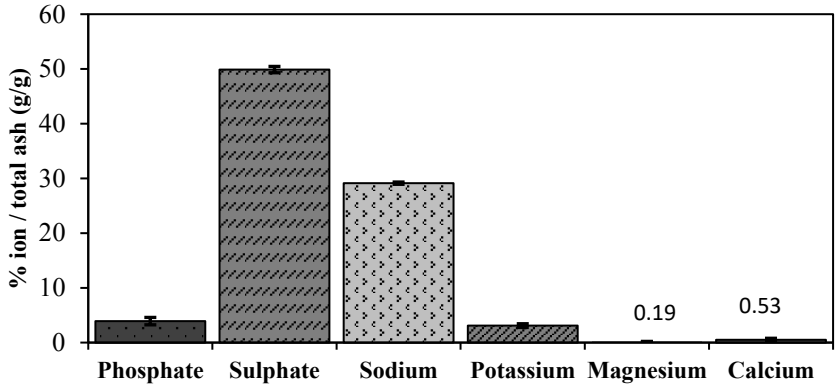

Figure 5. Percentage of each ion to the total inorganic content of NDF-cell wall (g/g). Bars represent the percentage of each ion in the total ash. Values are the average of four replicates (two biological replicates, each measured in two technical replicates) and error bars represent the standard deviation (SD).

3.4. Ultrastructure cell of *N. oleoabundans*

The cell wall morphology of *N. oleoabundans* was assessed by electron microscopy analysis using both a scan electron microscope (SEM) and a transmission electron microscope (TEM). TEM images of the *N. oleoabundans* revealed that the cell wall consists of two main layers: an outer-layer (O-layer) having a more electron-dense structure covered with hair-like structures and an internal inner-layer (I-layer), which has a lower electron density structure (Figure 6A and supplementary file 2, Figures D and E). The O-layer of the cell wall has a monolayer structure thinner than that of the I-layer. The thickness of the cell wall, determined based on an average of 200 images, was 200 nm. The hair-like structures account for 145 nm and the O-layer and I-layer were both 55 nm. The O-layer of the cell wall was observed in SEM also, but sputter coating might have masked some of the hair-like structures (Figure 6B and supplementary file 2, Figure C). After dividing, the O-layer accumulates in the medium, which was observed in both TEM and SEM images (Figure 6C and 5D; and supplementary file 2, Figures A, B and F). SEM images revealed that the daughter

cells have loose and wavy cell walls, whereas the O-layer of the cell wall in the mother cells appeared less wavy and fully stretched (Figure 6D).

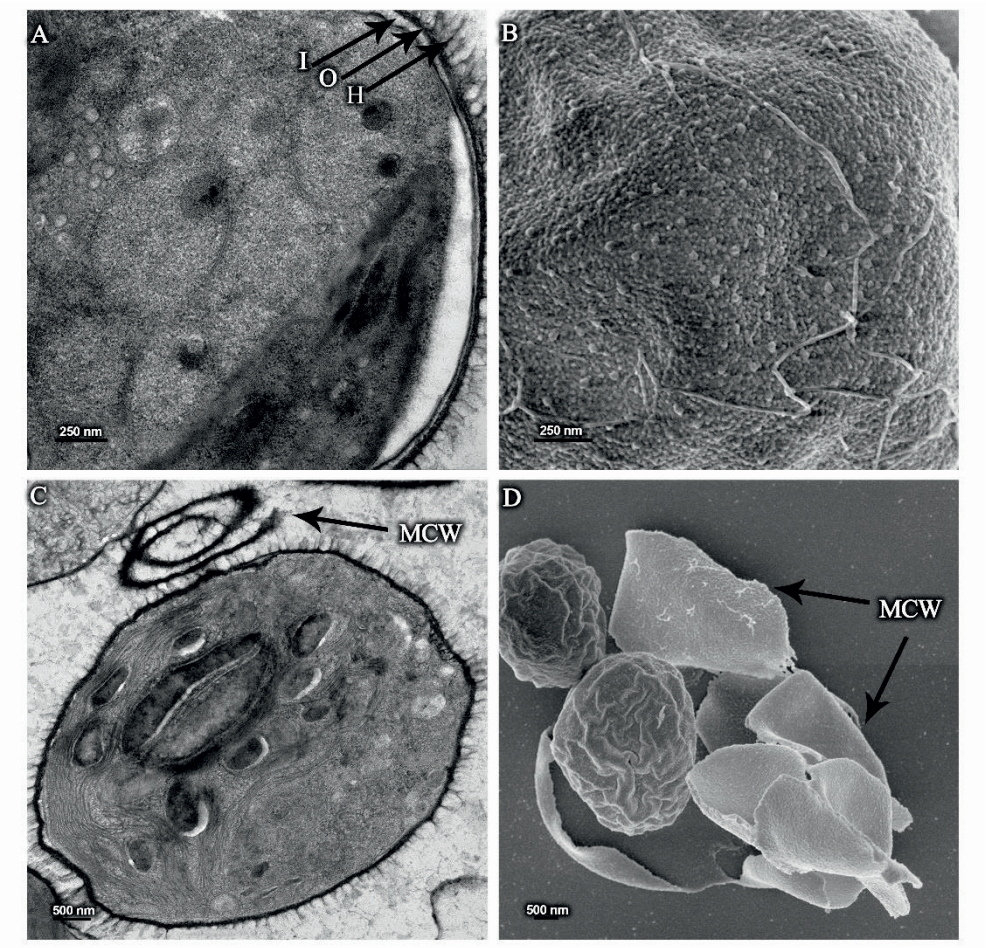

Figure 6. Electron microscopy images of *N. oleoabundans* cells. A, doubled-layered cell wall with hair-like structures (TEM). B, cell wall surface with hair-like structures (SEM). C and D, accumulation of maternal cell wall in the medium (TEM and SEM, respectively). I: internal-inner-layer of cell wall, O: external-outer-layer of cell wall, H: hair-like structures, MCW: maternal cell wall.

4. Discussion

4.1. Protein-rich cell walls of the *N. oleoabundans*

Unlike most of the cell walls in the plant kingdom, which are polysaccharide-rich , in *N. oleoabundans* proteins are the major component of the cell wall. The total nitrogen content in *N. oleoabundans* cell walls is 6.7%, indicating that they comprise 31.5% protein (% of total cell wall) (Figure 2). This revelation is consistent with other reports in the order of Chlorococcales, such as microalga *Scenedesmus obliquus*, which has a high protein content in the cell wall (Burczyk, 1973a; Burczyk, 1973b). It has been well-established from a variety of studies that the presence of nitrogen-containing biopolymers is a common feature in the Chlorococcaleae cell wall, although its content varies remarkably (Burczyk et al., 1999; Domozych et al., 2012; Voigt et al., 2014). Amongst nitrogen-containing biopolymers, the existence of glycoproteins in several green algae cell walls has been detected (Voigt et al., 2014; Voigt et al., 1994). Although specific functions of various glycoproteins in the majority of microalgae species cell walls are not yet known, the chaotrope-soluble cell wall glycoproteins number 1 (GP1), cell wall glycoproteins number 2 (GP2) and cell wall glycoproteins number 3 (GP3) in *Chlamydomonas reinhardtii* have proved to be precursors for the insoluble framework of the cell wall (Voigt et al., 2014). Considering the abundance of proteins in the *N. oleoabundans* cell wall, together with the taxonomical distribution of cell walls in Chlorophyta, it is tempting to hypothesise the existence of glycoproteins, which may have a significant function in the cell wall (Baudelet et al., 2017). Cell wall protein analysis revealed 16 different amino acids in *N. oleoabundans*. Valine, alanine, leucine, glutamic acids, glycine and aspartic acid are the dominant ones in the cell wall which is in line with earlier studies of various types of Chlorococcaleae algae (Burczyk et al., 1999). Hydroxyproline, an amino acid common in most land plants, was not found in our study. Due to the restrictions in this method, we were unable to detect asparagine, glutamine and arginine in the cell wall of *N. oleoabundans*. Furthermore, our results revealed a lack of methionine in the *N. oleoabundans* cell wall that may well have been degraded during the acid hydrolysis process.

4.2. *N. oleoabundans* belongs the class of glucosamine-rich rigid cell walls with high amounts of rhamnose and galactose

The carbohydrate content in the cell wall of *N. oleoabundans* accounts for 24.3% of the total cell wall biomass (Figure 2). Analysis of the sugar composition of the cell wall polysaccharides revealed that the most abundant monosaccharides in cell walls are rhamnose followed by galactose and glucuronic acids; while xylose, mannose, arabinose, glucosamine, glucose and galacturonic acid are present on a lower scale. The existence of high amounts of rhamnose-containing polysaccharides may contribute to cell wall rigidity. A previous study on the *Chlorella sorokiniana* cell wall

indicated that rhamnose, which is the most abundant monosaccharide, accounts for much of the cell wall resistance (Russell, 1995). The author observed that about 21.5% of the cell wall (percentage of dry weight) was resistant to an acetolysis treatment, an incubation with a mixture of concentrated sulphuric acid and acetic anhydride at 100 ˚C, which might result if a large amount of rhamnose exists in the cell wall. Besides rhamnose and galactose, glucosamine was the main sugar type in the *N. oleoabundans* cell wall. Consequently and consistent with the classification of cell walls based on the presence or absence of glucosamine in the "rigid cell wall", *N. oleoabundans* falls under the glucosamine enriched "rigid cell wall" group (Takeda, 1988a; Takeda, 1988b). The presence of glucosamine together with high amounts of rhamnose and galactose, confirms that *N. oleoabundans* belongs to "group 2" in Chlorophyta, similarly to the other members of this phylum (Baudelet et al., 2017). Out of all the species in this group, the cell wall of *N. oleoabundans* is most similar to *Chlorella* spp. and *Parachlorella* spp. (Chlorellaceae, Trebouxiophyceae) cell walls.

Cell walls in the plant kingdom generally have a complex structure including cellulose as a rigid network that is immersed in the matrix of glycoproteins and other polysaccharides (Banasiak, 2014; Fangel et al., 2012b). Results from this study exhibited only a trace amount of glucose (< 1%), revealing the lack or rather scarce amount of cellulosic polymer in the *N. oleoabundans* cell wall. It is reported that less evolved plants, Chlorophyceae, contain linear membrane-cellulosic-synthase-proteins, while rosette complexes, which are considered a main feature for being terrestrial, are absent (Banasiak, 2014; Fangel et al., 2012b; Sarkar et al., 2009). Low amounts of glucose, and possible traces of cellulose, together with the linear structure of the cellulosic-synthase-protein suggest that non-cellulosic polymers are the likely cause of rigidity in the *N. oleoabundans* cell wall. The lack of a polysaccharide-based cell wall, notably cellulose, in *N. oleoabundans* supports the theory that this species has evolved from ancestors before terrestrialization. It is believed that having a polysaccharide-based cell wall was a vital element that enabled the charophycean green algae, the ancestor of land plants, to make a successful transition to land (Harholt et al., 2016).

4.3. Biochemistry of *N. oleoabundans* cell wall lipids and inorganic components

Results of chloroform: methanol extraction revealed that the NDF-cell walls of the *N. oleoabundans* contain about 22.2% lipids (Figure 2). Reports on the amount and lipid composition in green microalgae cell walls are fragmentary and the information available is very general. In 1973, Burczyk mentioned that the cell wall of the microalga *S. obliquus* has about 9% of lipids (as a percentage of the extracted cell wall) of which about one third are waxes and phospholipids (Burczyk, 1973b). In the

early 1990s, research on the cell wall composition of some green microalgae revealed that seawater strains of *C. vulgaris*, *Kirchneriella lunaris* and a freshwater strain of *C. vulgaris* contained 10%, 12.5% and 15% of lipids, respectively (Abo-Shady et al., 1993). More recently, a study on the enzymatic cell wall degradation of *C. vulgaris* revealed that phospholipase A_1 is able to expand and stratify the O-layer of the cell wall due to the possible existence of phospholipids or phospholipid-like structures, even though the characteristics of these components were not identified (Gerken et al., 2013) . Despite the limited amount of analyses and reports on this topic, it is speculated that the lipids on cell walls could be cutins, waxes, algaenan-like structures or phospholipids (Burczyk, 1973b; De Leeuw et al., 2006; Gerken et al., 2013; Scholz et al., 2014).

The chromatography analysis of fatty acids in the *N. oleoabundans* cell walls revealed the existence of long-chain fatty acid (with more than 20 carbon atoms) along with saturated fatty acids C16-C18. These fatty acids have been reported as the main precursors in the elongation pathways of cutins and waxes (De Leeuw et al., 2006). An earlier study indicated that the aliphatic components in the *Chlamydomonas reinhardtii* cell wall were composed of C16:0 together with other fatty acids such as C16:1, C18:0, C18:1, C18:2 and C18:3 (Kondo et al., 2016). They proposed that *C. reinhardtii* has wax components, even though they were mainly different from land plants. They demonstrated that *C. reinhardtii* is not able to produce very long chain fatty acids with more than 20 carbon atoms and the lipid layer of the cell wall is essentially composed of TAG and alkanes embedded in a glycoprotein framework. While examining the annotated transcriptome of *N. oleoabundans*, we came across several putative enzymes relating to the wax and cutin-like biosynthetic pathway (Rismani-Yazdi et al., 2012). On account of this evidence it is tempting to hypothesise that *N. oleoabundans* is predominately formed by a wax/cutin-like structure regarding the lipid composition of its cell wall. This report is, to our knowledge, the first attempt to chemically characterize the primary lipids of *N. oleoabundans* cell walls, and it is an important step forward in understanding the cell wall properties of microalgae and how they function.

Approximately eight percent of *N. oleoabundans* cell wall was made up of inorganic ions, among which sulphate and sodium were the major components. It is known that marine algae are able to resist the saline environment owing to the sulphated polysaccharides in their cell walls (Aquino et al., 2011; Synytsya et al., 2015). It has been shown that sulphated polysaccharides are present in *N. oleoabundans*, as they grow in marine medium (Guzman-Murillo & Ascencio, 2000). A very recent report indicated that the cell walls of green microalgae belonging to Chlorophyta, *Ulva flexuosa* and *Cladophora glomerata*, are enriched in a polysaccharide composed of glucuronic acid and rhamnose linked to sulphate (Pankiewicz et al., 2016).

Considering the origins of *N. oleoabundans* in which severe saline and drought stress are a constant challenge, we would propose the presence of sulphated polysaccharide in the cell wall, thanks to the dedicated adaptations, which might allow this freshwater microalga to grow in a saline medium with seawater salt concentration.

4.4. *N. oleoabundans* cell walls have double layers

Morphologically, *N. oleoabundans* cell walls consist of two main layers each having different properties. Previous studies indicate that the O-layer of cell wall in some species of Chlorococcales is resistant to several lytic enzymes, such as cellulases, hemicellulase or lysozyme, as well as chemical agents, due to the existence of glycoproteins, and/or biopolymers containing glucosamine, and/or acetolysis resistant biopolymers (algeanans) (Atkinson Jr et al., 1972; Burczyk, 1986; Burczyk, 1973a; Derenne et al., 1992). The O-layer with a trilaminar structure, and its accumulation in the growth medium following cell division, has been reported as indicator of the existence of algaenan (Burczyk et al., 2014). A lack of this structure in *N. oleoabundans* suggests that the cell wall may not contain algaenan. Nevertheless, electron microscopy images depicted the accumulation of the maternal cell wall in the growth medium (Figures 6C and 5D; and supplementary file 2, Figures A, B and F). The O-layer of the *N. oleoabundans* cell wall is covered with hair-like structures, which, based on the TEM results, were observed on accumulated cell walls in the medium (maternal cell walls) and growing cells (Figure 6C). Previous studies indicated that these hair-like structures in *Chlorella* are linear polysaccharides of β-1,4-glucuronic acid and β-1,3-*N*-acetylglucosamine groups and may act as a defence mechanism against the PBCV-1 virus (Graves et al., 1999). Another study based on the enzymatic degradation of *C. vulgaris* cell walls, revealed that lysozyme is able to remove hair-like fibres from the O-layer of the cell wall (Gerken et al., 2013). Considering the taxonomic classification of the microalgae cell wall and the fact that *C. vulgaris* is closely related to *N. oleoabundans*, it could be hypothesised that the hair-like structures on the *N. oleoabundans* cell walls have a similar composition of those on *C. vulgaris* (Baudelet et al., 2017).

5. Conclusion

This manuscript is the first report of its kind on the detailed biochemical characterization and visualization of *N. oleoabundans* cell walls. Our results reveal that *N. oleoabundans* cell walls have a particularly unique composition and structure in comparison to higher plants. The high content of nitrogen-containing-biopolymers (mainly proteins) and the very limited amounts of glucose suggested that similar cell wall properties or functionalities can be achieved in diverse organisms with very different combinations of polymers. Herein we report the first characterization of the

lipids in the microalga cell wall, wax/cutin-like lipids, which might be a potential target for future cell wall disruption during the biorefining process. This study expands our knowledge on the cell walls of Chlorophyta, in particular *N. oleoabundans*, and may contribute even further to enable us to understand more precisely the evolution and diversity of the largest group of green algae.

Acknowledgements

This work was performed within the TKI AlgaePARC Biorefinery program with financial support from the Netherlands' Ministry of Economic Affairs in the framework of the TKI BioBased Economy under contract nr. TKIBE01009. The authors thank to Marcel Giesbers and Jan van Lent from Wageningen Electron Microscopy Centre of Wageningen University for the support with electron microscopy imaging and fruitful discussions and valuable input during the experiments.

Supplementary data

Supplementary file 1. Total fatty acid composition of *Neochloris oleoabundans* grown in freshwater medium. Values are calculated according to the peak area and presented as a percentage of composition.

Fatty acid	% composition
C16:0	17.8
C16:3	14.6
C18:0	2.4
C18:1	8.1
C18:2	30.9
C18:3	26

Supplementary file 2. Electron microscope images showing cell wall ultrastructure in *Neochloris oleoabundans*. A, B, accumulation of maternal cell wall in the medium (SEM). C, cell wall surface with hair-like structures (SEM). D and E, doubled-layered cell wall with hair-liked structures (TEM). F, accumulation of maternal cell wall in the medium (TEM). I: Inner-layer of cell wall, O: Outer-layer of cell wall, H: Hair-like structures, MCW: Maternal cell wall.

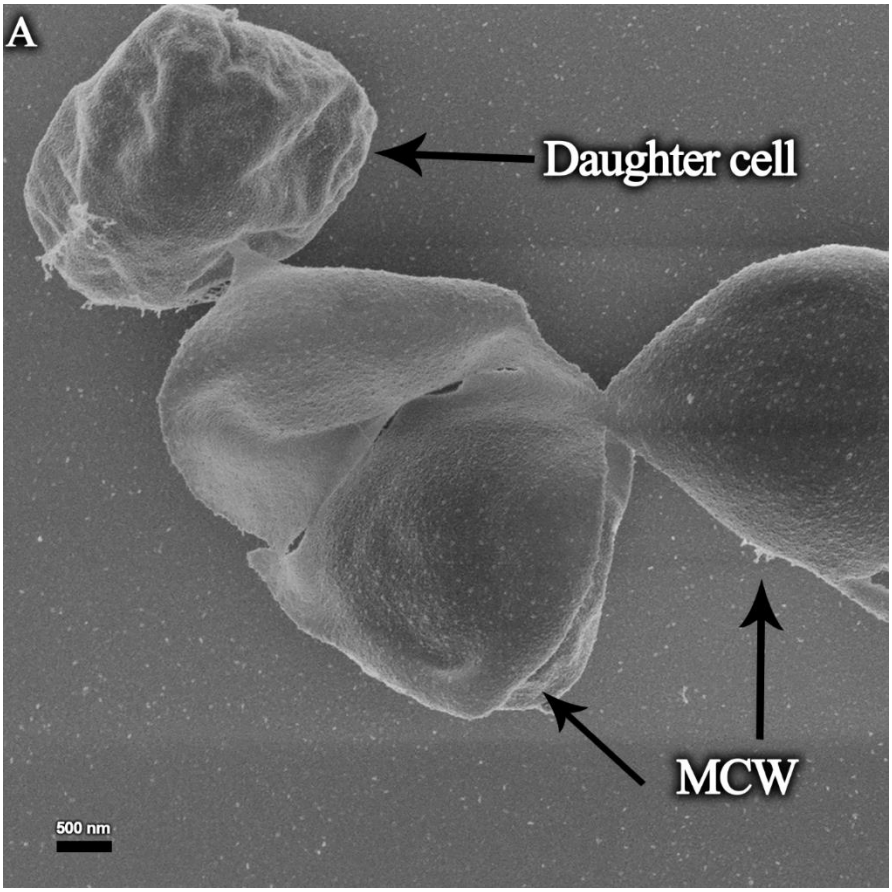

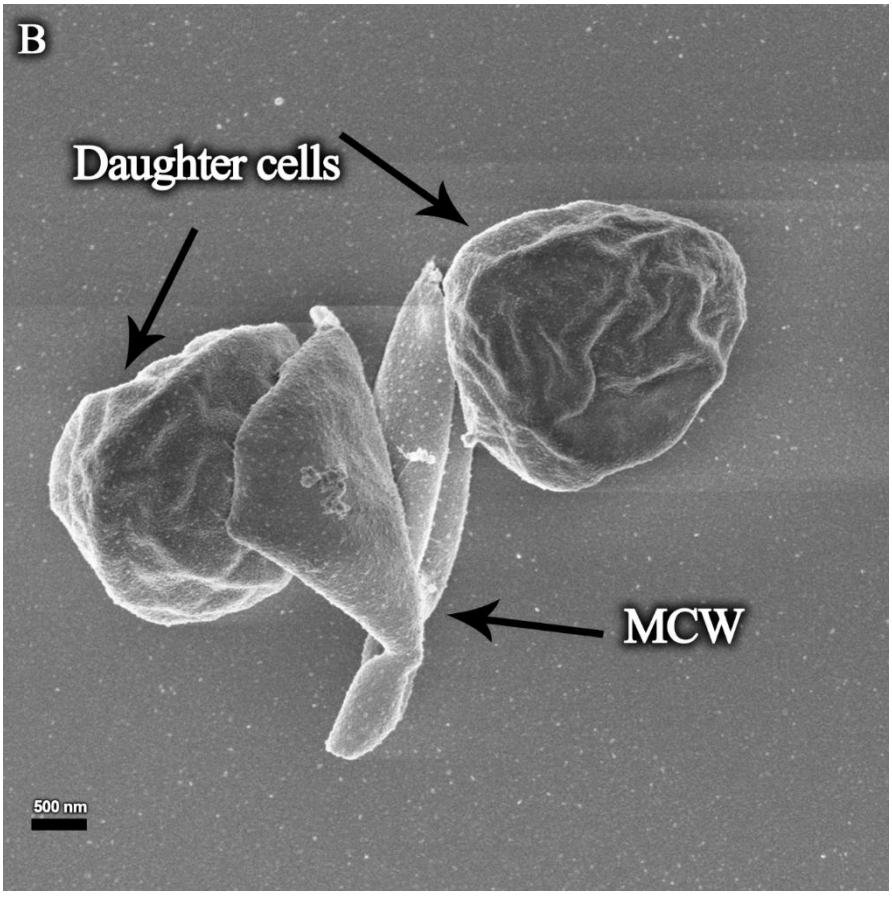
B
Daughter cells
MCW
500 nm

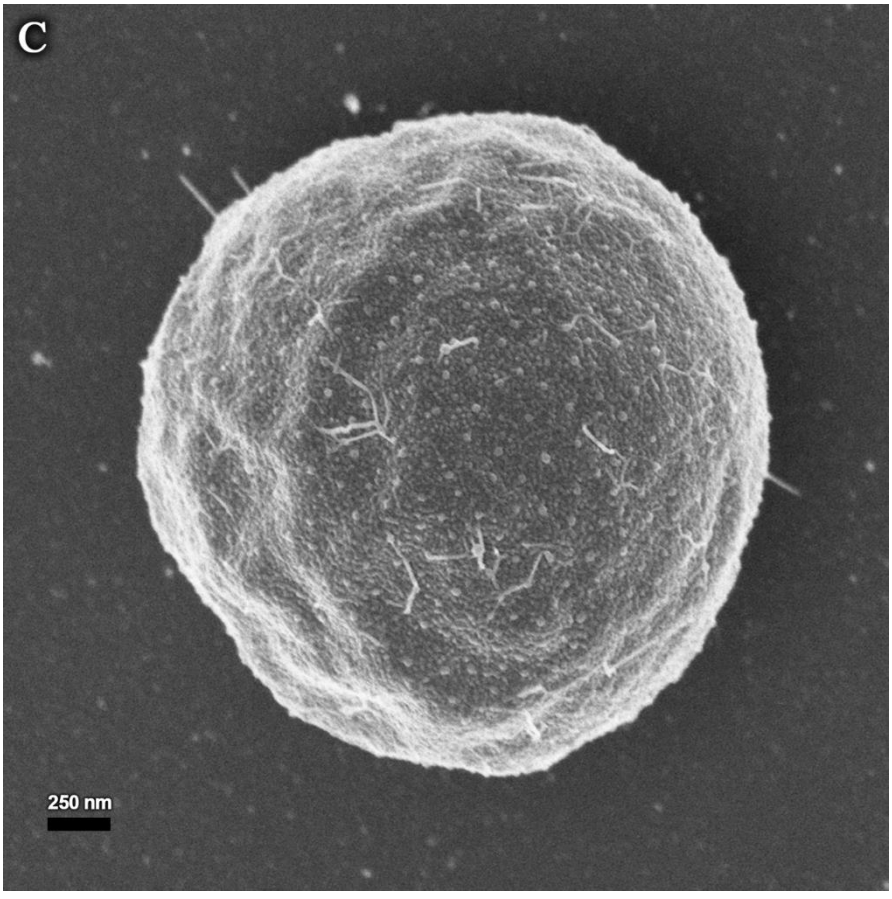
C
250 nm

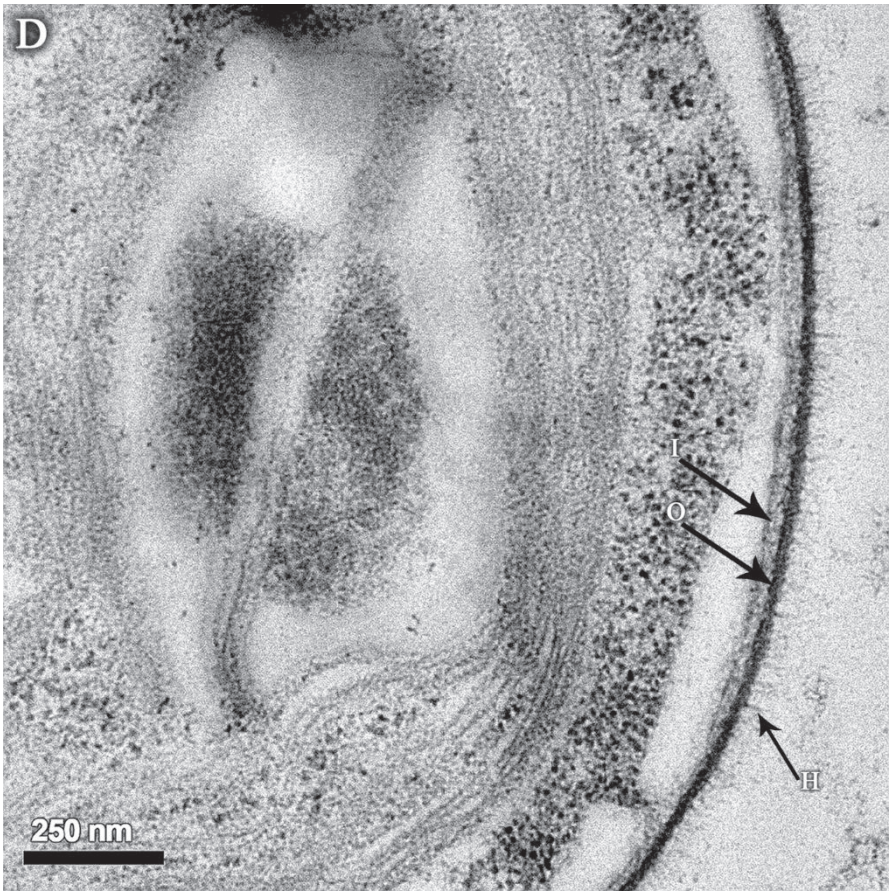
D
I
O
H
250 nm

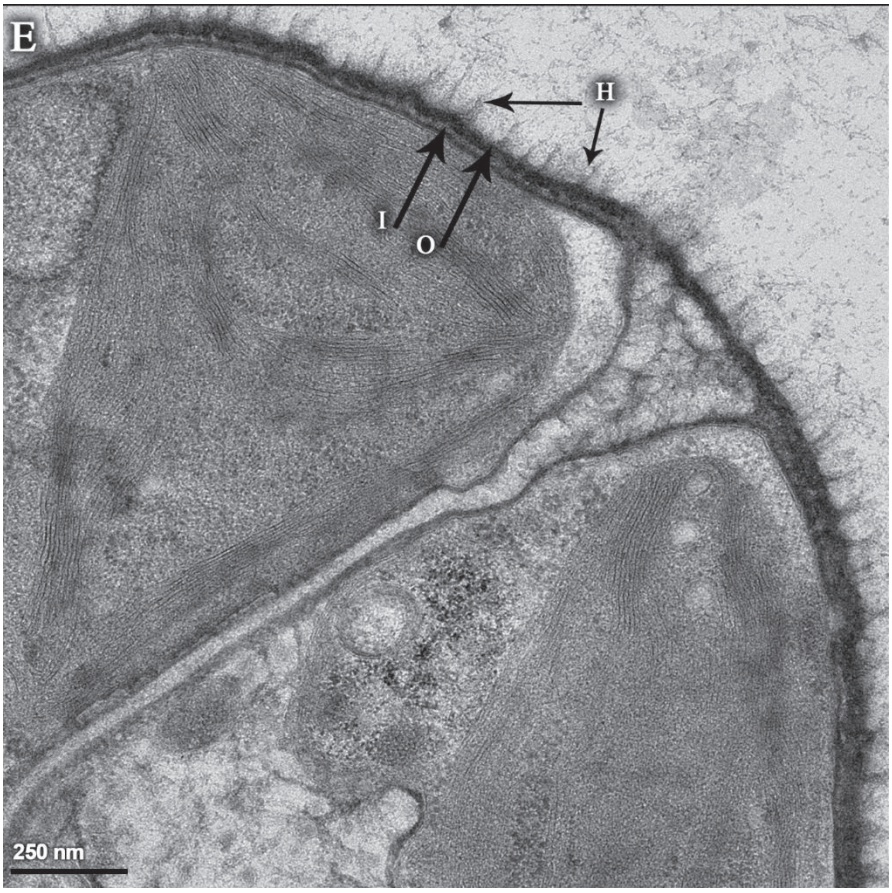
E
H
I
O
250 nm

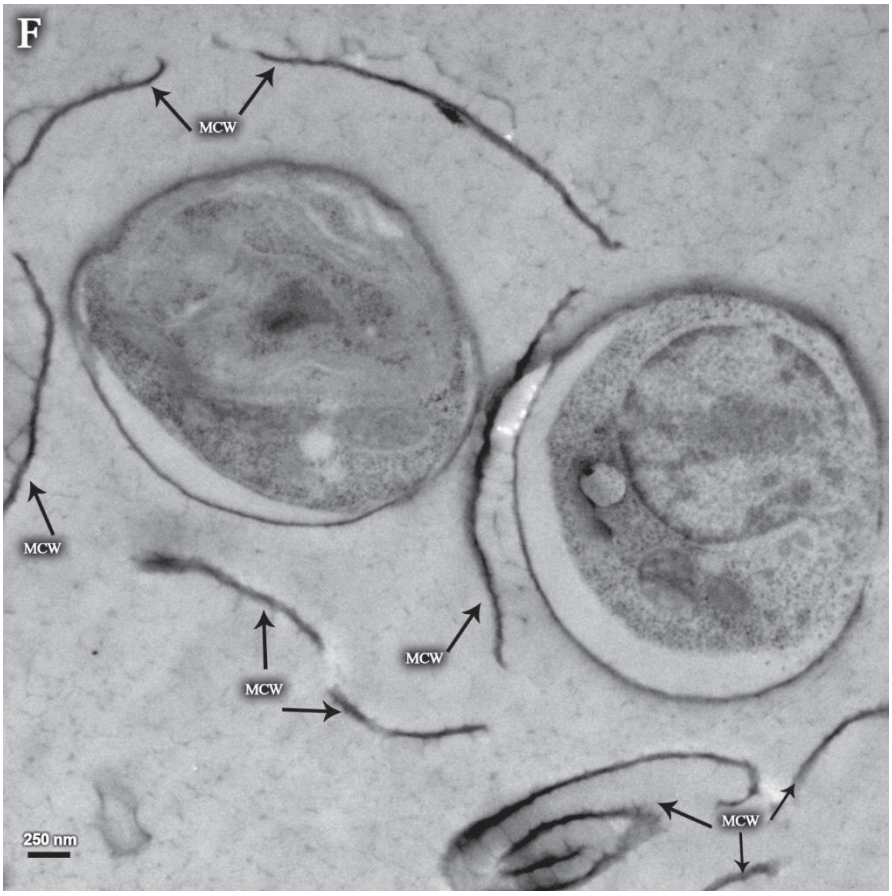
F
MCW
MCW
MCW
MCW
MCW
250 nm

CHAPTER 3

Neochloris oleoabundans cell walls have an altered composition when cultivated under different growing conditions

This chapter has been published as:

Behzad Rashidi, Annemarie Dechesne, Maja G. Rydahl, Bodil Jørgensen, Luisa M. Trindade (2019) *Neochloris oleoabundans* cell walls have an altered composition when cultivated under different growing conditions. Algal Res. 40: 101482

The impact that environmental factors have on the intracellular components of microalgae has been the focus of research for a number of decades. Despite that, their effects on the cell wall have received very little attention. In this study, we investigated how different growing conditions affect the cell walls of *N. oleoabundans*. The results revealed that the cell wall composition varied in that the modifications were different in the four cultivation media: freshwater nitrogen-replete (optimum culture) and -depleted conditions, and seawater nitrogen-replete and -depleted conditions. Nitrogen deficiency in freshwater cultivation was the only condition that significantly ($p<0.05$) increased the total content of carbohydrates in the cell wall. The three most abundant components of freshwater-cultivated cell wall polysaccharides were rhamnose, galactose and glucuronic acid whereas in seawater media the main components of cell wall polysaccharides were rhamnose, glucose and galactose. The combined results of the biochemical analyses and monoclonal antibodies epitope-binding revealed that *N. oleoabundans* cell walls are likely composed of sulphated polysaccharides enriched in mannose, β-(1→4)-D-mannans, and glucose as they grow in seawater. Salinity and nitrogen deficiency also had an impact on the nitrogenous components of the cell wall. Under these conditions we observed a decrease in glucosamine in the cell wall. The analysis of specific binding of monoclonal antibodies, revealed that the cell wall of *N. oleoabundans* is possibly enriched in arabinogalactan proteins (AGPs). Under salinity and nitrogen deficiency *N. oleoabundans* increased the proportion of the non-polar to polar amino acids in the cell walls. An increase of leucine in the cell walls may suggest that *N. oleoabundans* contains leucine-rich repeat proteins which are known to play a vital role in stress responses. This report provides new insights into microalgae cell wall biology and how cell walls are remodelled when growing under different conditions.

1. Introduction

The impact that environmental factors have had on the intracellular components of microalgae has already been the subject of research for a number of decades. In contrast, variations in cell wall composition and structure due to the impact of different environments have received limited attention. Adverse environmental factors can influence physiological processes and consequently have an impact on the regulation of cell wall biosynthesis, at both transcriptional and biochemical levels (Jeong et al., 2017; Tenhaken, 2015).

Nitrogen deficiency and salinity are two stress factors that have been used to modulate the intracellular composition in various microalgae species (Chen et al., 2017; Chu, 2017; Garibay-Hernández et al., 2013; Ghafari et al., 2018; Matich et al., 2018). It is clear that these factors play a significant role in the cell carbon partitioning, and one would expect these alterations to be visible in the cell wall as well. A few reports are now available on the effects of stress conditions on the algae cell wall. These include alterations in the cell wall composition or structure such as increased cell wall thickness which is associated with nitrogen deficiency (Solovchenko et al., 2015; Van Donk et al., 1997).

A great example on effects of stress condition on green microalgae cell wall has been recently published (Jeong et al., 2017). It was revealed that the increased thickness of the cell wall caused by nitrogen deficiency in *Nannochloropsis salina* is associated with up-regulation of genes encoding for cellulose biosynthetic enzymes, which resulted in an increase the cellulose content of the cell walls. Another study demonstrated that transition of *N. salina* from high to low saline culture increased the cell wall thickness, although detailed changes in biochemical composition are not yet available (Beacham et al., 2014).

Neochloris oleoabundans, is oleaginous unicellular green microalga belonging to the Chlorophyta phylum. Over the years, this microalga has been considered one of the most promising candidate industrial microalgae, due its high growth rate and biomass composition (Abu Hajar et al., 2017). *N. oleoabundans* is an edaphic freshwater green microalga which was originally isolated from the sand dunes in Saudi Arabia, an environment where the lack of water is a tenacious threat and cells can be exposed to saline or drought stress (S. Chantanachat & Bold, 1962). The cell wall is the outermost structure of the cell and the first part of the cell to be exposed to severe conditions. It therefore requires specific properties to guarantee cell viability. Owing to the plasticity of *N. oleoabundans* and its saline resistance mechanism, this alga can be cultivated in both freshwater or saline cultivation media, with seawater salt concentration (Arredondo-Vega et al., 1995; Jaeger et al., 2018; Popovich et al., 2012).

Recently, the cell wall composition of *N. oleoabundans* growing in freshwater condition was biochemically characterized and the morphology of the cell wall dissected by means of electron microscopy (Rashidi & Trindade, 2018). This report revealed that 56% of the cell wall is composed of carbohydrates and nitrogenous components such as amino sugars and proteins.

In this manuscript we aim to evaluate the effects of different cultivation media, freshwater nitrogen-replete (optimum culture) and -depleted conditions, and seawater nitrogen-replete and -depleted, on cell wall composition, with the main focus on carbohydrate and protein compositions. We expect that a lack of nitrogen could not only affect the carbohydrates but also have a direct impact on the nitrogenous components of the cell wall, such as amino sugars and proteins. The results revealed considerable variations in the biochemical composition of cell walls grown under different culture conditions. These results provide important insights into the biology of *N. oleoabundans* and will greatly contribute to our understanding of cell wall remodelling in green microalgae when they are exposed to adverse environments.

2. Materials and Methods

2.1. Biomass supply

N. oleoabundans (UTEX 1185, University of Texas Culture Collection of Algae) was pre-cultured in 100 ml sterilized fresh or seawater medium. Subsequent to reaching an optimum density (~ 0.2 g L-1), the culture was used to inoculate a vertical tubular photobioreactor (VT LGem, 1300 L working volume, Rotterdam, The Netherlands) installed inside a greenhouse at AlgaePARC facilities (Wageningen, The Netherlands). Details of the reactor are available on the manufacturer's website (www.lgem.nl). The same inoculations were used for the nitrogen-depleted experiments. The reactor was operated in a batch phase with the use of artificial light (7.2 kW), at an average temperature of 25°C and pH of 7.5. Concentration of the nutrients in the medium can be found in Table 1. The culture was monitored daily and the biological parameters including dry matter, optical density (530, 680, 750 nm) and quantum yield of the harvested points were recorded (supplementary file 1). Additionally, daily microscopic visualization in order to assess the cell morphology and possible contamination was conducted. Details of the measurements have already been described (Rashidi & Trindade, 2018). Biomass from different points in time of this batch pipeline production was harvested, centrifuged (80 Hz, ~3000g, 0.75 m3 h-1) using a spiral plate centrifuge (Evodos 10, Raamsdonksveer, The Netherlands), rinsed with water and dried in an oven at 60°C until a constant weight was achieved. The dried biomass at different points of harvesting was pooled and used as a starting material. Cell wall extraction was carried out in three replicates. The extracted cell wall materials were combined and used for further biochemical

characterization. All the biochemical analyses mentioned in this publication were performed at least with two technical replications and the values presented are the mean ± standard deviation (SD).

Table 1. Concentration of nutrients in the nitrogen-replete medium. For a nitrogen-depleted medium, amount of $NaNO_3$ is reduced and half of the concentration was used. Macronutrients and micronutrients are indicated based of mM and µM, respectively.

	Component	Freshwater	Artificial seawater
Macronutrients	$NaNO_3$	11.765	11.765
	$MgSO_4.7H_2O$	0.811	-
	$MgCl_2$	-	102.929
	NaCl	17.111	419.233
	$NaHCO_3$	9.523	9.523
	KH_2PO_4	2.939	1.469
	K_2HPO_4	-	1.148
	$CaCl_2.2H_2O$	0.680	-
	$CaCl_2$	-	4.775
	K_2SO_4	-	4.877
	$NaSO_4$		26.878
Micronutrients	NaEDTA	31.722	95.168
	H_3BO_4	141.329	128.481
	$FeSO_4.7H_2O$	20.142	60.493
	$MnSO_4.H_2O$	2.366	-
	$MnCl_2.4H_2O$	-	6.992
	$ZnSO_4.7H_2O$	0.765	2.292
	$CoCl_2.6H_2O$	0.210	0.630
	$CuSO_4.5H_2O$	0.080	0.236
	$(NH4)Mo_7O_{24}.4H_2O$	0.040	-
	$Na_2Mo_4.2H_2O$	-	0.619
	KI	0.301	-

2.2. Preparing samples to extract the cell wall

Cell wall preparation was carried out as described in (Rashidi & Trindade, 2018). In brief, 1 g of dried biomass was mechanically disrupted in a mill for 1 min at a frequency of 25 s-1 (Mixer Mill MM 200 -Retsch, Germany). Following this, three incubation cycles of chloroform: methanol (2:1) was used in order to remove the intracellular lipids. Each cycle was conducted at 60°C for 30 min continuously shaking at 600 rpm. After each incubation, samples were centrifuged and the supernatant was discarded. Subsequent to the last extraction, the residual pellets were dried in an oven at 60°C until a constant weight was achieved. When the lipids

had been removed from the sample, the biomass was de-starched by incubation in a buffer containing a cocktail of alpha-amylase. In summary, 25 mL of maleate buffer (0.01 M C4H4O4, 0.01 M NaCl, 0.001 M CaCl2, and 0.05% W/V NaN3) at pH 6.5 was added to the sample and then incubated for 90 min at 85°C. Once the sample had cooled down to room temperature, a cocktail of alpha-amylase (50 µL/25 mL, ANKOM Technology Corporation, Fairpoint, NY) was added to the suspension which was then incubated for 24h at 30°C. Subsequently, samples were centrifuged and the supernatant containing glucose derived from starch was discarded. All the centrifugal steps mentioned in this publication were conducted at 4200 g for 10 min unless stated otherwise.

2.3. Neutral Detergent Fibre (NDF) extraction of the cell wall

Cell walls from the oil-free de-starched sample were extracted in accordance with the established protocol developed by Ankom Technology (ANKOM Technology Corporation, Fairpoint, NY) as described in (Rashidi & Trindade, 2018). In short, the biomass was incubated at 100°C for 1 h in a 25 mL NDF buffer (104 mM sodium dodecyl sulphate, 50 mM ethylenediaminetetraacetic disodium salt (dihydrate), 17.8 mM sodium borate, 32 mM sodium phosphate dibasic (anhydrous), 79 mM sodium sulphite and 10 g/L triethylene glycol) and stirred constantly at 600 rpm. As soon as the incubation was accomplished, the suspension was then centrifuged and the supernatant discarded. The remaining pellets were washed twice using ultrapure water (Milli-Q®) and once with ethanol (96%). Subsequently, the pellets were then dried in an oven at 60°C until a constant weight was achieved. These pellets corresponded to the total cell wall and will be further referred as the NDF-cell wall.

2.4. Sulphuric acid hydrolysis and characterization of the cell wall carbohydrates

A total amount of carbohydrates in the NDF-cell wall of *N. oleoabundans* were measured subsequent to the sulphuric acid hydrolysis of polysaccharides as described earlier (Rashidi & Trindade, 2018). Briefly, 20 mg of dried NDF-cell wall was incubated in 1 mL of 72% (V/V) H2SO4 for 1 h at 30°C. The acid concentration was then diluted by adding the right amount of ultrapure water (Milli-Q®) to reach the final concentration of 6% (V/V). Incubation with the diluted acid concentration was further continued for 1 h at 121°C (autoclave). Following the hydrolysis, the hydrolysates were cooled down, neutralized and after filtration using a 0.45 µm filter, sugar content was analysed by means of High Performance Anion Exchange Chromatography (HPAEC, Dionex ICS5000+DC, CarboPac PA1, 2 x 250 mm, Thermo Fisher Scientific, Waltham, MA, USA) as described in (Rashidi & Trindade, 2018).

2.5. Immunolabelling of the *N. oleoabundans* cell wall components

Comprehensive microarray polymer profiling (CoMPP) of *N. oleoabundans* grown in either fresh or seawater nitrogen-replete was performed as previously described in (Fangel et al., 2012a; Kračun et al., 2017; Moller et al., 2007). Cell wall was isolated using a alcohol insoluble residue (AIR) procedure and used as a starting materials to extract the carbohydrates microarrays (Pettolino et al., 2012; Rydahl et al., 2017). In brief, the cell wall polymers were extracted sequentially from 10 mg of the AIR-cell wall using 50 mM 1,2-diaminocyclohexanetetraacetic acid (CDTA), pH 7.5, followed by extraction with 4 M NaOH with 0.1% m/V NaBH4, and extractions printed in four dilutions and two replicates giving a total of 8 spots per sample. The same amount of cell wall material was used for each sample. Nitrocellulose microarrays were printed as described previously by Pedersen et al.(2012) and Moller et al.(2007). Briefly, the printed arrays were probed with a panel of anti-rat and anti-mouse monoclonal antibodies (PlantProbes and Biosupplies). Antibodies were diluted in PBS containing 5% w/v milk powder to 1/10 and 1/1,000, respectively. For secondary antibodies, anti-rat and anti-mouse secondary antibodies conjugated to alkaline phosphatase (Sigma) were diluted in MPBS to 1/5,000. Developed microarrays were scanned at 2,400 dpi (CanoScan 8800F), converted into TIFFs and signals were measured using Array-Pro Analyzer 6.3 (Media Cybernetics). Data are shown in a heatmap in which the colour intensity is correlated to a mean spot signal value. A cut off, of 5 arbitrary units was applied.

2.6. Proteins and inorganic components of the cell wall.

Potential changes in the nitrogenous components of the cell wall due to the deficiency of nitrogen in the culture were further explored. To this end, the protein content was measured as described in (Rashidi & Trindade, 2018). In summary, a sample of 150 mg NDF-cell wall was dried in a convection oven for 1 h at 100°C and after cooling it down in a desiccator, the total nitrogen content was determined by combustion at 950˚C using a LECO analyser (LECO CN 628 Dumas analyser, LECO Corporation, USA). Total protein content of the cell wall was assessed by multiplying the Nitrogen to Protein (NTP) conversion factor with the nitrogen content. This conversion factor was calculated specifically for the NDF-cell wall of *N. oleoabundans* as reported previously (Rashidi & Trindade, 2018). Prior to characterizing the amino acids, a 20 mg sample of the NDF-cell wall was hydrolysed in 6 N HCl for 24 h at 100°C. Subsequent to hydrolysis, the amino acid characterization was carried out using the Gas Chromatography (GC) technique based on the EZ:faast™ method (Phenomenex Inc.). All the steps were carried out in line with the protocol annexed to the kit (Phenomenex).

Possible changes in the inorganic material of the cell wall under different environments were investigated. The inorganic content was assessed in line with the protocol described in (Rashidi & Trindade, 2018). Briefly, 100 mg ground dried NDF-cell wall in a pre-weighed glass tube was heated gradually in a muffle furnace for 5 h at 575°C and the contents were turned into ash. The inorganic residue was then cooled down to room temperature in a desiccator and the weight was recorded. To measure the cations and anions, approximately 3 mg of ash was dissolved in 1 ml of 3 M formic acid and incubated for 15 min at 99°C. Subsequent to dissolving, the solution was diluted 10 times with MQ water, filtered using a 0.45 µm filter and then the ions were characterized using the Ion Chromatography (IC) system 850 Professional (Metrohm Switzerland). The anions were determined by means of a Metrosep A 150, 150/4.0 mm column equipped with a Metrosep C5/5 Supp 4/6 Guard column and the cations with a Metrosep C4 Supp 4, 250/4.0 mm column equipped with a Metrosep A Supp 4/6 Guard column.

2.7. Statistical analysis

Significant difference between the each trait under the different growing conditions was assessed by two-way analysis of variance (ANOVA). The Fisher's unprotected least significant difference values were calculated at 5% probability. All statistical analyses were performed using Genstat (19th edition software, VSN International, Hemel Hempstead, UK).

3. Results

3.1. Composition of the cell wall carbohydrates alters according to different growing conditions

Analysis of the *N. oleoabundans* cell cultivated in the 4 different media resulted in significant differences ($p<0.05$) in the total content of cell walls between the growing conditions evaluated (Figure 1). Nevertheless, the total amount of carbohydrates in the cell wall did not show any significant differences ($p<0.05$) between the different treatments with the exception of cell cultivated in fresh water with nitrogen deficiency (Figure 2).

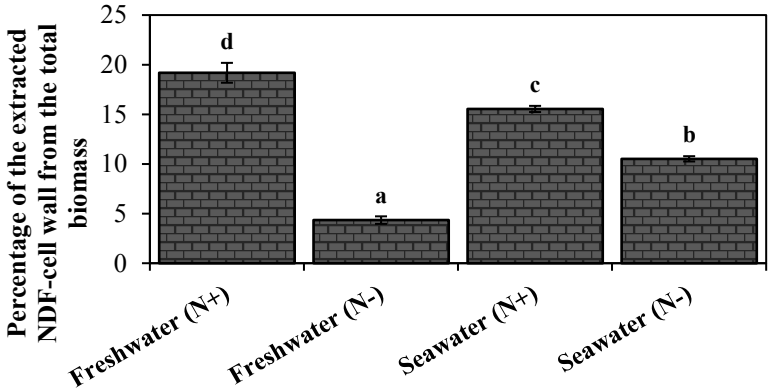

Figure 1. Percentage of the isolated cell wall in four different growing conditions. Values are the average from two technical replicates of pooled biomass and error bars represent the standard deviation (SD). Letters are based on the Fisher's unprotected least significant difference of cell walls amongst the different growing conditions.

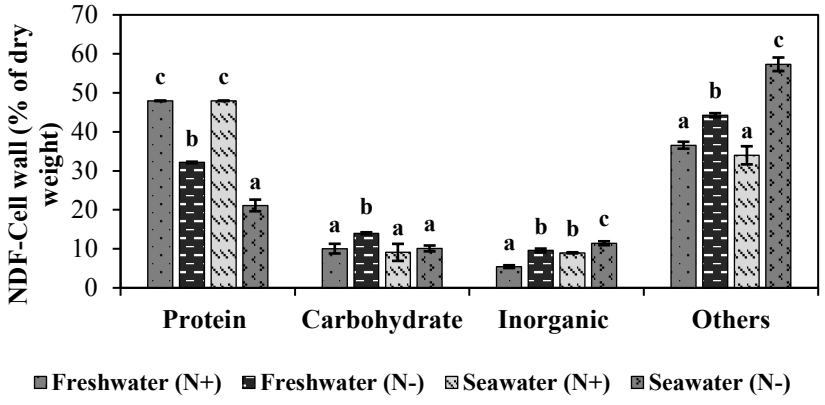

Figure 2. Percentage of the cell wall components in four different growing conditions. Values are the average from two technical replicates of pooled biomass and error bars represent the standard deviation (SD). "Others" fraction stand for the portion of the cell wall composition that remained uncharacterized. Letters are based on the Fisher's unprotected least significant difference of each cell wall component amongst cultures.

Under this condition, the total carbohydrates in the cell wall were about 14% (percentage of NDF-cell wall). Rhamnose, arabinose, glucosamine, galactose, glucose, mannose, xylose and glucuronic acid were the monosaccharides detected in the cell wall of *N. oleoabundans* independently of the media used for cultivation (Figure 3 and supplementary file 2).

Figure 3. Monosaccharides composition of *N. oleoabundans* cell wall polysaccharides. Bar chart represents a relative amount of each sugar to the total monosaccharides. Values indicates the average from two technical replicates of pooled biomass. Letters are based on the Fisher's unprotected least significant difference of each sugar amongst cultures and error bars represent the standard deviation (SD).

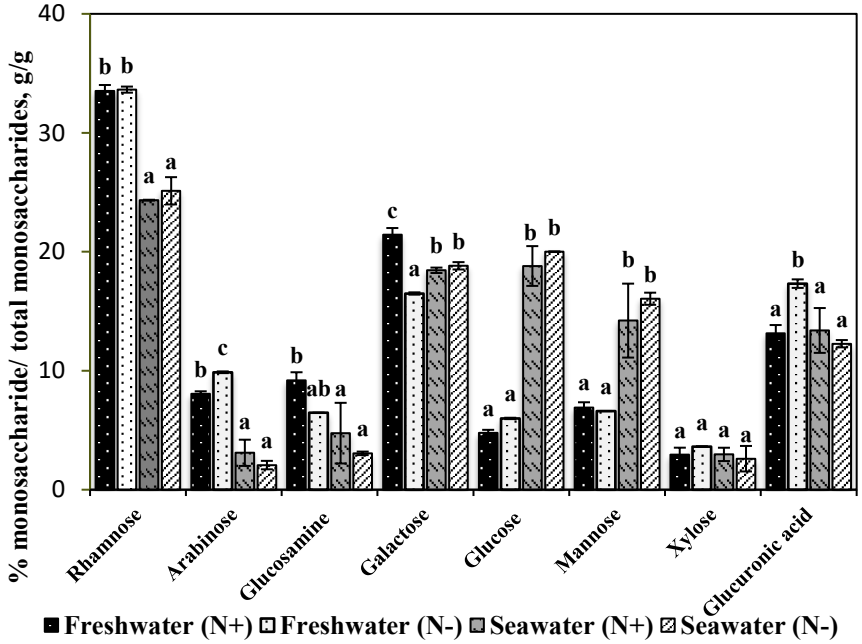

However, the proportion of the different monosaccharides was different. Rhamnose, galactose and glucuronic acid were the three most abundant monosaccharides in freshwater cultivations (~68% of total monosaccharides), whereas in seawater cultivations rhamnose, glucose and galactose constituted the main cell wall monosaccharides (63% of total monosaccharides). The proportion of monosaccharides remained relatively constant when cells were cultivated in seawater conditions (Nitrogen-deplete versus nitrogen-replete). Nitrogen depletion in freshwater cultivations resulted in a significant increase in the amount of arabinose and glucuronic acid and a reduced galactose content ($p<0.05$). Except for xylose, of which the content was similar in all growing conditions, we observed that there were alterations in the relative amount of almost all monosaccharides in seawater

cultivations, with or without nitrogen, as compared to the corresponding samples cultivated in freshwater conditions. Our results disclosed that glucose and mannose are the monosaccharides which increased the most in the cell wall carbohydrates of cells cultivated in saline media ($p<0.05$).

CDTA and NaOH-extracted glycans of *N. oleoabundans* cell wall, fresh and seawater nitrogen-replete cultivations, were probed with 38 monoclonal antibodies (mAbs). Figure 4 shows a heatmap of the relative abundance of the mAbs binding to specific cell wall components. Overall, the majority of the mAbs did not bind to the *N. oleoabundans* cell wall polymers. Walls of cell cultivated in both nitrogen-replete freshwater and seawater conditions revealed that they were composed of (1→4)-β-D-xylan/arabinoxylan. Additionally, our results indicated the possible existence of arabinogalactan proteins (AGPs) in the cell wall of *N. oleoabundans*. Monoclonal antibodies of JIM16 and LM14 showed a high binding affinity with the NaOH-extract of the freshwater cell wall (nitrogen-replete), whereas JIM13 indicated a high affinity with the CDTA-extract of seawater cell wall (nitrogen-replete). Remarkably, our results demonstrated the accumulation of (1→4)-β-D-mannan/galactomannan in *N. oleoabundans* cell walls grown in seawater condition, whereas these epitopes were either absent or inaccessible in freshwater cultivation.

Figure 4. Heatmap showing the binding of monoclonal antibodies (mAbs) to the extracted cell wall materials. Values are the average of the replications and indicate the relative abundance of the antibodies to glycan epitope of *N. oleoabundans* cell wall. Colour intensity in the heatmap is correlated to mean spot signals. The highest signal in each dataset was set to 100, and all other values were normalized accordingly as indicated by the colour scale bar.

3.2. Cell walls have a varied protein composition when grown under stress

Analysis of the protein content in the cell walls of microalgae cultivated under different conditions revealed that cell wall accumulated a high amount of proteins in both sea and freshwater cultivation provided there was a sufficient amount of nitrogen in the medium (Figure 2 and supplementary file 3). However, under nitrogen-depleted growing conditions, the protein content of the cell wall decreased significantly ($p<0.05$), in which nitrogen-depleted seawater showed the lowest content (19.3% of the NDF-cell wall). Further amino acid characterization revealed a decrease in the algae cell wall polar amino acids that were cultivated in fresh water under nitrogen depleted condition (Figure 5).

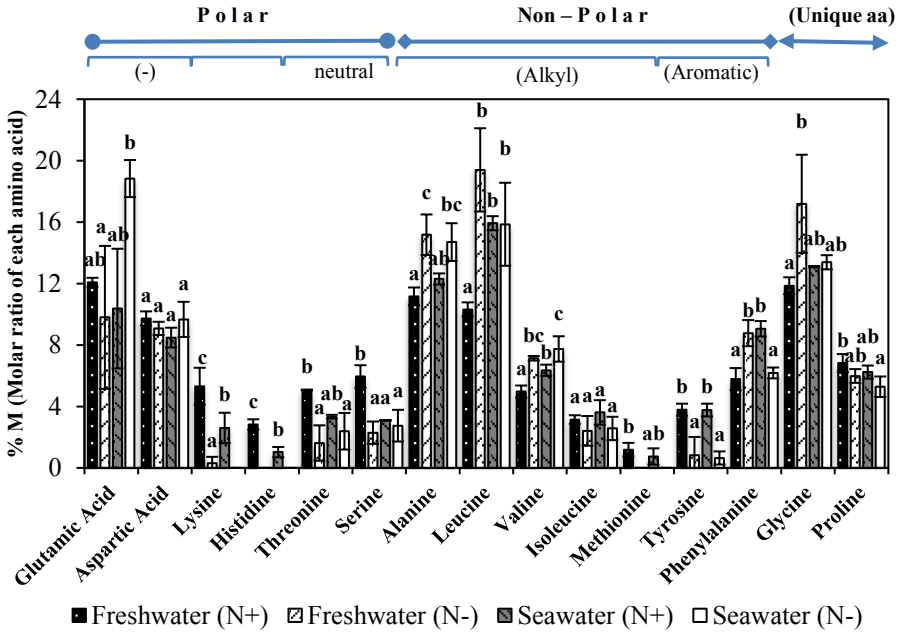

Figure 5. Detected amino acids composition of *N. oleoabundans* cell walls using EZ:faast™ method. Bar chart signifies a percentage of molarity (%M) of each amino acid to the total identified amino acid content. Values indicates the average from two technical replicates of pooled biomass and letters are based on the Fisher's unprotected least significant difference of each amino acid amongst cultures. Error bars represent the standard deviation (SD). Due to the intrinsic limitation of the EZ:faast™ method we were unable to detect asparagine, glutamine and arginine. Asparagine and glutamine are quantitatively converted to aspartic acid and glutamic acid during acid hydrolysis. Therefore, the absolute value of these two amino acids might be overrepresented. Cysteine and tryptophan were not detected in the cell wall, which is most probably due to the degradation during HCl hydrolysis.

This reduction was specifically on the positive-side-chain-amino acids, where lysine decreased dramatically and histidine reduced to undetectable amounts, as well as the polar-uncharged amino acids where the larger reductions were observed in serine and threonine. Cells cultivated in nitrogen-depleted seawater revealed a higher content of polar amino acids in the cell wall relatively to the nitrogen-replete culture ($p<0.05$). Positive-side-chain-amino acids were not detected in the cell wall of a nitrogen-depleted seawater cultivation. Aspartic acid and isoleucine remained constant in the different growing conditions.

Results of the inorganic portion of the cell wall revealed a higher accumulation of inorganic components in the nitrogen deficient cultures (Figure 2). Under nitrogen-replete growing conditions, the inorganic content of the cell wall decreased, with the lowest percentage being found in freshwater cultivation (~5%).

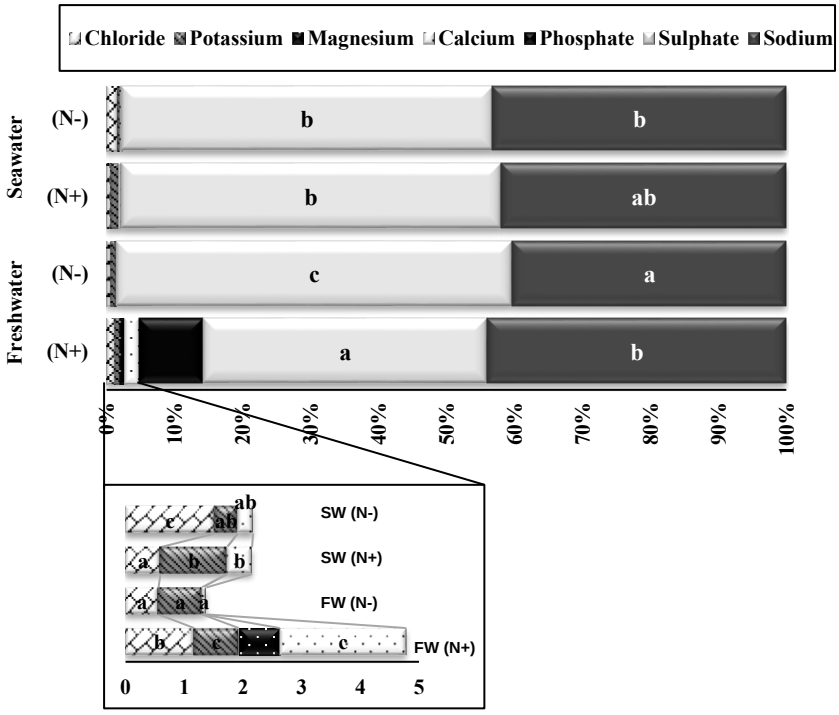

Figure 6. Percentage of each ion to the total inorganic content of NDF-cell wall (g/g). Bars represent the percentage of each ion in the total ash. Values are the average from two technical replicates of pooled biomass and error bars indicate the standard deviation (SD). Letters are based on the Fisher's unprotected least significant difference of each ion amongst cultures.

Ion chromatography analysis revealed that the cell wall is primarily composed of sulphate and sodium, adding up to almost 85% of the total ash content in a nitrogen-replete freshwater culture and 98% in other growing conditions (Figure 6).

Phosphate and magnesium were only detected in nitrogen-replete freshwater culture.

4. Discussion

Adverse growing conditions such as salinity and nitrogen depletion can influence cell physiology and consequently cell wall composition (Tenhaken, 2015). We observed an significant variation in the total content of cell walls between the growing conditions assessed (4% - 19% g/g, $p<0.05$). Under different growing conditions *N. oleoabundans* cells were able to change the composition of their cell walls. This variation highlights an important property of *N. oleoabundans* cell walls, which are plastic and can adapt to different growing conditions. In this study we have characterized the content and composition of carbohydrates, proteins and inorganic components, though microalgae cell wall might have other components, such as lipid, that may as well vary under the adverse growing conditions, but these were not object of our study.

Our results revealed that walls of *N. oleoabundans* cultivated under nitrogen-depleted conditions accumulated a higher content of carbohydrates, although this increase was not significant ($p<0.05$) in the seawater cultivation (Figure 2). Previous studies of other microalgae indicate that when cells were cultivated under nitrogen-depleted conditions an increase in polysaccharide content of the cell wall was observed (Baulina et al., 2016; Gorelova et al., 2014; Jeong et al., 2017). This result illustrates the ability of the *N. oleoabundans* cell wall to function as an additional type of sink for photo-assimilates accumulated under nitrogen stress. Seawater cultivation resulted in alterations in the monosaccharide profile of the cell wall as compared to the freshwater culture (Figure 3). Glucose and mannose content in the cell wall were abundantly increased when *N. oleoabundans* was cultivated in seawater ($p<0.05$). We have observed that the majority of the mAbs did not bind to the *N. oleoabundans* cell wall polymers. The most probable explanation is the absent of the epitopes in *N. oleoabundans* cell wall, which would not be surprising as these antibodies have been developed for other plant and algae species. Another explanation could be that the epitopes might have been inaccessible and/or possibly degraded during the extraction procedure. Nevertheless, results from monoclonal antibodies disclosed that (1→4)-β-D-mannan/galactomannan are the possible epitopes of the accumulated mannan in the seawater cultivated cell wall.

Although results from monosaccharides composition of the cell wall revealed the presence of mannose in a freshwater cultivation (~7% of total monosaccharides, g/g), evaluated monoclonal antibodies were unable to recognize the mannose-epitope(s). This may attributable to the existence of different epitope of mannose or inaccessibility of the same mannose-epitope in the cell wall of freshwater cultivation.

Previous studies on marine algae established that some microalgae are enriched in sulphated polysaccharides including β-(1→4)-D-mannans, (1→3)- β -L-arabinopyranans and other sulphated polysaccharides containing galactose, glucose and arabinose (Aquino et al., 2011; Fernández et al., 2012; Fernández et al., 2013; Synytsya et al., 2015). Marine algae are able to resist the saline environment on account of particular mechanisms such as sodium exclusion or accumulation of sulphated polysaccharides (Aquino et al., 2011; Gimmler, 2000; Muralidhar et al., 2015; Synytsya et al., 2015). The latter mechanism, which is unique to marine algae, is considered to be a strategy of adaptation in marine territories and is also existent in (some) halophyte terrestrial plants (Aquino et al., 2011; Synytsya et al., 2015). It has been reported that sulphated polysaccharides, which provide a gel-like matrix for a fibrous and crystalline component of the cell wall, are part of the cell walls of some marine species belonging to the phylum Chlorophyta (Percival, 1979; Synytsya et al., 2015). Considering the abundance of mannose, β-(1→4)-D-mannans, and glucose together with a high content of inorganic sulphate in the seawater cultivated *N. oleoabundans* cell wall, it is tempting to hypothesize the presence of sulphated polysaccharides which may contribute to the adaptation of this species in a saline medium.

Nitrogen-containing biopolymers are one of the main components in the microalgae cell wall belonging to the Chlorococcaleae, therefore it was not surprising that a restricted amount of nitrogen in the medium caused a reduction of the cell wall fraction in the total cell mass of *N. oleoabundans* (Burczyk et al., 1999; Domozych et al., 2012; Voigt et al., 2014). As depicted in Figure 3 there is a considerable reduction of glucosamine in the cell walls when they are cultivated under nitrogen depletion or saline medium. A recent transcriptomic study of *N. oleoabundans* cultivated under nitrogen depletion indicated a downregulation of glucosamine fructose-6-phosphate aminotransferase (GFAT) (Rismani-Yazdi et al., 2012). This enzyme is involved in the hexosamine (amino sugar) biosynthesis pathway, synthesizing glucosamine-6-phosphate (GlcN-6P) from fructose-6-phosphate (Fru-6P) which is derived from glucose. It has been demonstrated that nitrogen depletion in *Chlorella vulgaris* resulted in morphological alteration of the cell wall (Gerken et al., 2013). *C. vulgaris* growing in nitrogen-replete conditions contains hair-like fibres mounted on the outer layer of the cell wall, referred to as hyaluron, an unsulphated glycosaminoglycan structure composed of β-1,4-glucuronic acid and β-1,3-N-acetylglucosamine (Gerken et al., 2013; Graves et al., 1999; Van Etten et al., 2017). Under nitrogen-depleted conditions *C. vulgaris* lacks these hair-like fibres.

The change in cell wall mass under nitrogen-depleted conditions was predominantly attributed to a reduction in the protein content of the cell wall (Figure 1 and Figure 2). Localized cell wall proteins comprise enzymes, both in situ enzymes for

development and remodelling, and enzymes involved in biotic and abiotic responses; as well as glycine-rich proteins (GRPs), proline-rich proteins, extensins and hydroxyproline-rich glycoproteins (HRGPs) (Immerzeel, 2005; Showalter, 1993). Arabinogalactan proteins (AGPs) belong to the HRGPs and are found at the cell surface of a wide variety of plants and algae (Chudzik et al., 2005; Domozych et al., 2012; Immerzeel, 2005). The positive signal of the antibodies JIM16, JIM13 and JIM14 toward the arabinogalactan/arabinogalactan-protein antigens revealed the possible existence of AGPs in *N. oleoabundans* cell walls. In line with previous studies, these monoclonal antibodies have an affinity to AGP1 and AGP2 immunogens (Knox et al., 1991; Yates & Knox, 1994). The likely existence of arabinogalactan proteins in the *N. oleoabundans* cell wall supports its taxonomical classification into the phylum Chlorophyta, in which cell walls are known to contain AGPs (Baudelet et al., 2017). Despite these enlightening findings, questions still remain concerning the particular biological function of AGP1 and AGP2 in the *N. oleoabundans* cell wall. The exact function of AGPs in plant cells is still a matter of debate, yet cell division, cell extension, abiotic stress tolerance and cell viability are the main functions discussed in literature (Chudzik et al., 2005; Fernández et al., 2014; Showalter, 2001).

Polar amino acids were more abundant in the walls of cells cultivated in nitrogen-replete freshwater in comparison to all the other growing conditions (Figure 5). The final structure of a protein comprises polar/hydrophilic side-chain amino acids, which are normally located on the surface of the proteins and are in contact with the aquatic milieu, and non-polar/hydrophobic side-chain amino acids existing on the interface (Rosenberg, 1996). Changes in the abundance of amino acids, each with the different chemistry of side chain, alters conformation and structure of the protein. Amongst non-polar amino acids, the increase of leucine was considerable in the cell wall of *N. oleoabundans* grown in either seawater conditions or freshwater nitrogen-depleted culture. The significant increase of this amino acid ($p<0.05$) could indicate that *N. oleoabundans* cell walls contain leucine-rich repeat proteins. These proteins are part of a large variety of organisms and are reported to be involved in many developmental processes and responses to biotic and abiotic stress (Diévart et al., 2011; Kinoshita et al., 2017; Liu et al., 2017). Due to the intrinsic limitation of the EZ:faast^{TM} method, we were unable to detect asparagine, glutamine and arginine in the *N. oleoabundans* cell wall. Furthermore, our results revealed a lack of cysteine and tryptophan in the *N. oleoabundans* cell wall that may well have been degraded during the acid hydrolysis process.

Our findings herein clearly confirm that the cell wall composition of *N. oleoabundans* varies depending on the cultivation medium. Remodelling of this dynamic structure is key for the plasticity of this species to survive in a wide range of growing conditions.

5. Conclusion

In this study we have highlighted the importance of the *N. oleoabundans* cell wall in response to high saline and/or nitrogen-deficient mediums. Cell wall remodelling under saline conditions comprises the possible accumulation of sulphated polysaccharides enriched in mannose, β-(1→4)-D-mannans, and glucose. The likely abundance of sulphated polysaccharides together with non-polar amino acids, especially leucine, could well enable the cell to resist the saline environment. Nitrogen depletion also has an important effect on the cell wall composition, being the primary effect of this stress a substantial reduction in the nitrogenous components of the cell wall. This is the first study of this kind on the cell wall biology of *N. oleoabundans* which has enabled us to understand the complexity of remodelling the cell wall in response to salt and/or nitrogen deficiency.

Acknowledgement

This work is performed within the TKI AlgaePARC Biorefinery program with financial support from the Netherlands' Ministry of Economic Affairs in the framework of the TKI BioBased Economy under contract nr. TKIBE01009.

Supplementary data

Supplementary file 1. Biological parameters from different points in time of the batch pipeline production. FW(N+): Freshwater nitrogen-replete, FW(N-): Freshwater nitrogen-deplete, SW(N+): Seawater nitrogen-replete, SW(N-): Seawater nitrogen-deplete.

Medium	Time of harvest (h)	Optical density			Dry matter ($g\ L^{-1}$)	Quantum yield	pH
		550	680	750			
FW(N+)	186.7	3.03	3.77	2.53	0.82	0.68	6.9
	354.5	6.501	8.437	5.346	1.68	0.72	7.0
	693	1.97	2.4	1.56	0.52	0.69	7.2
FW(N-)	130	2.73	3.15	2.26	0.73	0.66	8.3
	321	5.03	5.12	4.57	1.44	0.60	7.9
SW(N+)	286	5.54	7	4.51	1.41	0.71	8.4
	425.5	2.95	3.72	2.58	0.83	0.59	8.4
	785.5	4.21	5.31	3.62	1.15	0.68	8.2
SW(N-)	137	2.52	3.05	2.10	0.68	0.75	7.8
	281	4.13	4.85	3.42	1.09	0.73	7.9
	449	4.185	4.195	4.01	1	0.45	7.73

Supplementary file 2. Monosaccharides composition of *N. oleoabundans* cell wall polysaccharides. Values represent a relative amount of each sugar to the total monosaccharides and they calculated from two technical replicates of pooled biomass. FW(N+)= Freshwater nitrogen-replete, FW(N-)= Freshwater nitrogen-deplete, SW(N+)= Seawater nitrogen-replete, SW(N-)= Seawater nitrogen-deplete. Rha= Rhamnose, Ara= Arabinose, GlcN= Glucosamine, Gal= Galactose, Glc= Glucose, man= Mannose, Xyl= Xylose, GlcA= Glucuronic acid.

Medium	Rha	Ara	GluN	Gal	Glc	Man	Xyl	GlcA	Total
FW(N+)	33.52	8.05	9.19	21.44	4.78	6.91	2.95	13.15	100
FW(N-)	33.63	9.87	6.46	16.49	5.99	6.61	3.62	17.32	100
SW(N+)	24.34	3.10	4.75	18.44	18.80	14.21	2.97	13.38	100
SW(N-)	25.12	2.07	3.05	18.82	20.01	16.05	2.60	12.27	100

Supplementary file 3. Total protein content of *N. oleoabundans* cell walls under different growing conditions. Protein content was calculated by means of nitrogen percentage and Nitrogen to Protein (NTP) conversion factor. KA (N-factor of the maximum upper limit), KP (N-factor of the minimum lower limit) and K (mean N-factor).Values are the average from two technical replicates. FW(N+): Freshwater nitrogen-replete, FW(N-): Freshwater nitrogen-deplete, SW(N+): Seawater nitrogen-replete, SW(N-): Seawater nitrogen-deplete.

Medium	NTP value			N content	Protein content
	KA	KP	K	(%DW)	(%DW)
FW(N+)	6.5	2.6	4.5	10.2	45.9
FW(N-)	6.6	1.4	4	6.8	27.2
SW(N+)	6.7	1.7	4.2	10.2	42.8
SW(N-)	6.8	1.7	4.3	4.5	19.3

CHAPTER 4

Changes in morphologic characteristics of *Neochloris oleoabundans* cell wall during the cell cycle

To be submitted as:

Behzad Rashidi, Maria J. Barbosa, Luisa M. Trindade. Changes in morphologic characteristics of *Neochloris oleoabundans* cell wall during the cell cycle.

The microscopic green microalga, *Neochloris oleoabundans*, is surrounded by a morphological and sophisticated biochemical cell wall. As is the case with other unicellular algae, the dynamic structure of the *N. oleoabundans* cell wall regulates the cell morphogenesis throughout the cell cycle by allowing the cell to grow and divide. Despite that, detailed morphological remodelling of the *N. oleoabundans* cell wall during a complete cell cycle has continued to remain elusive. On account of this, we have constructed a library of electron microscopy images for *N. oleoabundans* cell wall ultrastructures throughout its cell cycle, from the early growth up to cell division. We have portrayed that cell division in *N. oleoabundans* is based on autosporulation, indicating that the daughter cell synthesis occurs inside the maternal cell. SEM images revealed that the *N. oleoabundans* cell surface possesses a wrinkled network-like structure ornamented with irregular-shaped granules. We observed a variation in the level of cell surface wrinkling throughout the cell cycle. TEM images have enabled us to propose a model for the daughter cell wall regeneration in *N. oleoabundans* which has three main highlighted features: I- at an early stage of the light period (growth phase), and prior to the appearance of the daughter cell wall, the whole cell wall (WCW) doubled in thickness, II- daughter cell wall formation commences during the early light period, after the cells have been exposed to at least three hours of light, III- thickening of the daughter cell wall occurs mainly during the remaining period of light. Essentially, the findings in this study contribute to understanding the biology and remodelling of the cell wall in *N. oleoabundans*, and can be a platform to study cell wall regeneration in other (closely related) microalgae species.

1. Introduction

Neochloris oleoabundans is a terrestrial microalga belonging to the Chlorophyta phylum, which is surrounded by a biochemical complex cell wall, composed of carbohydrates, proteins, lipids and inorganic substances (Rashidi & Trindade, 2018; S. Chantanachat & Bold, 1962). These components combined together form the ultrastructure of the cell wall which morphologically consists of two main layers, a thinner inner layer and a more electron-dense outer layer (Rashidi & Trindade, 2018). This dynamic ultrastructure regulates the cell morphogenesis during the cell cycle by enabling the cell to grow and reproduce.

Research which focuses on circadian rhythms of *N. oleoabundans* during the cell cycle has revealed that cell division in this green microalga takes place by multiple fission, in which 2 to 8 daughter cells are released from the maternal cell (de Winter et al., 2013). It has previously been demonstrated that most of the unicellular green microalgae, particularly those surrounded by a cell wall, belonging to Trebouxiophyceae or Chlorophyceae class divide through auto-sporulation (Yamamoto et al., 2005; Yamamoto et al., 2007). During auto-sporulation, daughter cells, including their cell walls develop inside the mother cell.

Formation of the daughter cell together with the development of the maternal cell requires biosynthesis and cell wall component modification (Takeda & Hirokawa, 1978; Takeda & Hirokawa, 1979). Biochemical changes in the components of the cell wall have an automatic effect on how it functions and its morphology. In microalgae belonging to the class of Trebouxiophyceae the formation of the daughter cell wall can be classified into two clusters in accordance with the relative timing of cell wall synthesis (Yamamoto et al., 2005). In the first group otherwise referred to as the early-group, the daughter cell wall synthesis initiates during the early cell-growth phase prior to protoplast division. Whereas in the second group known as the late-group, the daughter cell wall synthesis follows protoplast division. In order to illustrate this, three microalgae belonging to the *Chlorella* genus comprising *C. vulgaris*, *C. sorokiniana*, and *C. lobophora* reveal an early-group behaviour whereas *Parachlorella kessleri* (formerly known as *Chlorella kessleri)* belongs to the late-group (Yamamoto et al., 2005).

Subsequent to the maturation of the autospores and formation of the daughter cell wall, the outermost layer of the cell (mother cell wall) sheds and the daughter cells are released from the auto-sporangium (Yamamoto et al., 2004). It has previously been observed that extracellular proteolytic enzymes are responsible for the liberation of the daughter cell by targeting the auto-sporangium (Fukada et al., 2006; Kubo et al., 2009; Satoh & Takeda, 1989). After liberating the daughter cell,

remnants of the mother cell walls remain in the medium (Rashidi & Trindade, 2018; Somogyi et al., 2013).

Different studies have shown that some microalgae intrinsically form a synchronized culture within their natural environment or in a photo-bioreactor which has been adjusted to different periods of dark/light periods (Bišová & Zachleder, 2014; León-Saiki et al., 2018; Pokora et al., 2017; Tamiya et al., 1953). This characteristic is the key for evolving microalgae divided by multiple fission (Bišová & Zachleder, 2014). In these species cell growth takes place during light (day), while cell division occurs at night (the dark period). By this means they make the maximum use of daylight for photosynthesis and growth. Previous studies on *N. oleoabundans* proved that the daily light/dark cycles are required for synchronization. (de Winter et al., 2017b; de Winter et al., 2013) The authors have demonstrated that during 16 hours of light and 8 hours of dark periodic cycles, cell cultures converted into a synchronous state, in which phases of growth and division took place during periods of light and dark, respectively (Figure 1). Synchronous culture enables the study of intracellular biomass alterations in *N. oleoabundans* during the cell cycle development (De Winter et al., 2017a; de Winter et al., 2013).

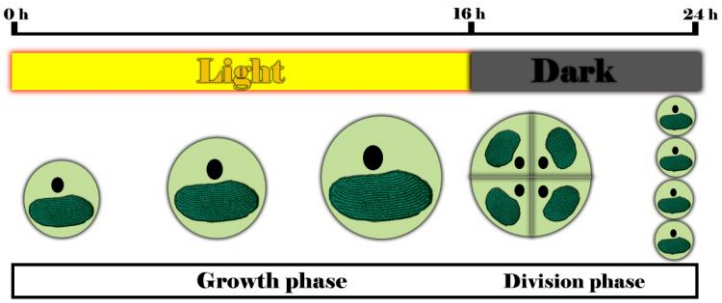

Figure 1. Schematic cell cycle of synchronized *N. oleoabundans* during 16 h light and 8 h dark cycle. Synchronized *N. oleoabundans* cells grow during the light and divide during the dark period. Division in *N. oleoabundans* occurs by multiple fission. This figure is adapted and modified from (de Winter et al., 2017b).

In contrast to intracellular biomass, only a few studies have been carried out to investigate the microalgae cell wall development in synchronous cultures. As a result, there is an urgent need to expand our knowledge in this context. This prospective study, therefore, was designed to investigate the morphological generation and development of the *N. oleoabundans* daughter cell wall in a synchronous culture, during a 24 hour cell cycle. High-pressure freezing and fast freeze substitution methods were used to preserve the morphology of the cell, and thus minimized the chance of cellular artifacts which often occur during the conventional preparation method (Bobik et al., 2014; Lonsdale et al., 1999;

Yamamoto et al., 2005). Results from this study have generated a fresh insight into the cell wall biosynthesis and development of *N. oleoabundans* during the cell cycle.

2. Materials and methods

2.1. Photo-bioreactor set-up to produce synchronous cultures

Synchronous cultures were produced as described in (De Winter et al., 2017a). In brief, *N. oleoabundans* was pre-cultured in a 250 ml Erlenmeyer flask containing 100 ml adjusted BBM medium at pH 7.5 (Klok et al., 2013). The culture was shaken continuously in an incubator at 120 RPM with a light intensity of 40 µmol m^{-2} s^{-1} (16 h light, 8 h dark) at a temperature of 25 °C. After reaching optimum density, the culture was used to inoculate a sterile 1.8 L Flat Panel Photo-bioreactor (PBR) (Labfors 5 Lux Flat Panel, Infors HT, Switzerland) containing a sterile medium (Klok et al., 2013). The light intensity at the front of the reactor was produced by the LED panel and set up initially at 50 µmol m^{-2} s^{-1}. In order to prevent environmental light contamination, a black cover was placed on the back of the reactor. Subsequent to inoculation, the system was operated in a batch mode and the ingoing light intensity was gradually increased in order to allow the microalgae to adapt to the new light intensity and prevent photo-inhibition. The reactor was switched from batch mode to turbidostat when the biomass concentration reached 0.5g L^{-1}. In the turbidostat, the incoming and outgoing light intensity was set at 500 µmol m^{-2} s^{-1} and 50 µmol m^{-2} s^{-1}, respectively. Throughout the growth and increasing the biomass concentration the outgoing light intensity gradually decreased. When the light intensity at the back of the reactor dropped to 50µmol m^{-2} s^{-1}due to cell growth, the culture was diluted by pumping in some fresh medium. The culture was only diluted during the light period. The experiment was conducted during 16 h of light and 8 h of dark photoperiod in which light was provided in a 'block' form. This indicates that the reactor was instantly exposed to maximum and minimum light intensity, 500 µmol m^{-2} s^{-1} and 0 µmol m^{-2} s^{-1}, at the beginning and end of the light period, respectively. For both batch and turbidostat modes the temperature and pH were set at 30˚C and 7.5±0.2, respectively and the culture was continuously sprayed with 1 L min^{-1} air enriched with 2% $_{(v/v)}$ CO_2. *N. oleoabundans* cells were synchronized when the culture reached a steady state, in which the daily dilution rate and biomass concentration remained constant. Cell growth was monitored on a daily basis by quantifying the optical density (OD_{680} and OD_{750} nm), dry weight, and the culture volume harvested daily (overflow) as outlined in (Kliphuis et al., 2010).

Once the cells had reached this phase, daily quantifications were made on 3 more consecutive days. If all parameters remained constant after three days, the culture was considered to be synchronized. The number of cells and their size were examined in order to further validate synchronization and monitor the cells

population during light and dark periods. For this purpose, samples of the light period (3, 6, 9. 12, 15 h after turning the light on) and samples of the dark period (1, 3, 5, 7 h after turning the light off) were collected from the PBR, diluted 200 times and then quantified using a Multisizer™ 3 Coulter Counter® (Beckman Coulter, Fullerton USA, 50 lm orifice).

2.2. Time-series imaging of synchronous culture

In order to visualize the remodelling of the cell wall during the cell cycle, a library of time-series imaging was constructed by means of electron and optical microscope images. To this end, synchronous samples were collected at during different phases of the cell cycle. The first sample was taken at the beginning of the light period (0 h) and the remaining samples from this period were taken every three hours (3, 6, 9, 12, 15 h). During the dark period, samples were taken 2 and 5 h after dark. In order to improve monitoring the morphology of cell wall development, an additional time point was set 7 h after the dark period began and visualized by means of a transmission electron microscope. Approximately 20 images were captured in each phase and further processed using ImageJ 1.51f software (National Institutes of Health, USA, free download available at http://rsbweb.nih.gov/ij/). In brief, each image was modified for background correction, smoothed and sharpened in accordance with the software settings. Subsequent to defining the scale of each image using a line selection tool (Analyze > Set Scale), the size of at least 4 different cells was measured (Analyse > Measure). The cell/cell wall diameter of each cell was measured at 4 different locations. Values mentioned in this publication are based on an average of 16 replicates.

Optical microscope. 1 mL synchronous culture was collected from the PBR and visualized using a light microscope (Leica DM 2500, Germany) and the corresponding software LAS V4.4.0. We used immersion oil which had been modified for microscopy use on a 100x objective lens (Immersion oil acc. to ISO 8036, Merck, Germany).

Transmission Electron Microscope (TEM). Preparation of the samples and their visualization was performed as previously outlined in (Rashidi & Trindade, 2018). In brief, *N. oleoabundans* cells were harvested, centrifuged (1000 g, 1 min) and re-suspended in 2% gelatine. Sufficient amount of samples were transferred into the sample holders which had previously been dampened with hexadecene and frozen instantaneously using a high-pressure freezing instrument (HPM-010 Blazer, ABRA Fluid AG, Switzerland). The frozen samples were then suspended in a substitution solution containing a mixture of acetone, osmium tetroxide and uranyl acetate. The substitution process was initiated at a temperature of -90°C in homemade apparatus and continued for about 5 h until a temperature of 0°C had been reached. The

substituted samples were rinsed 3 times with acetone and later were embedded in gradient concentrations of resin polymer (Lowicryl HM20) at 5°C for 3 days. The embedded cells were capsulated and polymerized for 3 days at a temperature of 50°C. Thereafter, the samples were trimmed and sectioned using a microtome (Leica UC7, Leica Inc.) with an extremely sharp diamond knife in order to produce 60 nm ultra-sections. Later on, the sections were then adhered to the grids and post-stained by placing the grids in uranyl acetate and a citrate buffer. Samples were visualized using a transmission electron microscope (JEOL JEM 1400 plus, JEOL, USA, Inc.).

Scanning Electron Microscope (SEM). Time-series SEM imaging was performed according to our previously described protocol (Rashidi & Trindade, 2018). In brief, samples collected at different phases of the cell cycle development were instantly mixed with a solution of 3% glutaraldehyde in a PBS buffer and incubated on a poly-L-lysine coverslip. Subsequent to 2 h incubation, the coverslips were rinsed 3 times in a PBS buffer and the samples were post-fixed using 1% O_SO_4 for 1 h. When fixation had been accomplished, the cells were then dehydrated using an ethanol gradient and later they were dried by the means of a critical point dryer (Leica EM CPD300). Lastly, slips were mounted onto the carbon pad and coated with 15 nm Tungsten using a sputter-coater. The cells were then visualized using a FEI Magellan 400 microscope at a voltage acceleration of 2 kV (Magellan 400, FEI, Eindhoven, The Netherlands).

3. Results

3.1. Synchronous cultures follow a cyclic growth and dividing pattern

During the steady phase and for 3 consecutive days, the daily overflow, optical density at 680 and 750nm and dry weight remained constant and was 3200 (g), 2.7 OD_{680}, 2.1 OD_{750} and 0.9 (g/L), respectively. Monitoring the cell diameter and number of *N. oleoabundans* cells during the steady phase confirmed a successful synchronization of the culture (Figure 2). Synchronous cultures developed a cyclic behaviour for both the number of cells and their diameter.

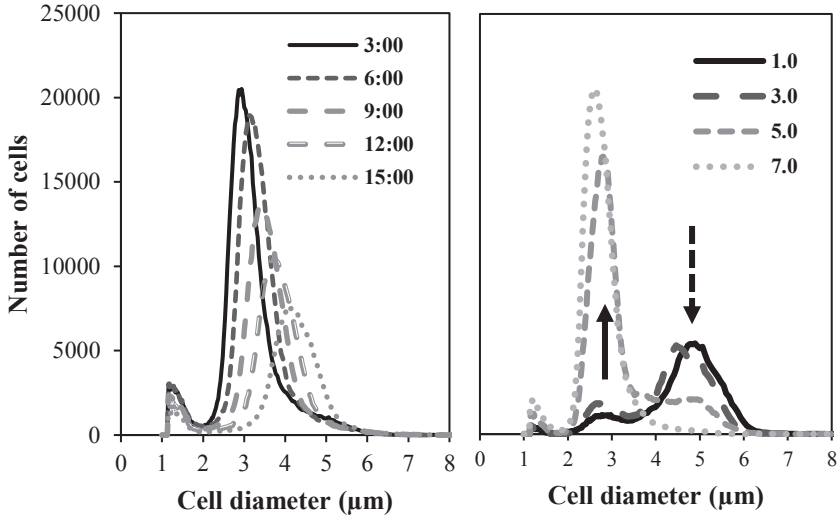

Figure 2. Cell number and diameter distribution in the samples taken during the light (left) and dark (right) periods. Synchronous cultures were produced using a photoperiod of 16 h light and 8 h dark. The sampling time-points are based on the hours after the imposition of light (left) and hours after the starting of the dark period (right). The dashed arrow shows the reduction in the population of mother cells and the unbroken arrow indicates the growing population of daughter cells.

As can be seen in Figure 2, the cell size and diameter during the light period depicted a normal distribution and bell curve, whereas during the dark period they displayed a bimodal distribution. The two peaks in the bimodal distribution of the dark period samples were related to both the mother and daughter cells. An average weight of a cell's diameter was determined at all points of time during both light and dark periods (Figure 3).

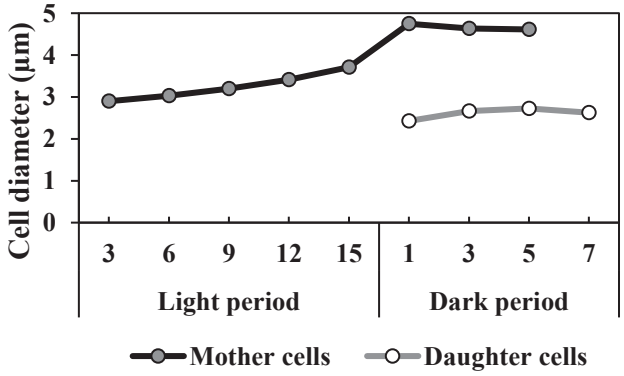

Figure 3. Weighted average of the cell diameter calculated in the samples collected during the light and dark periods. Synchronous cultures were produced using a photoperiod of 16 h light and 8 h dark. The sampling time-points are based on the hours after the beginning of light and dark period.

During the light period, *N. oleoabundans* cells grew steadily and expanded their size. At the end of the light period (15h after the light period began), we observed a rapid cell growth which continued until the dark period began. The cell diameter that increased during the light period was accompanied by a reduction in the number of cells. This reduction was due to the turbidostat control as the light absorbed in the culture was set at constant. As the dark phase began, the cells began to divide and produced the daughter cells (see the unbroken arrow in Figure 2). The weighted average of the newly released daughter cells was 2.4 μm. Whereas the calculated weighted average of the daughter cells displayed a slight expansion in the cell size during the dark period, the most obvious increase in cell size was observed during the light period (Figure 3). Throughout the dark period, the population of daughter cells increased and the highest density was recorded before starting the light period.

3.2. *N. oleoabundans* cells elongate during the light period

SEM and light microscopic images of cell growth during the light period are presented in Figure 4. At the beginning of the light period (0 h), the cells were roughly tri-oval in shape and their surface was wavy and wrinkled (Figure 4, 0a-0c and supplementary Figure 1, 0a). The longer and shorter axis of the cell were 2.5 and 2.3 μm, respectively. The hatched mother cell walls were observed in the medium using both optical and SEM imaging (Figure 4, 0a and 0b and supplementary Figure 1, 0b). Three hours after starting the light period, the cell walls had stretched slightly and the cells were oval in shape (Figure 4, 3a-3c and supplementary Figure 1, 3a-3b). The longer and shorter axes of the cells were 2.6 and 2.3 μm, respectively. The cell surface was still wavy, although smoother and more stretched than at the initial point in time of the set light period (Figure 4, 3c and supplementary Figure 1, 3b). At the following evaluation point in time (6 h after starting the light period), the cells were approximately round in shape and had a stretched surface (Figure 4, 6a-6c and supplementary Figure 1, 6a-6b). Cell diameter was approximately 2.8 μm. The mother cell walls were still observed in the culture (Figure 4, 6 b). Almost half way through the light period (9 h), the cells were round in shape and were 3 μm diameter. At this point in time , the cell surfaces were more stretched and smooth than at previous points during the light period (Figure 4, 9c and supplementary Figure 1, 9a and 9b). Twelve hours after starting the light period, the cells were more elongated (3.3 μm), and appeared spherical in shape (Figure 4, 12b and supplementary Figure 1, 12a and 12b). During the last evaluation point during the light period, the cells were undergoing a chloroplast division phase (Figure 4, 15a). At this point, the maternal cell walls were surrounded by an almost symmetrical scar which had presumably been caused by division site phase (Figure 4, 15b and 15c and supplementary Figure 1, 15a and 15b). The cell diameter at this stage was approximately 3.8 μm.

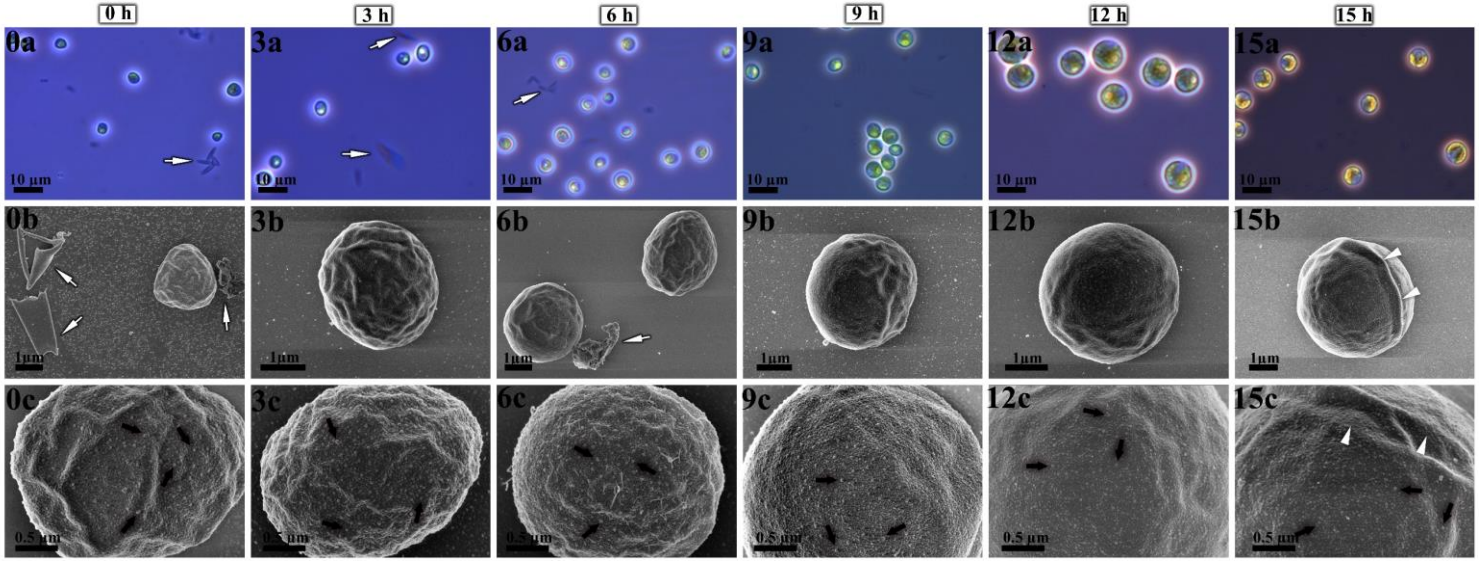

Figure 4. Optical and scanning electron microscopy images of synchronized *N. oleoabundans* cells during the light period. Throughout the light period, *N. oleoabundans* cells elongated and increased their size. 0 h, cells presented a tri-oval shape and had a wavy and wrinkled surface. 3 h, cell wall was slightly stretch and cells were oval in shape. 6 and 9 h, cells were round in shape and their surface were more stretch and less wrinkled than in previous time points.12 h, cells were spherical in shape and showed a smooth surface. 15 h, division of chloroplast started. In this time point, we have noticed an almost symmetrical scar (arrowheads) which possibly correspond to the division site. The remnants of mother cell walls were observed in the medium and are indicated with white arrows. Cells from all time points were ornamented with irregular granules on their surface (black arrows).

TEM images enabled the visualisation of nanoscale developments of the maternal and daughter cell walls, and they are depicted in Figure 5.

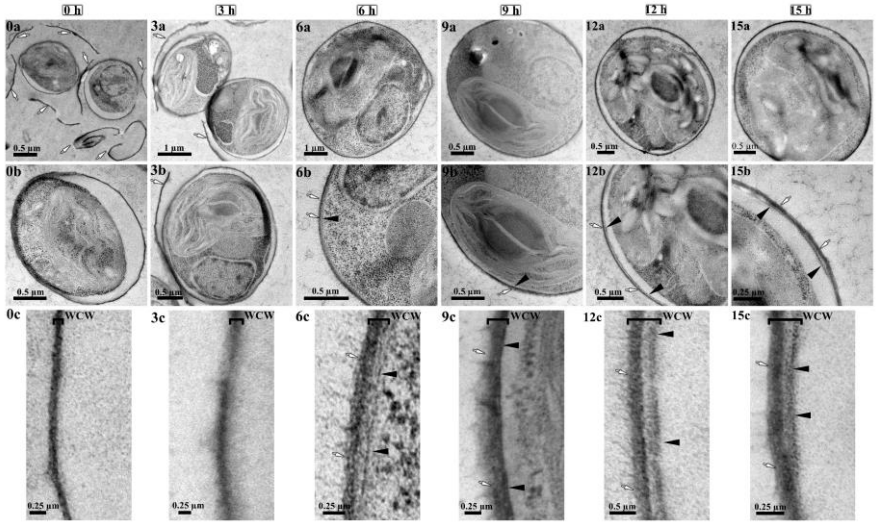

Figure 5. Transmission electron microscopy images of synchronized *N. oleoabundans* cells during the light period. Throughout the light period, *N. oleoabundans* cells grew and daughter cell wall developed inside of the mother cell. 0 and 3 h, cell wall appeared as a single electron-dense layer (whole cell wall). 6, 9, 12, 15 h, microscopically detectable daughter cell wall developed inside the mother cell. The mother and daughter cell wall are indicated with white arrow and black arrowhead, respectively. The remnants of the hatched mother cell walls were observed in the medium and are indicated with white arrows (0a, 3a and 3b).

Analysing the cell wall morphology revealed distinct differences between the samples taken during the first 3 hours of the light period in comparison to other points in time. During the first 3 hours of the light period, the cell walls appeared as a single electron-dense layer (Figure 5, 0c and 3c). Most of the hatched maternal cell walls were totally detached from the daughter cells, although in some cells fragments of the maternal cell wall still remained attached (Figure 5, 0a and 3b). The cell wall thickness at 0 and 3 h was 20 and 37 nm, respectively. , The daughter cell wall was detected microscopically 6 hours after the light period began (Figure 5 , 6c, 9c, 12c and 15c). With the exception of the 9 h samples, in which the cell wall appeared as a bilayer, the whole cell wall (WCW) at other points in time, 6, 12 and15 h, displayed a multilayer structure: a thick electron-dense outer-layer, a middle layer which has a lower electron density and a thin electron-dense inner-layer. The latter layer corresponds to the newly developed daughter cell wall. The thickness of the maternal cell wall (electron-dense outer-layer) was 33 nm 6 h after the light period began. We observed a gradual increase in its thickness during the light period, and by the end of the period (15 h) this layer was 40 nm thick. The daughter cell wall was 7 nm thick

when collected at either 6 and 9 h. At 12 h after the light period began, the daughter cell wall had expanded substantially and reached 15 nm. Subsequent to this point in time the thickness of the daughter cell wall did not increase any further.

3.3. *N. oleoabundans* cells reproduce during the period of darkness

N. oleoabundans cell walls were visualised during the period of darkness with SEM and light microscopic imaging and the results are depicted in Figure 6.

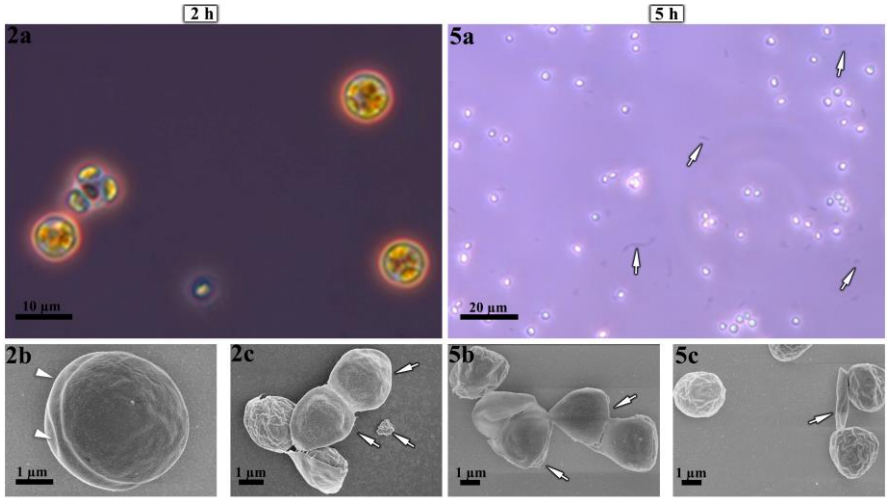

Figure 6. Optical and scanning electron microscopy images of synchronized *N. oleoabundans* cells during the dark period. Throughout the dark period, *N. oleoabundans* cells divided and produced daughter cells. 2 h, two different populations of the cell were observed: mother cells, which were the most abundant population and had an almost symmetrical scar (showed by arrowheads), and, daughter cells. 5 h, daughter cells were the most abundant cells in the culture. In this time point, it was possible to observe an enormous accumulation of mother cell wall remnants (white arrows).

During the initial phase of cell reproduction (2 h), we observed two different cell populations. The most abundant population corresponded to maternal cells which exhibited a symmetric scar. The daughter cell population was also visible although less abundant (Figure 6, 2a and 2b, and supplementary Figure 2, 2a and 2b). At this stage the size of the daughter cells and mother cells was 2.4 nm, average of the longest axis and the shortest axis, and 3.9 um, respectively. Five hours after the dark period began, the majority of the cells had divided completely, and the daughter cell had become the most abundant population in the culture (Figure 6 , 5a, 5b and 5c, and supplementary Figure 2, 5b). In both SEM and light microscopic images, we observed the accumulation of the hatched maternal cell walls during the dark period in the medium. At the end of this period, remnants of the maternal cell wall were everywhere in the culture, and this marked the end of the cell cycle (Figure 6 , 5a , 5b and 5c, and supplementary Figure 2, 5a).

Three samples from different points in time were examined using a transmission electron microscope in order to improve cell wall morphology monitoring and development throughout the reproduction phase (Figure 7).

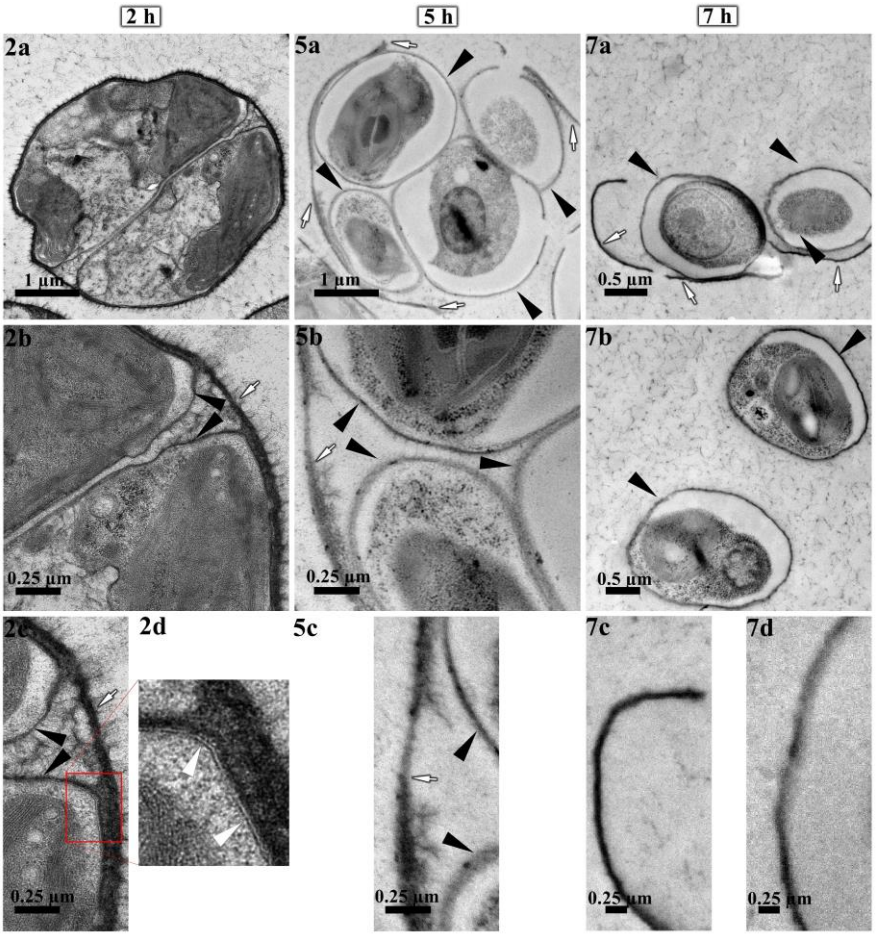

Figure 7. Transmission electron microscopy images of synchronized *N. oleoabundans* cells during the dark period. Throughout the dark period, *N. oleoabundans* cells divided and produced daughter cells. 2 h, first protoplast division occurred and two daughter cells with their own walls developed. The formation of the daughter cell walls occurred on the surface of the invaginating plasma membrane and thus decorated the triangular-like space between the mother and daughter cell wall. The upper daughter cell in 2a, has initiated the second the chloroplast division. 5 h, cells completed the second chloroplast and protoplast division. In this stage mother cell wall ruptured partially to release the daughter cells. 7 h, daughter cells released from the mother cells. The ruptured mother cell wall remained partially attached to some of the daughter cells. The black arrowheads and white arrows indicate the daughter and mother cell walls, respectively. The white arrowheads show the plasma membrane.

The first protoplast division occurred at the beginning of the dark period (Figure 7, 2a-2c). At this stage, the wall formation in two daughter cells was visible (Figure 7,

2b and 2c). The thickness of the daughter and maternal cell walls were 15 and 45 nm, respectively. Furthermore, we noticed at this stage, after finishing the first chloroplast and protoplast division, the cells began initiating the second chloroplast division. As can be observed in Figure 7, 2a, one of the daughter cells completed the second chloroplast division, while the other was still in process. 5 h after the dark period commenced, the cells completed the second chloroplast and protoplast division (Figure 7, 5a). At this stage the daughter cell wall was 19 nm thick. At this point we also observed a partial rupture in the mother cell wall which enabled it to liberate the daughter cells. The thickness of the mother cell wall was the same as at the previous point in time. In the last evaluated time point, most of the daughter cells were liberated from the maternal cells. The hatched maternal cell walls were still attached to some of the daughter cells albeit loosely (Figure 7, 7a). The thickness of the daughter cell wall at this point in time was about 20 nm.

4. Discussion

Despite its importance as a dynamic and rigid structure throughout the cell cycle, the ultrastructure of *N. oleoabundans* cell wall has been given very little attention in literature. The cell wall represents the skeleton of the cell throughout its life cycle. It is conceivable that the cell wall has to be morphologically and biochemically dynamic during cell growth and reproduction. It is a known fact that the circadian clock enabled the synchronization of *N. oleoabundans* (de Winter et al., 2013). On account of this knowledge, our investigation focused on characterizing the *N. oleoabundans* cell wall morphology and structure at different points in time throughout the cell cycle.

SEM images throughout the cell cycle indicated that the *N. oleoabundans* cell wall exhibits a wrinkled network-like structure, having an undulated surface ornamented with irregular granules on the surface. These features are in accordance with the previous observations of differing algae belonging to Chlorophyta phylum (Asselborn et al., 2015; Baudelet et al., 2017; Eliáš et al., 2010; Huss et al., 2002). It has been suggested that a network-like structure on the outer surface of the cell is due to cell wall thickening (Baudelet et al., 2017; Dempsey et al., 1980). Throughout the cell cycle, however, we have observed a variation in the level of the wrinkles on the cell's surface. At the onset of the light period we noticed that the cell surface was more wavy and wrinkled compared to other points in time throughout the light period (Figure 4). TEM visualization of the cell from the first point in time of the light period revealed that the intracellular components were situated far from the cell wall (Figure 5). Although, we observed that 3 h after the beginning of the light period, the cell wall had stretched slightly and the intracellular components had almost covered the entire cell; the size of the cell had only increased slightly. However, on the contrary, the cell wall (Whole cell wall) had thickened to approximately twice its size. This might

indicate that the cell wall deposition and perhaps its stiffness are the primary needs in the early stages of its development and must occur prior to the expansive growth.

Expansive growth of the algae cells is based on turgor pressure, which described as a force within the cell that pushes the plasma membrane toward the cell wall. Turgor pressure facilitates the irreversible (plastic) and reversible (elastic) wall deformation and consequently regulates the cell shape (Lalitha Sridhar et al., 2018; Ortega, 2016). The absence of strong expansive growth during 3 h after the light period began, might be attributable to turgor pressure which is probably about the same at these two points in time. A plausible explanation for the similarity of turgor pressure may relate to the osmotic pressure that is essential for absorbing water from the medium and subsequently generates turgor pressure.

Six hours after the light period began, we observed the morphological formation of the daughter cell wall inside the mother cell. This observation evidenced that division in *N. oleoabundans* is based on auto-sporulation. In accordance with the present results, previous studies have demonstrated that division in Trebouxiophyceae and Chlorophyceae is generally via auto-sporulation (Yamamoto et al., 2007; Yamamoto et al., 2003)

It has been recently demonstrated that the *N. oleoabundans* cell wall is biochemically and morphologically similar to *Chlorella spp* and *Parachlorella spp*. (Chlorellaceae, Tre-bouxiophyceae), and is therefore expected to follow a similar pattern of the daughter cell wall formation (Rashidi & Trindade, 2018). In line with the suggested models for Trebouxiophyceae, daughter the cell wall formation can be illustrated by two models depending on the timing of the daughter cell wall synthesis (Yamamoto et al., 2004; Yamamoto et al., 2005). We observed that *N. oleoabundans*, is comparable to *Chlorella vulgaris*, and belongs to the early-group, in which cell wall synthesis commences during the cell-growth phase. In the early-group model, even though the daughter cell wall deposition occurs at the outset of the growth phase, the cell wall formation rate is substantially higher at the end of the cell cycle when autospores mature and hatch at a later stage.

In contrast to the early-group model proposed for Trebouxiophyceae, in *N. oleoabundans* we have observed that approximately 75% thickness of the daughter cell wall was formed during the growth phase (light period). This observation has enabled us to point out that the pattern of the daughter cell wall formation in *N. oleoabundans*, a Chlorophyceae microalgae, is different from the algae belonging to Trebouxiophyceae. We, therefore, propose a new model for *N. oleoabundans* which has three main highlighted characteristics (Figure 8). I- at the early stage of the light period, and before the daughter cell walls appear, the whole cell wall (WCW) doubled its thickness, II- daughter cell wall formation commences during early light period,

when the cell has been exposed to at least to three hours of light, III- thickening of the daughter cell wall occurs mainly during the light period.

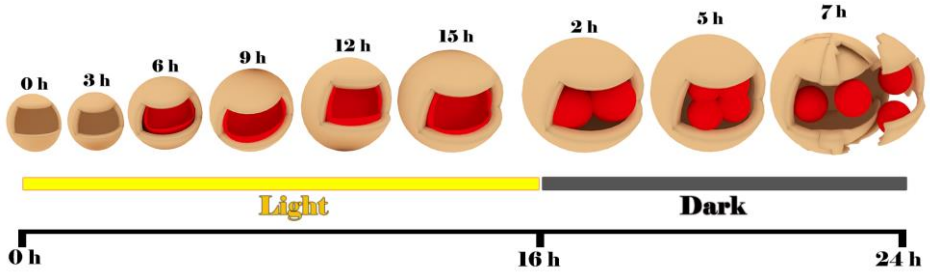

Figure 8. Schematic model for the daughter cell wall formation and development in *N. oleoabundans* (Chlorophyceae). At the beginning of the light period and before formation of the daughter cell wall, whole cell wall (light brown coloured) doubles its thickness. After 6 h of light, the daughter cell wall (red coloured) starts to develop inside of the mother cell. Daughter together with mother cell wall enlarge their thickness throughout the light period. At early of the dark period, first protoplast division occurs and two daughter cells with their own cell walls are developed. Throughout the dark period a second protoplast division occurs and four daughter cells are formed. In the last stage of the dark period, the mother cell wall ruptures and daughter cells are released.

During the light period, the maternal cell wall also thickened along the daughter cell wall deposition. At the end of the light period we observed a symmetrical scar on the surface of the cell, which presumably corresponds to the division site and formation of the cleavage furrow. This morphological trait in *N. oleoabundans*, which was also observed at the beginning of the dark period, can be used as a visible marker to identify the cells that have completed the last stage of the growth phase. At the beginning of the dark period, cells which had begun their chloroplast division continued to synthesize the daughter cell walls on the surface of the invaginating plasma membrane. Invagination of the daughter cell walls together with the plasma membrane decorated the triangular-like space between the mother and daughter cell walls at dividing plate (Figure 7). This feature has previously been reported in other microalgae dividing by auto-sporulation (Yamamoto et al., 2004; Yamamoto et al., 2005; Yamamoto et al., 2003). Furthermore, it has also been made known that the dividing plane of the daughter cell walls in *Nannochloris bacillaris* and *Nannochloris coccoides*, Trebouxiophyceae, comprises (1,3)-β -glucans at specific developmental stages (Yamamoto et al., 2003). During the dividing process, daughter cell walls thickened slightly and by the end of the process were 20 nm thick. We have not observed an increase in the thickness of the liberated daughter cell wall during the dark period.

Subsequent to completion of the protoplast division and cytokinesis, mother cell walls had been ruptured and the daughter cells liberated. It has also been observed that extracellular proteolytic enzyme, mainly subtilase-like serine protease, is

accountable for liberating the daughter cells in several microalgae (Fukada et al., 2006; Kubo et al., 2009; Matsuda et al., 1995; Satoh & Takeda, 1989; Schlösser, 1981). While probing the annotated transcriptome of *N. oleoabundans*, we found several transcripts describing subtilase-like serine enzymes (Rismani-Yazdi et al., 2012). In view of this evidence together with the fact that more than 30% of the *N. oleoabundans* cell wall is protein, it is tempting to hypothesise that subtilase-like serine enzymes are involved in liberating daughter cells by targeting the mother cell walls (Rashidi & Trindade, 2018).

Morphological changes in the cell wall, e.g. thickness, during the cell cycle, are regulated biochemically. Recently, it has been reported that *N. oleoabundans* cell walls belong to the class of glucosamine-rich rigid cell walls with high amounts of rhamnose, galactose and traces of glucose (Rashidi & Trindade, 2018). During the cell cycle, biochemical changes in the glucosamine-rich rigid fraction of the cell walls as well as the other fractions, namely hemicellulose, have been reported for *C. vulgaris* (Takeda & Hirokawa, 1978; Takeda & Hirokawa, 1979; Takeda & Hirokawa, 1982). They observed that during the cell-growth phase, the hemicellulose content of the cell wall increased in proportion to the cell surface enlargement, while the rigid-cell wall hardly changed at all. Nevertheless, the amount of the rigid-cell wall as assessed by its glucosamine content, increased considerably throughout the cell division phase. On account of this evidence that the cell wall of *N. oleoabundans* is morphologically and biochemically similar to that of Chlorella spp, it is quite possible that similar patterns of alteration occurred in the two aforementioned fractions of the cell wall during a complete cell cycle of *N. oleoabundans*. In order to validate these expectations, further research with more focus on cell wall biochemical alteration during the cell cycle is recommended.

5. Conclusion

Cell wall synthesis and development is arguably one of the key processes throughout the microalgae cell cycle. To guarantee a prosperous completion of the cell cycle, the molecular machineries of the cell necessitate that the cell wall is morphologically and biochemically modifiable. This is the first study to report on how the *N. oleoabundans* cell wall develops during a complete cell cycle. Electron microscopic images portrayed that cell division in *N. oleoabundans* is based on auto-sporulation, meaning that daughter cell/cell wall synthesis occurs inside the mother cell. Morphological observation of *N. oleoabundans* during the cell cycle enabled us to propose a model for cell wall regeneration. Accordingly, the thickening of whole cell wall (WCW) at a high rate during the early growth stage, formation of the daughter cell wall at an early stage during the growth phase and a higher deposition of daughter cell wall during the growth phase in comparison to the division phase, are

three main factors for the proposed model. Insights gained from this study form the basis for further studies which aim to explore the cell wall biology and remodelling in *N. oleoabundans*. Moreover, the proposed model in this study may be a possible framework for studying the cell wall regeneration in closely related microalgae species.

Acknowledgement

This work was performed within the TKI AlgaePARC Biorefinery program with financial support from the Netherlands' Ministry of Economic Affairs in the framework of the TKI BioBased Economy under contract nr. TKIBE01009. The authors thank to Marcel Giesbers and Jan van Lent from Wageningen Electron Microscopy Centre of Wageningen University for the support with electron microscopy imaging and fruitful discussions and valuable input during the experiments. The authors thank in particular Rick Wieggers for his contribution to produce the synchronous culture.

Supplementary data

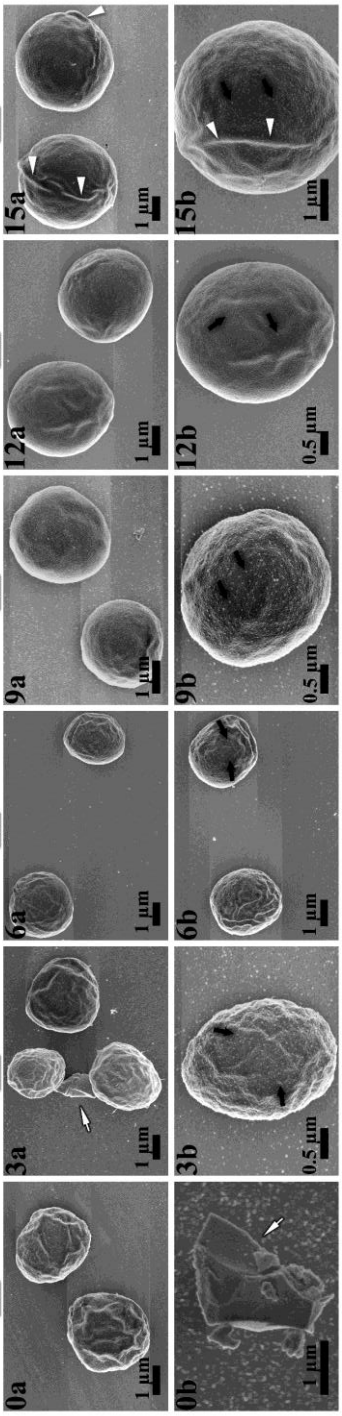

Supplementary Figure 1. Additional scanning electron microscopy images of synchronized *N. oleoabundans* cells during the light period. Throughout the light period, *N. oleoabundans* cells elongated and expanded their size. 0 h, cells had a wavy and wrinkled surface. 3 h, cell wall was slightly stretched and cells were oval in shape. 6 h and 9 h, cells surface were more stretched and less wrinkled than the previous points in the time. 12 h, cells were spherical in shape and had the smoothed surface. 15 h, cells were observed in a chloroplast division phase. In this time point, we observed an almost symmetrical scar on the cell surface (arrowheads), which possibly correspond to the division site. The remnants of mother cell walls still were observed at beginning of the light period and indicated with white arrows. Cells from all the time points were ornamented with irregular granules on their surface (black arrow).

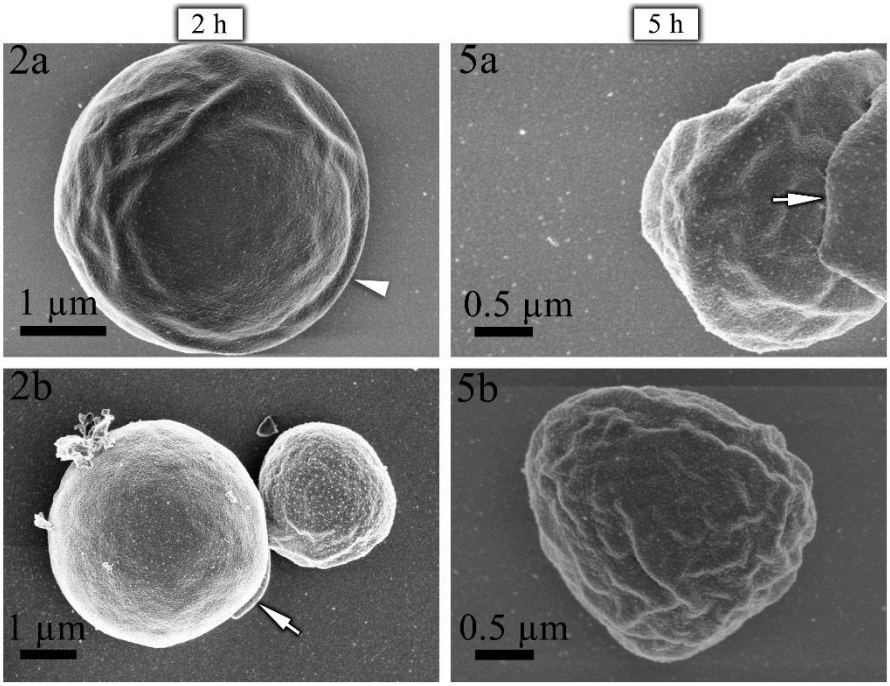

Supplementary Figure 2. Additional scanning electron microscopy images of synchronized *N. oleoabundans* cells during a dark period. Throughout the dark period, *N. oleoabundans* cell divided and produced daughter cells. 2 h, mother cell was observed with an almost symmetrical scar (arrowheads). Mother cell wall ruptured partially and liberated the daughter cells. 5 h, in this time point, most of the daughter cells were released from mother cell. The remnants of mother cell wall were still attached partially to some of the daughter cells (white arrows).

CHAPTER 5

Comparative transcriptomics reveals changes in cell wall carbohydrate composition of *Neochloris oleoabundans* throughout the cell cycle

To be submitted as:

Behzad Rashidi, Luisa M. Trindade. Comparative transcriptomics reveals changes in cell wall carbohydrate composition of *Neochloris oleoabundans* throughout the cell cycle.

Cell wall biosynthesis and modification are key processes for the growth and division of green microalgae such as *Neochloris oleoabundans*. In spite of its importance, the molecular mechanisms underlying cell wall development throughout the cell cycle remain unidentified. To gain insights in these processes, we analysed the biochemical composition of the cell wall and investigated the transcriptome at different stages of development through the cell cycle. The results of the biochemical analysis disclosed that the relative amount of glucosamine, galactose, glucose and rhamnose in the cell wall changed substantially during the cell cycle. Results of the transcriptomic analysis correlated well with biochemical compositional characterization as well as with the localization of the cell wall carbohydrates observed with a multi-mode confocal microscope. Transcriptomic results suggest that during the cell-growth phase, an increase in glucose was regulated by an upsurge in the bulk of uridine diphosphate glucose (UDP-D-Glu). Throughout the cell cycle, we observed an interplay between the production and degradation of a chitin/chitin-like structure, with the highest content during the division phase, which is likely related to the formation of the new daughter cell walls. Together, our results revealed fundamental molecular determinants leading to the biosynthesis and modification of cell wall carbohydrates in *N. oleoabundans*. These new findings shine a light on a highly coordinated cell wall carbohydrate machinery of *N. oleoabundans* cell wall and provide a basis for understanding the cell wall synthesis in green microalgae.

1. Introduction

A vast majority of green microalgae are outlined by a cell wall that plays essential roles in their life cycle. It shapes the cell, protects it from stresses and provides a dynamic structure to allow growth and morphological plasticity throughout the cell cycle.

On account of evolution and perhaps different adaptive purposes, cell walls across the plant kingdom, including green microalgae, are biochemically and structurally diverse (Baudelet et al., 2017; Harholt et al., 2012; Jensen et al., 2018). Apart from the diversity of the cell wall among different species, structural properties of the cell wall might also change in response to environmental factors or throughout the life cycle. In microalgae, depending on the species, a portion of the photosynthesis fixed-carbon is integrated into cell wall polysaccharides, and the specific molecules might be different in accordance to the developmental phases of the algal cell (Baudelet et al., 2017; Rashidi & Trindade, 2018; Takeda, 1993). Some of these changes have been observed on the cell wall of *Chlorella ellipsoidea* (Takeda & Hirokawa, 1978; Takeda & Hirokawa, 1979). The cell wall of this species is composed of two fractions, an alkali-soluble part known as hemicellulose, and an alkali-insoluble residue named as rigid-cell wall. Previous reports described an increase in hemicellulose content during the cell-growth phase, while the rigid-cell wall remained nearly unchanged. Nevertheless, the amount of the rigid-cell wall, measured as glucosamine content, increased considerably throughout the cell division phase.

Neochloris oleoabundans is a promising industrial microalga candidate with convergence interested in its utilization as an alternative green feedstock, though little information on the synthesis of its cell wall is available (Abu Hajar et al., 2017; Matich et al., 2018; Suarez Ruiz et al., 2018). We recently described the composition and morphology of unsynchronized *N. oleoabundans* cell wall cultured in a batch state (Rashidi & Trindade, 2018). When compared to other plants or green microalgae, *N. oleoabundans* possesses a unique cell wall composition and structure, in particular in its constituent polysaccharides. In contrast to most of the members of the plant kingdom, the cell wall of *N. oleoabundans* contains a rather scarce amount of glucose and thus, at the most, only trace of cellulose. *N. oleoabundans* cell wall belongs to the class of glucosamine-rich rigid cell walls with high amounts of rhamnose and galactose (Ghafari et al., 2018; Takeda, 1993).

Electron microscopic observations portrayed that propagation in *N. oleoabundans* is based on autosporulation, meaning that daughter cells syntheses occur inside of the mother cell (Figure 7, Chapter 4). Although the detailed morphological remodelling of cell wall throughout the cell cycle was disclosed, biochemical and transcriptional

regulation have remained concealed. Formation of the daughter cells together with the development of the mother cell require a sophisticated biosynthetic machinery to biosynthesize and modify the cell wall components during the cell cycle.

With the aims to identify the biochemical adjustments and the genetic determinants that underlie the cell wall development, we have sequenced and compared the transcriptome profiles of *N. oleoabundans* derived from four different time points during the cell cycle. In parallel, cell walls from the same time points were extracted and their composing carbohydrates were characterized. To our knowledge, this is the first transcriptomic study of *N. oleoabundans* cell walls. Our results provide new insights into the genes and putative enzymes that regulate the cell wall biosynthesis of this Chlorophyta microalga during the cell cycle. The knowledge reported herein is also a guideline for uncovering the cell wall biosynthesis and modification in other (closely related) green microalgae.

2. Materials and methods

2.1. Photobioreactor set-up to produce the synchronized cells

Synchronous cultures were produced using the procedure described in (De Winter et al., 2017a). In brief, *N. oleoabundans* was pre-cultured in 100 ml adjusted Bold's Basal medium (BBM) at pH 7.5(Klok et al., 2013). Subsequent to reaching an optimum density, the culture was used to inoculate a sterile 1.8 L flat panel Photobioreactor (PBR) (Labfors 5 Lux flat panel, Infors HT, Switzerland) which was filled with the same medium used during pre-culture. Following inoculation, the system was operated in batch mode and the ingoing light intensity gradually increased in order to allow the microalgae to adapt to the new light regime and thus preventing photo-inhibition. The reactor was switched from batch mode to turbidostat when the biomass concentration reached to almost 0.5 g L^{-1}. In the turbidostat, the ingoing and outgoing light intensities were set up to 500 µmol m^{-2} s^{-1} and 50 µmol m^{-2} s^{-1} , respectively. The experiment was conducted with a 16 h day (light) and 8 h night (dark) photoperiod. The temperature and pH were set up to 30˚C and 7.5±0.2, respectively and the culture was continuously sparged with 1000 mL min^{-1} air enriched with 2% $_{(v/v)}$ of CO_2. *N. oleoabundans* cells were in the synchronized state when culture reached the steady state in which the daily dilution rate and biomass concentration were constant. Cell growth was monitored daily by measuring the optical density (OD_{680} and OD_{750} nm), dry weight, and amount of daily overflow as described by Kliphuis et al. (2010). To further validate the synchronization and monitor the cells population during light and dark periods, cell number and cell size were measured using a Multisizer™ 3 Coulter Counter® (Beckman Coulter, Fullerton USA, 50 lm orifice). The experiment conducted with two Photobioreactors which were cultivated simultaneously and used as biological replicates. Cells from four different stages of the cell cycle were harvested as follows: I- sample at the beginning

of the light (further termed as sunrise), II- sample 8 hours after the beginning of the light period (further termed as midday), III- sample 16 hours after the beginning of the light period (further termed as sunset) and sample 4 hours after the beginning of the dark period (further termed as midnight), and the transcriptome profiles together with their cell wall carbohydrate composition were compared (Figure 1).

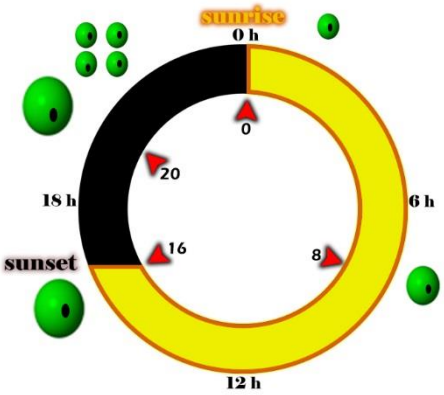

Figure 1. The schematic figure represents the cell cycle in *N. oleoabundans*. The red arrowheads indicate the sampling points for the cell wall biochemical analysis and RNA sequencing. The figure is adapted from (de Winter et al., 2013)

1.1. Cell wall carbohydrate composition throughout the cell cycle

Cell wall extraction of *N. oleoabundans* was performed according to the protocol described in (Rashidi & Trindade, 2018). In this protocol, 1 g ground biomass was incubated in a chloroform: methanol solvent and a cocktail of alpha-amylase (50 µL/25 mL, ANKOM, FFA) in order to remove the intracellular lipids and starch, respectively. In the next step, Neutral Detergent Fibre (NDF) buffer [104 mM sodium dodecyl sulphate, 50 mM ethylenediaminetetraacetic disodium salt (dihydrate), 17.8 mM sodium borate, 32 mM sodium phosphate dibasic (anhydrous), 79 mM sodium sulphite and 10 g/L triethylene glycol] was used to extract the cell wall from oil-free de-starched biomass. Lastly, the pellets were dried in an oven and further used for follow-up experiments, named as NDF-cell walls.

To begin the process of carbohydrates characterization, twenty mg of dried NDF-cell walls were hydrolysed using H_2SO_4 hydrolysis method (Rashidi & Trindade, 2018). Next, hydrolysates were cooled down, neutralized and after filtration using a 0.45 µm filter, the sugars content was characterized by means of High Performance Anion Exchange Chromatography (HPAEC, Dionex ICS5000+DC, CarboPac PA1, (2 x 250

mm) connected to Pulsed Amperometric Detector (PAD) as previously described (Rashidi & Trindade, 2018). Cell wall hydrolysing and carbohydrate characterization were performed with minimum of two technical replicates for each of the time points.

1.2. Isolation of total RNA and DNase digestion

Similar time-points as used for cell wall carbohydrates characterization, were used to extract the RNA (Figure 1). Microalgae samples were collected from PBR, transferred into RNA-free falcon tubes, stored in ice and immediately centrifuged at 4°C for 5 min (4200 *g*). Instantly, the supernatants were discarded, pellets were frozen in liquid nitrogen and stored at -80°C freezer until further processing. Total RNA was extracted and purified using the RNeasy Lipid Tissue Mini Kit (Cat. No. 74804, Qiagen, USA) independently for each of the biological replicates. All the steps for RNA isolation and further digestion and removal of the contaminating DNA were performed as described in the manufacturer's protocol.

1.3. Preparation of RNA-seq library and BGISEQ-500 sequencing

RNA-seq library preparation and sequencing on BGISEQ-500 platform sequencing technology was performed at Beijing Genomics Institute (BGI-Shenzhen, Shenzhen, China). In brief, the mRNA enrichments were carried out by means of oligo (dT)-attached magnetic beads. The quality of the RNA was then assessed using a 2,100 Bioanalyzer (Agilent Technologies) and only high-quality samples were used in the subsequent steps to construct the sequencing library. Subsequent to mRNA enrichment, a fragmentation reagent was used to hydrolyse mRNA molecules into smaller strands. Next, random hexamer (N6)-primed reverse transcription was used to make a double-strand cDNA (dscDNA). The synthesized cDNA was then subjected to the end-repairing and later was 3′adenylated. In the next step, adaptors were ligated to the 3′ end of adenylated cDNA fragments and following the purification of the ligation products, several rounds of PCR amplification was used to enrich the cDNA templates. In the last step, double strand PCR products were heated and after denaturation, the single strand DNAs were circularized using splint oligo sequence. The single strand circular DNAs (ssCir DNA) were constructed and used as the final library for sequencing following the standard BGISEQ-500 sequencing platform.

1.4. De novo assembly and annotation

Sequencing data generated from the BGISEQ-500 sequencing platform, referred to as raw data, went through a quality control check. In brief, low-quality reads, reads that contained more than 20% bases with lower quality than 10, reads with the adaptors, and reads in which unknown bases (N) were more than 5% were removed

using an internal software developed at BGI. Subsequent to quality filtering, the clean reads were stored in FASTQ format. High quality reads were de novo assembled using Trinity software v2.0.6 without a reference genome with the following parameters: -min_contig_length 150 –CPU 8 -min_kmer_cov 3 -min_glue 3 -bfly_opts '-V 5 -edge-thr=0.1 -stderr' (Grabherr et al., 2011). The transcripts assembled with Trinity were further clustered using TGICL clustering software v2.0.6 with the following parameters: -l 40 -c 10 -v 25 -O '-repeat_stringency 0.95 -minmatch 35 -minscore 35' (Pertea et al., 2003). The final unigenes generated with TGICL were distributed into two groups: cluster unigenes (prefix of CL) which composed several unigenes with shared similarity of more than 70%, and singleton unigene.

Functional annotation of the entire assembled sequences was carried out by aligning the sequence to seven different public databases. BLAST v2.2.23 with default parameter was used to blast the sequences to the NCBI nucleotide sequence (NT) database, NCBI non-redundant protein sequence (NR), Eukaryotic Orthologous Groups (KOG) database, Kyoto Encyclopedia of Genes and Genomes (KEGG) database and SwissProt (=Uniprot). Based on the results obtained at NR database, Blast2GO v2.5.0 program was used to perform Gene Ontology (GO) annotation of the sequences (Conesa et al., 2005). Lastly, InterProScan5 v5.11-51.0 software was used to search the proteins function (Quevillon et al., 2005). Transdecoder v3.0.1 with default parameters was used to identify the coding sequences (CDs) (https://github.com/TransDecoder/TransDecoder/releases). Thus the longest Open Reading Frame (ORF) was extracted and then the Pfam protein homologous sequences were searched against SwissProt and Hmmscan to predict the coding regions.

1.5. Analysis of expression level and differentially expressed unigenes

Clean reads from each sample were mapped to the reference using Bowtie2 v2.2.5 with the following parameters: -q -phred64 = -sensitive -dpad 0 -gbar 99999999 -mp 1,1 -np 1 -score-min L,0,-0.1 -I 1 -X 1000 -no-mixed -no-discordant -p 1 -k 200 (Langmead & Salzberg, 2012). The expression levels were then calculated using RSEM v1.2.12 with default parameters and their abundances were reported as Fragments Per Kilobase of transcript per Million mapped reads (FPKM). Pairwise comparisons of expression levels among the samples were conducted using NOIseq and PossionDis algorithms (Audic & Claverie, 1997; Tarazona et al., 2011). The parameters for identifying the significant DEGs using NOIseq were a fold change ≥ 2.00 and a probability ≥ 0.8 and using PossionDis were a fold change ≥ 2.00 and a False Discovery Rate (FDR) ≤ 0.001. Pairwise comparisons were conducted for all the time points, nevertheless, we have only discussed the comparison between

sunrise and midday, sunrise and sunset, and sunrise and midnight, the most relevant time points.

1.6. Functional analysis of differentially expressed genes (DEGs)

Relevant DEGs were further analysed for GO classification and distributed into three groups including molecular function, cellular component and biological process. The GO functional enrichment was performed using the R function Phyper and the terms with an FDR lower than 0.01 were presumed significant. Moreover, based on the KEGG annotation we classified the DEGs according to the official classification. The functional enrichment of identified pathways was performed using Phyper with the same criteria used for GO functional enrichment.

1.7. Localization of cell wall polysaccharides using a multi-mode confocal microscope

Based on the results from biochemical analyses and transcriptomic study, intracellular localizations of specific cell wall carbohydrates were visualized by a confocal microscopy. Two fluorescent dyes were utilized with this purpose: Wheat Germ Agglutinin (WGA) labelled with CF® 488A (Biotium Inc., CA, USA) which binds to sialic acid and N-acetylglucosamine, and pontamine fast scarlet (also known as S4B and Direct Red 23) which can stain cellulose-based polysaccharides (Sigma-Aldrich, Sant Louis, Missouri, MO, USA). Aliquots of frozen samples (stored at -80°C) from the exact time points used for the transcriptomic experiments were thawed gradually in PBS buffer at 0°C. Next, a sufficient amount of the sample was transferred to a 12 mm Ø poly-L-lysine coverslip and incubated at 30°C. Subsequent to 1 h incubation, the coverslips were rinsed 3 times in PBS buffer and later the samples were fixed in 4 % formaldehyde solution in PBS buffer. After a 30 min fixation at room temperature, samples were 3 times rinsed with PBS buffer and then stained for 30 min at 40°C. With the intention to enhance dye penetration efficiency, Dimethyl sulfoxide (DMSO) (20 % $_{v/v}$) was added as a carrier into the stain solutions. The final concentrations of the stains were 0.01 % and 0.1 % for WGA and S4B, respectively. Subsequent to the staining, samples were rinsed (3 times) with PBS buffer and mounted cell-side down on top of the microscope slides bearing a droplet of Fluoromount™ aqueous mounting medium (Sigma-Aldrich, Sant Louis, Missouri, MO, USA). The coverslips were sealed to the microscope slide by adding a sufficient amount of nail polish to the edges. Control samples, without dye, were prepared based on the same procedure as stated above and used to validate the staining procedure. Finally, preparations were visualized using a Leica SP8X-SMD fluorescence multi-mode confocal microscope equipped with a 63×1.20 NA water immersion objective with a coverslip thickness correction collar (Leica Microsystems). The white light laser was tuned to 488 nm to excite all fluorophores;

the emission ranges were 500-540 nm for WGA, 560-620 nm for S4B and 710-740 nm for chlorophyll autofluorescence. For all measurements, a size-adjustable pinhole was set to 102 and 88 µm for WGA and S4B, respectively. The captured images were further processed using ImageJ 1.51f software (National Institutes of Health, USA, free download available at http://rsbweb.nih.gov/ij/). The default function of the software was used to smooth and sharpen the images.

2. Results

2.1. High accumulation of glucose and glucosamine in the cell wall of *N. oleoabundans* during the growth and division phases, respectively

Cell wall carbohydrates were quantified at four different time points of the cell cycle and the results are presented in Figure 2, A.

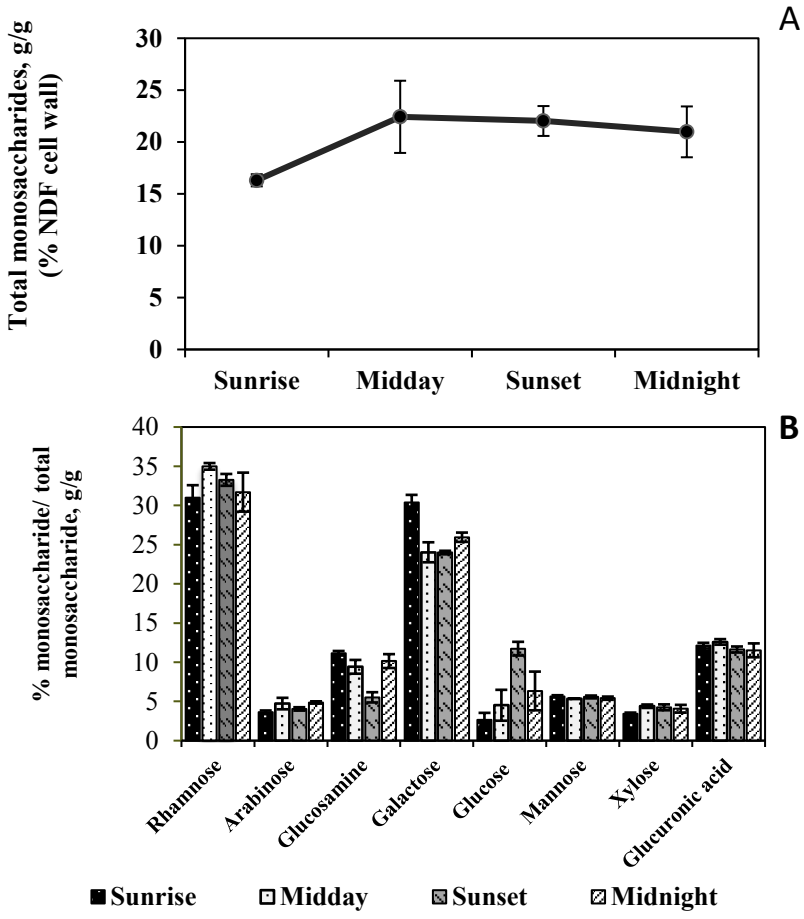

Figure 2. A, Percentage of the total carbohydrates in the cell wall of *N. oleoabundans* during the cell cycle. B, Monosaccharides composition of *N. oleoabundans* cell wall polysaccharides during the cell

cycle. Bar chart represents a relative amount of each sugar to the total polysaccharides. Values in both panels are the average of four replicates (two biological replicates, each measured in two technical replicates). Error bars represent the standard deviation (SD).

Compositional analyses revealed that the total amount of the carbohydrates in the cell walls were different throughout the cell cycle. In particular, the walls of the cells at 0 h (sunrise) were significantly different compared to the cell walls at other time points during the cell cycle. *N. oleoabundans* cells at 0 h (sunrise) contained less carbohydrates in contrast to the other time points. Monosaccharides content of *N. oleoabundans* cell wall during the cell cycle consisted of rhamnose, arabinose, glucosamine, galactose, glucose, mannose, xylose and glucuronic acid (Figure 2, B). Throughout the cell cycle, considerable fluctuation in the relative amount of some sugars was observed. Among all the sugars evaluated, however, glucose, galactose, glucosamine and rhamnose showed the largest changes in their relative content. Whereas glucose was accounted for the lowest portion of the total monosaccharides in the daughter cell wall, at sunrise (2.6%), along the day its content increased progressively and it became the third most abundant monosaccharide of *N. oleoabundans* cell walls at the end of the light period (11.7%). Rhamnose content of the cell wall increased throughout the light period and walls of both cells from midday and sunset accumulated higher amounts of rhamnose than the wall of cell at sunrise. Unlike glucose and rhamnose, during the day galactose and glucosamine content of the cell wall decreased. Galactose content of the cell walls from samples at midday and sunset was about the same, though it was significantly lower than in the cell wall at sunrise. Glucosamine cell wall content displayed a downward trend during the day, with the lowest concertation measured at sunset. Interestingly, during the division process in the night, we observed that the cell walls were enriched in glucosamine and galactose contrasting to the last sample of the day.

Alterations in the relative content of N-acetylglucosamine and cellulose/cellulose-like polysaccharides were monitored by means of confocal microscopy. Figure 3 represented the binding affinity of WGA to the cell wall N-acetylglucosamine throughout the cell cycle. It pointed out that all over the light period cell wall N-acetylglucosamine-like constituents decreased, whereas not long after starting the cell division, cell walls increased the content of this component.

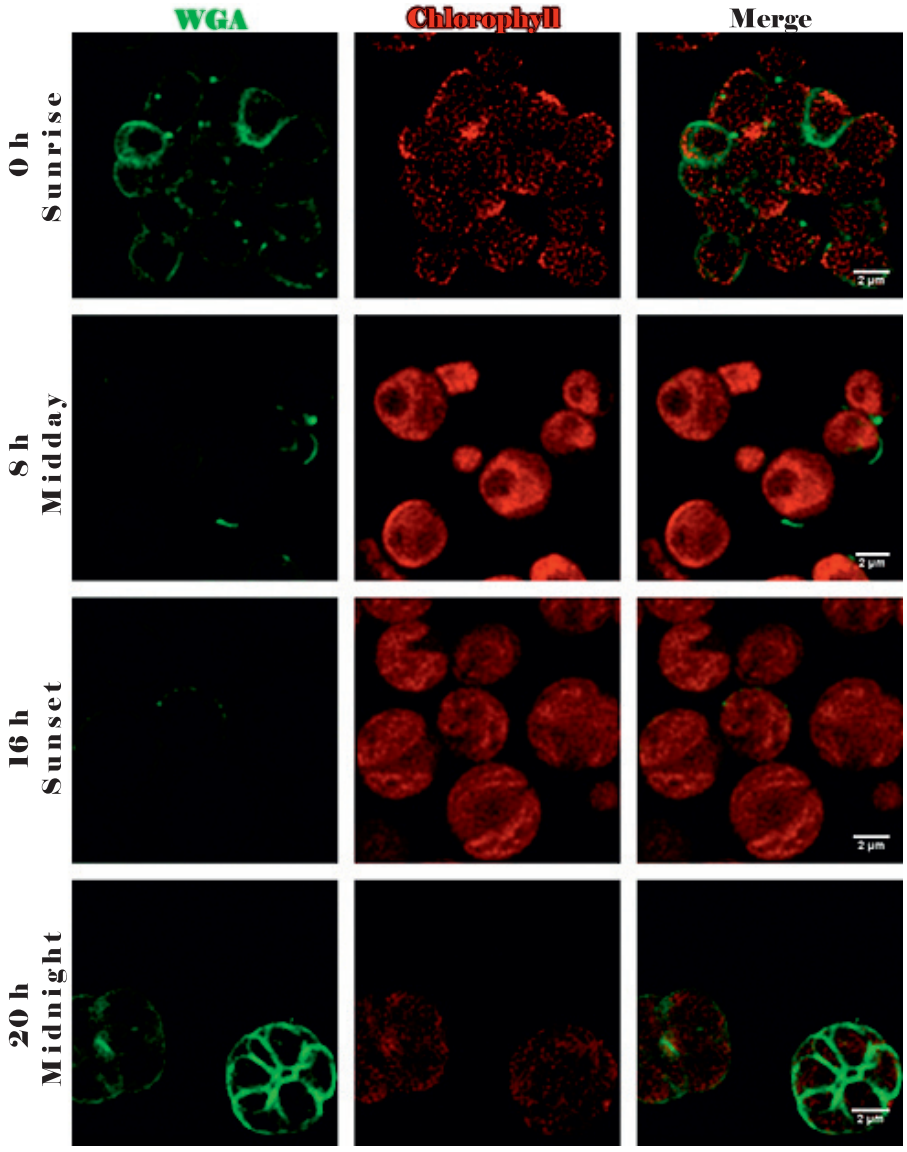

Figure 3. Visualization of *N. oleoabundans* cell wall stained with Wheat Germ Agglutinin (WGA) labelled with CF® 488A (WGA). Fluorescence of the WGA in the presence of N-acetylglucosamine can be seen in the first column with green colour. The second and third columns indicate the chlorophyll and merged channels, respectively.

Cellulose-based polysaccharides staining of the cell wall with S4B displayed a different pattern throughout the cell cycle. As it shows in Figure 4, through the light period, from sunrise to sunset, *N. oleoabundans* cell walls showed an incremental increase in cellulose/cellulose-like polysaccharides.

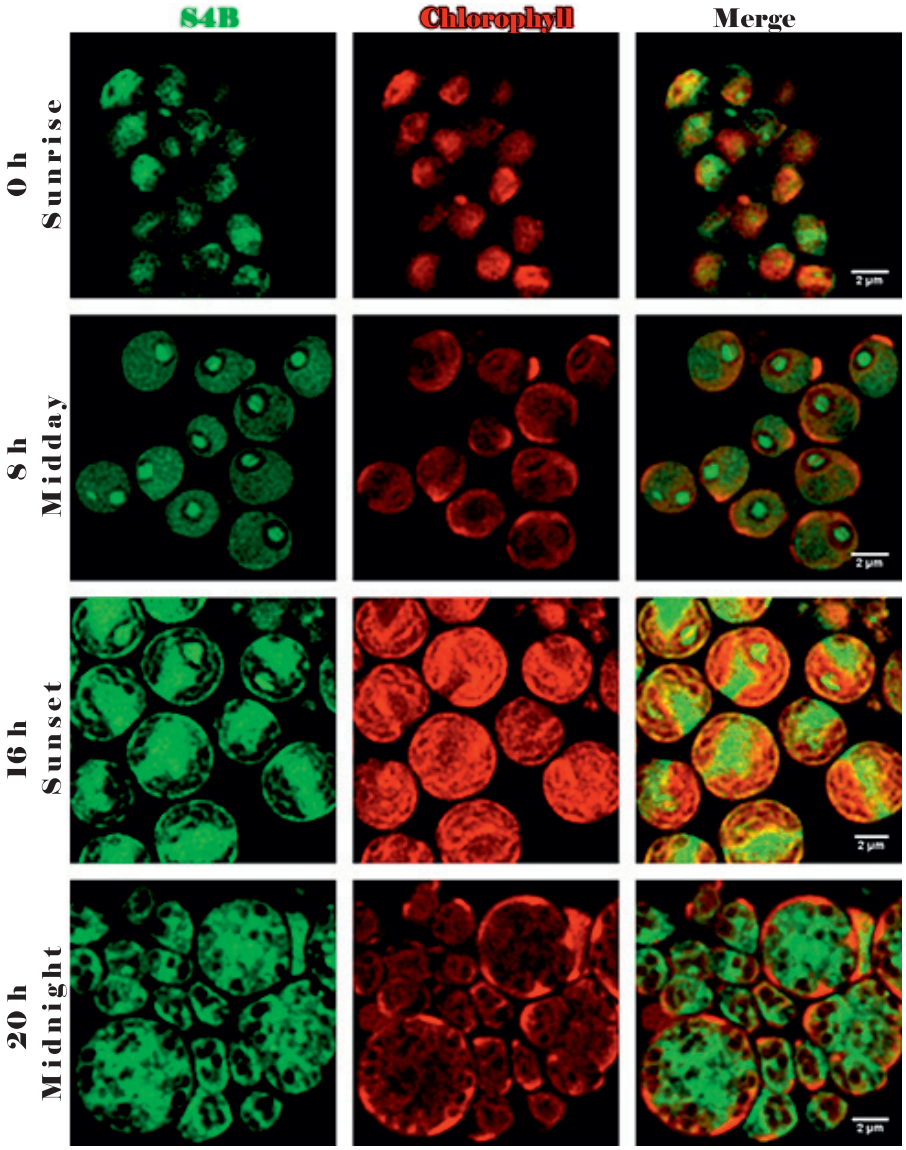

Figure 4. Imagining of *N. oleoabundans* cell wall stained with pontamine fast scarlet (also known as S4B and Direct Red 23). First column displays fluorescence of the S4B in the presence cellulose (cellulose-like) polysaccharides. The second and third columns indicate the chlorophyll and merged channels, respectively.

Midnight cell walls were also showed a binding affinity to the S4B fluorescent dye, whereas their emitted intensities indicating the cellulose/cellulose-like content of the cell wall, were somewhat weaker than sunset sample.

2.2. High throughput sequencing, de novo transcriptome assembly and functional annotation

For each sample, more than 74 megabytes (MB) raw data was generated and, after filtering, over 72 (MB) of clean reads was obtained (Additional file 1). Overall, we assembled 76595 All-Unigenes (longest transcripts achieved by overlying the unigenes of the samples from different time points) with lengths ranging from 300 (nt) to ≥ 3000. The mean length and N50 of the All-Unigenes were 2517 and 3772 (nt), respectively. Altogether, 80.3% of the total unigenes were annotated using the seven functional databases and amongst all, NR showed the highest percentage of significant annotation (77.7%) (Additional file 2). Based on the results of NR database functional annotation, we calculated the top-hit species distribution of *N. oleoabundans* to the close species (Figure 5).

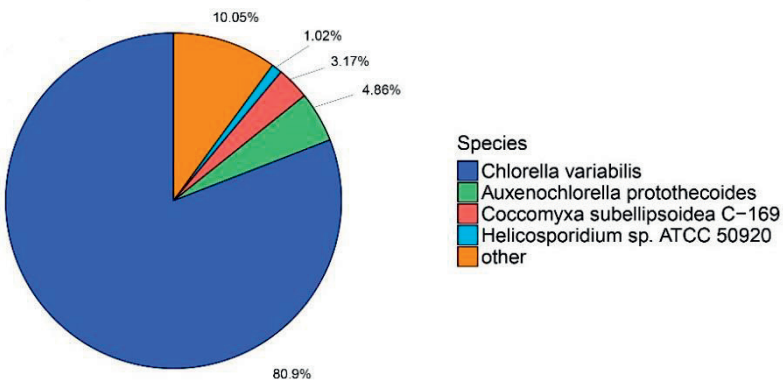

Figure 5. Distribution of top-hit species according to NR database functional annotation.

The majority of the unigenes were annotated to the *Chlorella variabilis* (80.9%) followed by *Auxenochlorella protothecoides* (4.86%), Coccomyxa subellipsoidea *C*-169 (3.17%) and *Helicosporidium sp.* ATCC 50920 (1.02%).

2.3. Cell wall-related pathway analysis of differentially expressed unigenes

In order to identify the main biological pathways involved in cell wall biosynthesis and development of *N. oleoabundans* we characterize the differential expressed genes (DEG) for three pairwise comparisons presented in this study: sunrise-VS-midday, sunrise-VS-sunset and sunrise-VS-midnight. Significant differentially expressed genes (DEGs) were identified based on a defined threshold of a probability equal or higher than 0.8 and a fold change equal or higher than 2.

Altogether, the DEGs were mapped to 131 pathways in sunrise-VS-midday, 130 pathways in midday-VS-sunset, and 133 pathways in sunrise-VS-midnight.

Changes in the monosaccharides content of the cell wall, specifically, rhamnose, glucosamine, galactose, and glucose, coincided with deviations of several genes involved in the pathways of amino sugar and nucleotide sugar metabolism, galactose metabolism and cellulose and callose biosynthesis. We observed a strong up-regulation in the expression of genes involved in the conversion of galactose into UDP-D-Glu and other intermediate sugars. The reconstructed pathway based on the identified putative enzymes is illustrated in Figure 6. Overall, transcripts coding for the enzymes involved in degradation of the D-Gal showed a strong up-regulation in their expression as compared to the sunrise sample. In contrast, the over-expression of transcripts coding for the enzyme in charge of the conversion of galactan to D-Gal was only observed during the division phase (midnight). This reaction was catalysed with beta-galactosidase (EC: 3.2.1.23) and targeted the terminal non-reducing D-Gal residues in galactan.

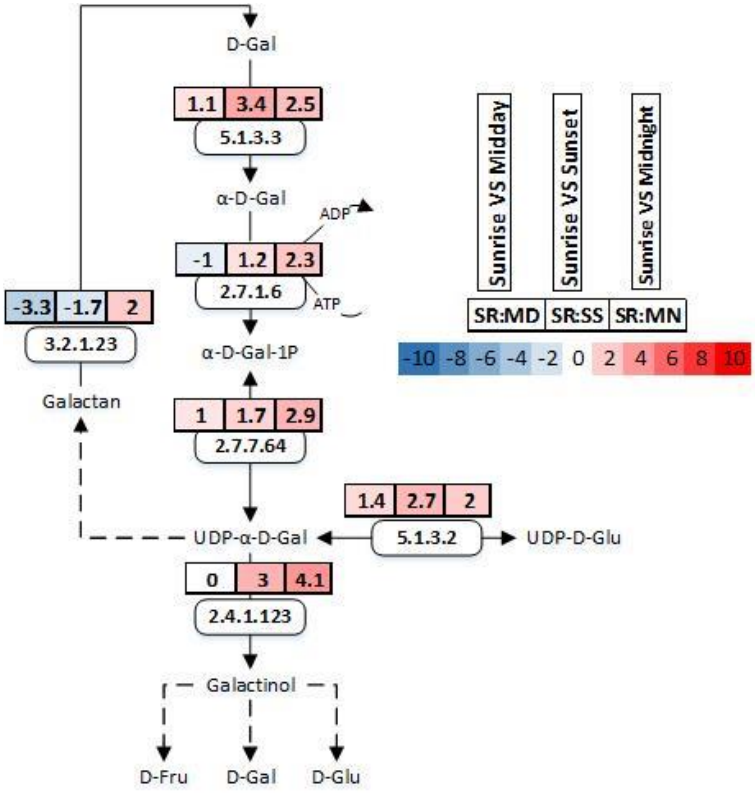

Figure 6. Reconstructed galactose metabolism pathway in *N. oleoabundans*. Key enzymes are indicated with EC number. The single expression levels that are shown in each pairwise comparison were the added up value from the corresponding transcripts.

To reconstruct the pathways involving glucose and rhamnose metabolism, we have specifically focused on the transcripts coding for the enzymes related to UDP-D-Glu (Figure 7). The nucleotide sugar, UDP-D-Glu, is an active form of glucose involved in several reactions such as the biosynthesis of cellulose, callose and hemicellulose. We observed that all the enzymes related to the accumulation of UDP-D-Glu were subjected to the transcriptional regulation throughout the cell cycle.

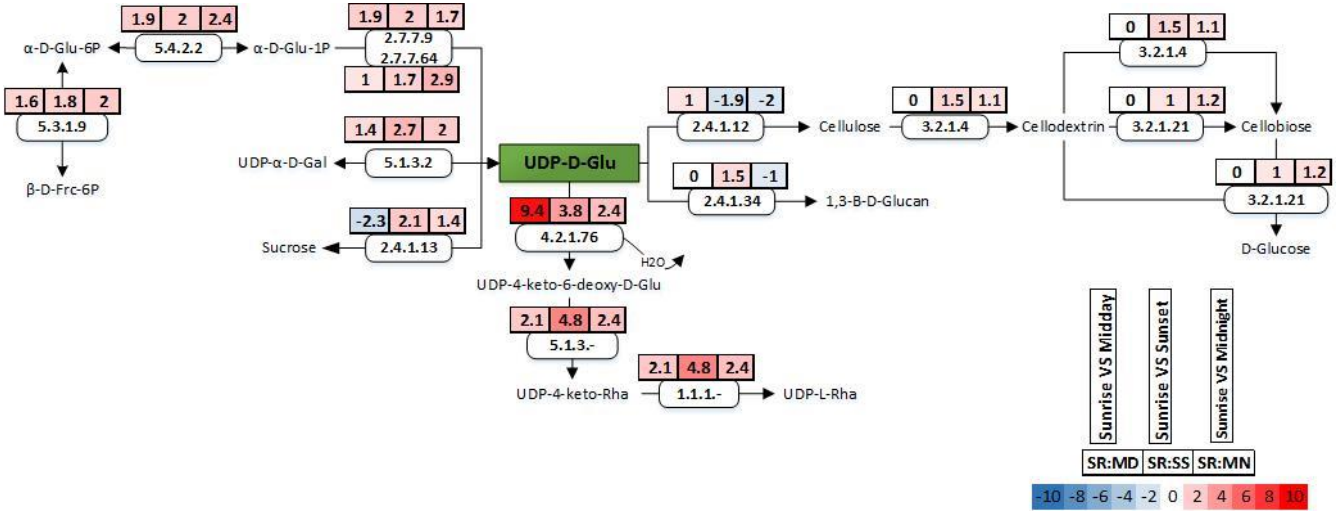

Figure 7. Reconstructed pathway of glucose-based polysaccharides and rhamnose metabolisms in *N. oleoabundans*. Key enzymes are indicated with EC number. The single expression levels that are shown in each pairwise comparison were the added up value from the corresponding transcripts.

The synthesis of the cellulose, catalysed by cellulose synthase (EC: 2.4.1.12), was transcriptionally induced at midday, whereas transcripts annotated to the 1,3-beta-glucan synthase to further form the callose were merely up-regulated at sunset. Besides the biosynthesis of cellulose, we identified a pronounced induction of transcripts coding for enzymatic hydrolysing of cellulose, cellodextrin and cellobiose. The identified transcripts annotated to the putative glycosylases, cellulase (EC: 3.2.1.4) and cellobiase (EC: 3.2.1.21), were increased in their abundance during sunset and midnight. Additionally, we observed a strong transcriptional induction of putative enzymes UDP-glucose 4,6-dehydratase EC: 4.2.1.76 and 3,5-epimerase/4-reductase EC:5.1.3.- 1.1.1.-, which sequentially converts the UDP-D-Glu to UDP-L-rhamnose (UDP-L-Rha). These marked up-regulations were spotted all over the cell cycle.

Strong changes were observed in the expression of genes involved in the metabolism of amino sugars. The reconstructed pathway built upon the identified putative enzymes is displayed in Figure 8. Interestingly, we noticed that all the putative enzymes in hexosamine biosynthesis pathway, catalysing the consecutive reactions of D-Frc-6P to chitin, were upregulated at the end of the light period and reached to a maximum during the division phase at midnight. Furthermore, we observed that the expression of putative glycosylases targeting chitin was altered (Figure 8). Chitinase (EC: 3.2.1.14) was up-regulated during the division phase at midnight. Along with chitinase, we observed downregulation of beta-N-acetylhexosaminidase (EC: 3.2.1.52) throughout the cell cycle, Noteworthy, glucosamine-6-phosphate deaminase (EC: 3.5.99.6), responsible for removal of an amine group from GlcN-6P and synthesis of D-Fru-6P, substantially decreased in abundance throughout the cell cycle.

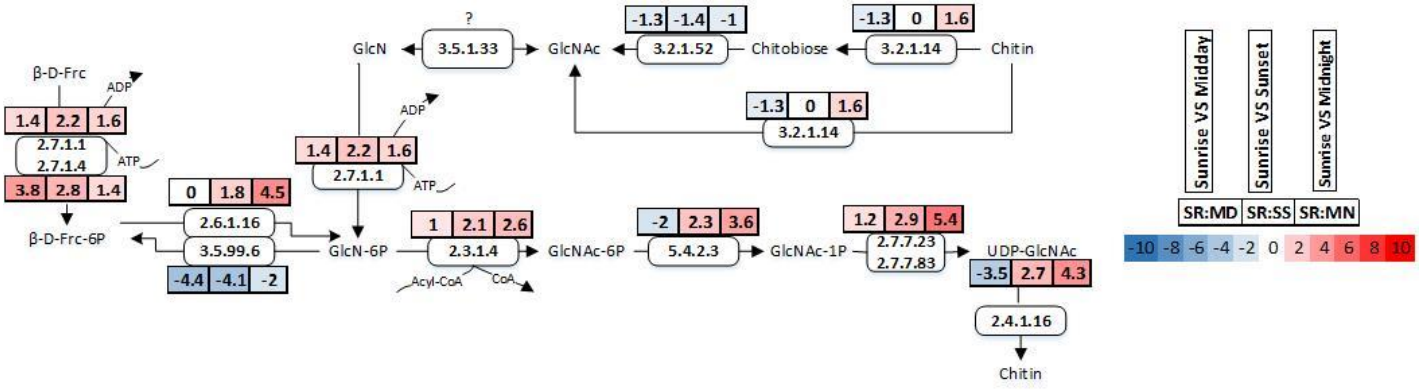

Figure 8. Reconstructed pathway of amino sugar and nucleotide sugar metabolisms in *N. oleoabundans*. Key enzymes are indicated with EC number. The single expression levels that are shown in each pairwise comparison were the added up value from the corresponding transcripts.

3. Discussion

Recently, we have shown that during the propagation in *N. oleoabundans*, daughter cell walls are formed inside of the mother cell (Chapter 4 of this thesis). Thus, complex and highly coordinated processes are needed to regulate the synthesis and modification of both, daughter and mother cell walls. In this study, we have addressed the intriguing research question on how cell wall is chemically built and transcriptionally regulated throughout the cell cycle.

Galactose, glucose, rhamnose and glucosamine are the main four *N. oleoabundans* cell wall carbohydrates subjected to modifications throughout the cell cycle. Glucosamine content increased significantly during the cell division phase at midnight. A similar pattern was previously reported for other Chlorophyta microalgae. (Takeda & Hirokawa, 1978; Takeda & Hirokawa, 1979; Yamamoto et al., 2005). The cyclic variation in glucosamine content of the cell wall was well correlated with transcriptomic data (Figure 8). Overall, we noticed a strong transcriptional induction of the putative enzymes toward chitin synthesis (EC: 2.6.1.16, EC: 2.3.1.4, EC: 5.4.2.3, EC: 2.7.7.23 2.7.7.83 and EC: 2.4.1.16). Although at the end of the light period the transcript levels of these putative enzymes were moderately upregulated, during the division phase they were considerably more abundant. The existence of chitin or chitin-like structures in the algae cell walls is infrequent, though it was reported that some Chlorellaceae algae cell walls are enriched in N-acetylaminoglucan (chitin) (Baudelet et al., 2017). A great example of this family are *Chlorella* species, which are recognized for this characteristic (Kapaun & Reisser, 1995). Despite finding that *N. oleoabundans* cell wall accumulates chitin/chitin-like structure during the division phase, questions still remain on the exact biological function of these components. It was previously hypothesized that the progressive increase in glucosamine content of the cell wall during the division phase is related to the formation of new daughter cell walls, though the clear cause-effect relation remains unclear (Takeda & Hirokawa, 1978). Our transcriptomic data suggest that the cell wall development and morphogenesis in *N. oleoabundans* is not only controlled by chitin synthase enzymes but also by chitinase, involved in the degradation of chitin. Upon the hydrolysis of chitin to the constituent monomer, GlcNAc, further deacetylation and deamination might occur to re-produce D-Frc-6P. Although the putative deacetylase (EC: 3.5.1.33) was absent from our annotation, we measured a strong up-regulation of deaminase (EC: 3.5.99.6) in the sunrise sample. The consequent accumulation of D-Frc-6P during the light period might be one of the reasons for the accumulation of glucose-based polysaccharide in the cell wall. It has been reported that the highly active deacetylation and deamination of chitin might result in cellulose-like polysaccharides, the structural homologue of chitin (Beier & Bertilsson, 2013).

An interplay between the production and degradation of chitin has been described in several models for fungal and yeast cell walls, though it has never been suggested for green microalgae (Bartnicki-Garcia, 1973; Selvaggini et al., 2004). The “unitary model” is one of the proposed models in which the wall growth is based on the balance between the biosynthetic and hydrolytic processes. In this model, hydrolytic enzymes such as chitinase partially hydrolyse the existing cell wall polymers. This sufficient cell wall lysis creates the starting points to deposit the new building blocks and further allows the turgor-driven expansion of the cell surface.

The hydrogen bonds between the hydroxyl group of glucose-based polymers (such as cellulose and callose) are milder than the bonds between the acetyl-amine group in chitin. In view of that, we suggest that the (partial) conversion of chitin-like structure to glucose-based component can be an exceptional strategy in *N. oleoabundans* cell wall, which facilitates the expansion of the cell surface during the growth phase.

Although *N. oleoabundans*, like other plant cell walls, accumulates glucose-based polysaccharide, its content in non-synchronous culture was reported to be negligible (Rashidi & Trindade, 2018). In this research, however, we observed that the amount of glucose measured throughout the cell cycle varied largely, ranging from 2.6% to 11.7% NDF-cell wall. Changes in glucose content of the *N. oleoabundans* cell walls were in accordance with the alterations observed at the transcriptional level, and together provided a clearer picture of the process. Altogether, we can conclude that the molecular determinants leading to the synthesis of glucose-like polysaccharides in *N. oleoabundans*c cell wall are manifold. We proposed three main functional routes that might play a role in the regulation of the bulk of UDP-D-Glu, as a dominant glucose donor for synthesizing cellulose and callose: I, the degradation of chitin to D-Frc-6P and further conversion to D-Glucose 1-phosphate (D-Glu-1P) and UDP-D-Glu; II, the conversion of galactose into UDP-D-Glu; III, the conversion of sucrose into UDP-D-Glu. On the basis of the proposed pathways, we observed an increase in the flux of UDP-D-Glu at the middle and end of the light period, which led to the accumulation of cellulose and callose, respectively.

Previously, it was reported that throughout the cell cycle, *Chlorella vulgaris* cell wall constituents exhibited differences in affinity to the fluorescent dye Fluostain I (Calcofluor White M2R), which targets the cellulose-like structure (Yamamoto et al., 2004). They observed a moderate increase in the fluorescence intensity, representing the content of cellulose-like components during the growth stage.

Accumulation of callose (1,3-β-D-glucans) as another glucose-based polysaccharide has also been reported in the cell wall of some green algae (Herburger & Holzinger, 2015; Yamamoto et al., 2005; Yamamoto et al., 2003). Immunoelectron microscopic

observations in earlier research investigating *Parachlorella kessleri* cell wall synthesis revealed the accumulation of 1,3-β-D-glucans in an internal space of the cell wall during the last phase of daughter wall development (Yamamoto et al., 2005).

Callose synthesis is catalysed by a complex of membrane-associated enzymes comprising callose synthase (EC: 2.4.1.13), sucrose synthase (EC: 2.4.1.13) and UDP-glucuronosyl transferase (Nedukha, 2015). Remarkably, during the light period, we noticed concurrent changes in transcripts abundance of putative sucrose and callose synthases. It is known that plant membrane-associated sucrose synthase channels the UDP-Glu derived from sucrose to synthesize callose (Amor et al., 1995). Considering that, it is tempting to speculate that in *N. oleoabundans* the required donor nucleotide sugar to synthesize callose is derived from sucrose. The specific biological function of callose accumulated at the end of the growth phase in *N. oleoabundans* cell wall is yet unknown. However, callose accumulation in multicellular green algae is known to be a regulatory factor for the developing septae during cytokinesis (Herburger & Holzinger, 2015; Scherp et al., 2001).

Besides glucose-based polysaccharides, we observed changes in the rhamnose and galactose contents of the cell wall during the cell-growth phase. Takeda and Hirokawa (1978) reported changes in the hemicellulose content of *Chlorella ellipsoidea* during the cell cycle. In line with this observation, we noticed a strong transcriptional induction of putative enzymes coding for UDP-L-Rha, which potentially plays a role in the rhamnose content of the cell wall. Decreases in galactose content of the cell wall during the growth phase might achieve by up-regulation of transcripts encoding for the enzymes involved in galactose degradation.

4. Conclusion

The results from this study showed that the *N. oleoabundans* cell wall is highly dynamic. Glucosamine, glucose, galactose and rhamnose were the main carbohydrates in which their contents undergo controlled variations. Increase in the bulk of UDP-D-Glu throughout the growth phase was possibly related to the degradation of chitin and the conversion of galactose and sucrose. During the division phase, we have observed an increase in chitin/chitin-like structure, which plausibly relates to the formation of the new daughter cell wall. Our findings shed new light on cell wall carbohydrate machinery of early-evolved unicellular microalgae, which can guide to understand the underlying genetics of other (closely related) microalgae. Furthermore, putative enzymes and metabolic routes identified in this study can supply exquisite prospect for further functional characterization and genetic improvement.

Acknowledgement

This work is performed within the TKI AlgaePARC Biorefinery program with financial support from the Netherlands' Ministry of Economic Affairs in the framework of the TKI BioBased Economy under contract nr. TKIBE01009. The authors thank Marcel Giesbers and Jan van Lent from Wageningen Electron Microscopy Centre of Wageningen University for the support with electron microscopy imaging and fruitful discussions and valuable input during the experiments. The authors thank in particular Rick Wieggers for his contribution to produce the synchronous culture. Last but not least, authors would like to express their appreciation to Arjen Bader for his contribution in confocal microscopy experiment.

List of abbreviations

BBM: bold's basal medium
DEGs: differentially expressed genes
D-Frc: beta-D-fructose
D-Frc-6P: beta-D-fructose 6-phosphate
D-Galactose: D-Gal
D-Glu-1P: D-glucose 1-phosphate
DMSO: dimethyl sulfoxide
FDR: false discovery rate
FPKM: fragments per kilobase of transcript per million mapped reads.
GlcN: glucosamine
GlcN-6p: D-glucosamine 6-phosphate
GlcNAc: N-acetyl glucosamine
GlcNAc-1P: N-acetyl-alpha-D-glucosamine 1-phosphate
GlcNAc-6P: N-acetyl-D-glucosamine 6-phosphate
GO: gene ontology
KEGG: kyoto encyclopedia of genes and genomes
KOGs: EuKaryotic orthologous groups
NDF: neutral detergent fibre
NR: NCBI non-redundant protein sequence
NT: NCBI nucleotide sequence database
ORF: open reading frame
PBR: photobioreactor
PCA: principal component analysis
UDP-D-Glu: UDP-glucose/ uridine diphosphate glucose
UDP-GlcNAc: UDP-N-acetyl-alpha-D-glucosamine
UDP-L-Rha: UDP-L-rhamnose
UDP-α-D-Gal: UDP-alpha-D-galactose
WGA: wheat germ agglutinin
α -D-Gal-1P: alpha-D-Galactose 1-phosphate
α-D-Gal: alpha-D-galactose

Sample	Total Raw Reads(Mb)	Total Clean Reads(Mb)	Total Clean Bases(Gb)	Clean Reads Q20(%)	Clean Reads Q30(%)	Clean Reads Ratio(%)
Midday-I	74.63	72.66	7.27	96.43	88.39	97.35
Midday-II	74.64	72.28	7.23	96.82	89.47	96.84
Midnight-I	74.65	72.82	7.28	96.75	89.28	97.55
Midnight-II	74.65	72.49	7.25	96.13	87.56	97.11
Sunrise-I	74.65	72.6	7.26	96.42	88.46	97.25
Sunrise-II	74.64	72.49	7.25	96.53	88.72	97.12
Sunset-I	74.64	72.94	7.29	96.83	89.44	97.72
Sunset-II	74.64	72.87	7.29	96.81	89.34	97.62

Additional file 1. RNA-seq raw data and filtering statistics for each of the biological replicates.

Additional file 2. Summary of *N. oleoabundans* functional annotation against seven functional databases.

Database	Number of unigene	Percentage
Total	76,595	100%
Nr	59,489	77.67%
Nt	32,068	41.87%
Swissprot	33,135	43.26%
KEGG	43,633	56.97%
KOG	40,343	52.67%
Interpro	42,167	55.05%
GO	48,066	62.75%
Intersection	15,948	20.82%
Overall	61,506	80.30%

CHAPTER 6

General discussion

1. Introduction

Over the past years there has been a growing interest from both industry and academia in the utilization of microalgae biomass to produce commodities in different bio-based sectors, namely for fuel, food and feed (Dixon & Wilken, 2018; Khan et al., 2018). This is mostly a consequence of an increasing world population, exhaustion of fossil fuel, alarming levels of the atmospheric carbon dioxide and social and political consciousness. The intracellular valuable components of microalgae are confined within the cell wall, which is a tenacious layer located outside of the cell membrane. The existence of such a persistent layer is a barrier that needs to be removed before the intracellular content can be reached.

One of the main obstacles towards the exploitation of microalgae entire biomass resides in the lack of biological knowledge to deconstruct the cell wall effectively while keeping the functionality of the internal components. Generating knowledge on the biochemical and structural configurations of the cell wall is a precondition to formulate a mild disruption method. The aim of this research was to gain new insights into the *Neochloris oleoabundans* cell wall building blocks. A range of biochemical, microscopy and molecular experiments were performed in order to uncover the *N. oleoabundans* cell wall composition, morphology and development throughout the cell cycle. In this chapter, the insights uncovered in the previous chapters of this thesis are discussed and put into a meaningful context.

2. Polysaccharide-deprived cell wall of *N. oleoabundans*

N. oleoabundans, as an early-evolved green microalga, is one of the 6000 species of Chlorophyta phylum that is deprived of polysaccharides in the cell wall. We have observed that more than 75% of the. *N. oleoabundans* cell wall is composed of non-polysaccharide-based polymers (**Chapter 2**). Encompassing a highly sophisticated sturdy cell wall that provides support and acts as a defensive barrier is indeed one of the key explanations for the successful colonization of land plants in terrestrial ecosystems. It is postulated that having a polysaccharide-based cell wall was an imperative element that enabled the Charophyta green algae, the ancestor of land plants, to make a successful transition to land (Harholt et al., 2016). In the same order, the lack of this polysaccharide-based cell wall structure in most of the Chlorophyta algae might be a possible reason for their unsuccessful development on the land. It must be pointed out that some Chlorophyta algae made as well a transition to land, though they failed to evolve a complex body plant. *N. oleoabundans* is an example of this group and originally belongs to the terrestrial ecosystem, the sand dunes in Saudi Arabia. We hypothesized that a rather scarce polysaccharide content in *N. oleoabundans* cell wall is one of the reasons for the unsuccessful transition of this microalga to land.

3. Shortage of glucose-based polymers in *N. oleoabundans* cell wall

Carbohydrate characterization revealed a very low amount of glucose (<1%), implying lack or a rather scarce amount of cellulosic polymer in the *N. oleoabundans* cell wall (**Chapter 2**). Cellulose biosynthesis originated in the most ancient extant group of living organisms, cyanobacteria (Roberts et al., 2002; Sørensen et al., 2010). However, its specific development throughout the evolution has been distinctly different between Charophyta and Chlorophyta (Banasiak, 2014; Sørensen et al., 2010). The terminal complex of cellulose synthases in Chlorophyta is linear, while in Charophyta a rosette configuration has been developed, resembling the Cellulose Synthase Complexes (CSC) in (higher) plants. Low amount of glucose and possibly traces of cellulose, together with lack of rosette structure suggests that cell wall properties and functionalities in *N. oleoabundans* are likely associated with non-cellulosic polymers.

4. Rhamnose-containing polysaccharides and chitin-like structures, possible explanations for rigidity of *N. oleoabundans* cell wall

Biochemical characterization of *N. oleoabundans* cell wall polysaccharides revealed that the most abundant monosaccharide is rhamnose (**Chapter 2**). A high amount of rhamnose may be responsible for the rigidity of *N. oleoabundans* cell walls, which is supported by results reported for other Chlorophyta algae (Baudelet et al., 2017). *Chlorella sorokiniana* cell walls revealed to be resistant to harsh acetolysis treatment (boiling acetic anhydride and concentrated sulphuric acid), and this was attributed to the existence of a large amount of rhamnose-containing polysaccharides in the cell wall (Russell, 1995). It is generally recognized that 6-deoxysugars, such as rhamnose and fucose, and lignin are among the few organic compounds able to resist this severe treatment (Fry, 1986; Russell, 1995).

As a result of our work, we hypothesize the existence of chitin-like structure in *N. oleoabundans* cell wall, which might contribute to the cell wall rigidity as well (**Chapter 2**). After cellulose, chitin is the second most common natural polymer on Earth and the most abundant one in the ocean (Durkin et al., 2009). This polymer is present in the exoskeletons of insects, egg shells of invertebrates and the cell wall of fungi, bacteria and some Chlorophyta algae (Baudelet et al., 2017; Shao et al., 2018). The existence of chitin is reported in the cell wall of organisms with a high abundance of glycoproteins (Rahman & Halfar, 2014). Chitin polymers individually, or in association with proteins provide structural strength to the cell wall. Although the presence of chitin has been reported in microalgae, its structural complexity and biochemical properties remain unknown. A few reports, for example, described that in the glucose-deprived cell wall of *Chlorella sorokiniana*, *Chlorella vulgaris* and *Chlorella kessleri*, the remaining residues after an alkali-treatment in their cell wall

contain glucosamine, which possibly underpins its strength (Takeda, 1993). In general, linkages between acetyl-amine groups in chitin-like structures are stronger than the hydrogen bonds of glucose-based polymers such as cellulose. This biochemical feature, might, therefore, play a central role in the rigidity of *N. oleoabundans* glucosamine-rich cell wall.

5. Uniqueness of *N. oleoabundans* cell wall across the plant kingdom

Although plant cell walls are characterized for carbohydrate-rich cell walls and a network of cellulose microfibrils; early-evolved plant, Chlorophyta microalgae, greatly differ in their cell wall compositions. A carbohydrate-deprived cell wall and rather scarce content of glucose-based polysaccharides in *N. oleoabundans* reflect the importance of other components to confer several physiochemical properties to the cell wall. As already discussed, the chitin-like components together with rhamnose-containing polysaccharides in *N. oleoabundans* might provide rigidity in the cell wall, a property that is achieved through the cellulose microfibrils in most of the land plant.

Amongst all the constituent cell wall components of *N. oleoabundans*, proteins /glycoproteins were the most abundant biomolecules (31.5% of NDF-cell wall) (**Chapter 2**). The abundance of proteins in *N. oleoabundans* cell wall is one of the main reasons for its uniqueness, as compared to other members of the plant kingdom. We have shown the presence of arabinogalactan proteins (AGPs) in *N. oleoabundans* cell wall (**Chapter 3**). These nitrogen-containing biopolymers are known to be present in the cell wall of several Chlorophyta algae (Baudelet et al., 2017). We have also identified different types of AGPs in the cell walls and these differ depending on the growing media, some were present only in freshwater while others only in seawater-cultivated *N. oleoabundans* cell walls. Our hypothesis is that different AGPs are synthesized in response to different abiotic stresses (Showalter, 2001).

A high amount of lipids is another reason for the distinctive structure of *N. oleoabundans* cell wall (**Chapter 2**). The lipophilic outer layer, cuticle, is an essential constituent of the land plants and protect them from ultraviolet irradiation and desiccation (Kondo et al., 2016; Riederer & Schreiber, 2001). We have shown that wax-like structures are part of the *N. oleoabundans* cell wall lipids and these might play a similar role as the cuticle layer of land plants. Only a few studies on cell wall-lipid of microalgae have been reported. In *Chlamydomonas reinhardtii*, lipids are either embedded or located at the surface of a glycoprotein network (Kondo et al., 2016). In another terrestrial alga, *Klebsormidium flaccidum*, it was reported that a cuticle-like hydrophobic layer on the cell wall surface is composed of lipids and glycoproteins (Kondo et al., 2016). The presence of glycoproteins with embedded

lipids is perhaps a complex system in terrestrial algae to protect the cells against several stress conditions.

Studying the morphology of *N. oleoabundans* cell wall provides additional support to its uniqueness. Through the exhaustive visualization of cell wall ultrastructure by means of different electron microscopy analyses, we were able to create a reference library, which reflects the morphological complexity of the cell wall throughout the cell cycle (**Chapter 4**). We showed that propagation (replication) in *N. oleoabundans* is based on autosporulation. In this mode of cell division, daughter cells, which have their own cell walls, are formed within the mother cell. We demonstrated that due to this nature of division, the cell wall throughout the cell cycle is mostly doubled. The outer electron-dense layer is the original maternal cell wall, which is carpeted with hair-like structures. Subsequent to the maturation of daughter cells, maternal cell wall sheds and releases the daughter cells. It has shown that cell wall proteolytic enzymes are responsible for the liberation of some microalgae daughter cells (Fukada et al., 2006; Kubo et al., 2009). On account of that, we hypothesized that in *N. oleoabundans*, the accumulation of hatched maternal cell walls in the medium is due to enzymatic reactions (**Chapter 5**). The potential implications of this observation are further commented in the below sections of this Discussion.

6. Cell wall dynamism of *N. oleoabundans*

Plant cell walls are highly dynamic. The dynamism of plant cell walls includes changes in composition and architecture in response to various stresses as well as developmental alteration throughout the cell cycle and/or developmental stage of the plant. Inimical environmental factors can influence physiological processes and, consequently, have an impact on the cell wall biosynthesis and structure. Insight in cell wall-adaptation/alteration in response to harsh environmental signals requires a thorough understanding of its regulation and modification of the various components. The impact of nitrogen deficiency and salinity on cell wall modulation of some microalgae have been reported previously (Chen et al., 2017; Ghafari et al., 2018). Results from **Chapter 3** of this thesis substantiated that variation in *N. oleoabundans* cell wall carbohydrate composition was notably dependant on the growing conditions. However, while different growing media were able to vary the total carbohydrate content of the cell wall, its relative quantity was still low when compared to other constitutive components (e.g. proteins). Nevertheless, the monosaccharides profile of the cell wall was significantly different in the different growing conditions. A key discovery in the carbohydrate characterization of seawater-cultivated cell wall was the abundance of glucose and mannose. We hypothesized that glucose and mannose can be the monomers of sulphated polysaccharides presented in the cell wall, by which a gel-like matrix is formed in the cell wall (**Chapter 3)**. This

mechanism, which is present in marine algae, is reported to be essential for their adaptation to the saline environment (Synytsya et al., 2015). The existence of sulphated polysaccharides in the cell wall of *N. oleoabundans* might be related to its origin, the sand dunes in Saudi Arabia, where salinity and perhaps drought stress are daily challenges. Additionally, we have observed that the protein content of the *N. oleoabundans* cell wall varies depending on the growing conditions. Nitrogen deficiency in the culture medium substantially lowered the protein content of the cell wall and alter the abundance of the constitutive amino acids (**Chapter 3**). We have noticed that salinity and nitrogen deficiency increased the proportion of the non-polar to polar amino acids. The significant increase of leucine, a non-polar amino acid, suggested that *N. oleoabundans* cell wall might contain leucine-rich repeat proteins. These proteins have been previously reported to be involved in the tolerance to many biotic and abiotic stresses (Liu et al., 2017).

Modification of plant cell wall might also occur during the cell cycle. We observed that glucosamine, glucose, galactose and rhamnose were the main components of cell wall polysaccharides that their contents changed throughout the cell wall development (**Chapter 5**). We hypothesized that the variation in glucose and glucosamine might articulate an interplay among the mechanical features of the cell wall. A partial conversion of chitin-like polysaccharides to glucose-based polymers might facilitate the turgor-driven expansion of the cell surface throughout the growth phase.

As a key message of this work, we prove that the cell wall is not just a rigid barrier of the cell. In contrast, its regulated dynamism makes it an operational and functional structure that modulates the growth and interaction of the cell with the environment.

7. Implication of knowledge, from biology to biorefinery

Biological breakthroughs on the biochemical composition, structure and molecular determinants of *N. oleoabundans* cell wall can enhance the utilization of this green feedstock microalga. In reliance on its polysaccharide composition, enzymatic treatments with carbohydrate hydrolases can be considered as a promising approach to weaken the cell wall prior to reaching the internal commodities of interest. However, the unusual and previously undescribed polysaccharides of microalgae cell wall limit the application of commercially available enzyme (cocktails). Future advances in the detailed chemical characterization of *N. oleoabundans* cell wall polysaccharides, with focusing on structural configuration and available linkages, might lead to the identification of new cell wall disruption methods or identification the promising hydrolytic enzymes.

In the same vein, the protein-rich cell wall of *N. oleoabundans* insinuates the possibility of using proteases to break/weaken the cell wall. To evaluate this hypothesis, we performed a test in which the freshwater cultivated *N. oleoabundans* was incubated for 1 h at room temperature with 0.5% papain (w/w), a commercial endopeptidase enzyme. Images from transmission electron microscopy proved our hypothesis and portrayed that the protease (papain) is able to denature the *N. oleoabundans* cell wall (Figure 1).

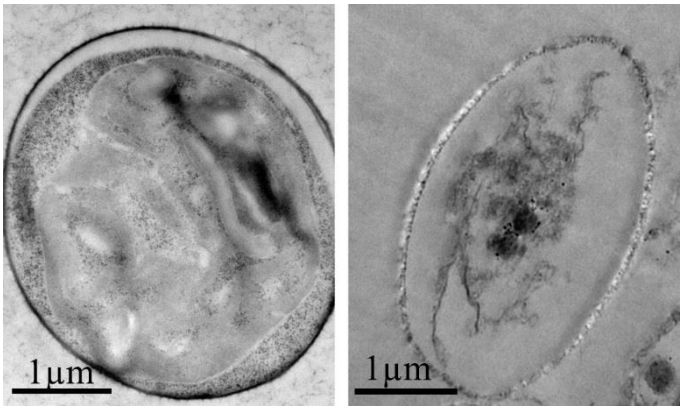

Figure 1. Images from Transmission Electron Microscope (TEM). Image on the left side displays the natural cell ultrastructure of *N. oleoabundans*. Image on the right side shows the impact of protease on the cell/cell wall of *N. oleoabundans*. Protease was able to target both intracellular and extracellular proteins of the *N. oleoabundans* cell and denatured them.

Nevertheless, we observed that together with the constitutive cell wall proteins, the intracellular proteins were denatured as well. Though, enzymatic treatment of *N. oleoabundans* with commercially available proteases can (still) be a possible approach to disrupt the cell wall and thereafter extract the intracellular lipids, sugars and non-bio-functional proteins/peptides.

8. Future perspective: microalgae autolysis via cell wall-degrading enzymes

A breakthrough cost-effective cell wall disruption method to substitute the traditional energy-consuming approaches is an urgent need for the successful downstream processing of microalgae. Understanding the biological and physiological mechanisms involved in cell wall biosynthesis and degradation will likely provide new tools for the identification of effective and specific cell wall-degrading enzymes.

Cell wall autolysis occurs naturally during particular events throughout the cell cycle, i.e. “cell division”. As previously explained, the autolysis of the cell wall during the cell division process allows the liberation of the daughter cells from the maternal cell.

These specific cell division autolysis enzymes, known as autolysins, are capable of degrading the cell wall at a particular site and a certain phase of the cell cycle. Previous reports indicated that the cell wall autolysis enzymes are mostly subtilase-like serine proteases (Kubo et al., 2009). These enzymes are able to cleave the peptide bonds of several peptides on the carboxyl side. Computational analyses of the sequenced algal genomes have shown that these proteases, are well represented in Chlorophyta phylum (Demuez et al., 2015).

In the context of the thesis, detailed morphological alteration underlying the cell wall development and later autolysis to liberate the asexually-generated daughter cells have been elucidated (**Chapter 4**). While exploring the transcriptome of synchronized *N. oleoabundans* throughout the cell cycle, we identified several potential unigenes annotated as “subtilase-like serine protease” (**Chapter 5**). Most of these identified unigenes showed differential expression throughout the cell cycle, with the highest expression levels during daughter cells liberation, implying their potential role in the asexual cell division. Based on this inspection, we adventure to suggest the existence of this autolysis enzyme as a cell-cycle regulated mechanism in *N. oleoabundans*. Further research is needed to demonstrate the potential application of “subtilase protease” as a specific tool for cell wall deconstruction.

References

Abo-Shady, A.M., Mohamed, Y.A., Lasheen, T. 1993. Chemical composition of the cell wall in some green algae species. *Biologia Plantarum*, **35**(4), 629-632.

Abu Hajar, H.A., Riefler, R.G., Stuart, B.J. 2017. Cultivation of the microalga Neochloris oleoabundans for biofuels production and other industrial applications (a review). *Applied Biochemistry and Microbiology*, **53**(6), 640-653.

Amor, Y., Haigler, C.H., Johnson, S., Wainscott, M., Delmer, D.P. 1995. A membrane-associated form of sucrose synthase and its potential role in synthesis of cellulose and callose in plants. *Proceedings of the National Academy of Sciences of the United States of America*, **92**(20), 9353-9357.

Aquino, R.S., Grativol, C., Mourão, P.A.S. 2011. Rising from the Sea: Correlations between Sulfated Polysaccharides and Salinity in Plants. *PLOS ONE*, **6**(4), e18862.

Arredondo-Vega, B.O., Band-Schmidt, C.J., Vazquez-Duhalt, R. 1995. Biochemical composition of Neochloris oleoabundans adapted to marine medium. **83**(335), 201-205.

Asselborn, V., Fernández, C., Zalocar, Y., Parodi, E.R. 2015. Effects of chlorpyrifos on the growth and ultrastructure of green algae, Ankistrodesmus gracilis. *Ecotoxicology and Environmental Safety*, **120**, 334-341.

Atkinson Jr, A.W., Gunning, B.E.S., John, P.C.L. 1972. Sporopollenin in the cell wall of Chlorella and other algae: Ultrastructure, chemistry, and incorporation of 14C-acetate, studied in synchronous cultures. *Planta*, **107**(1), 1-32.

Audic, S., Claverie, J.M. 1997. The significance of digital gene expression profiles. *Genome Research*, **7**(10), 986-995.

Banasiak, A. 2014. Evolution of the cell wall components during terrestrialization. *Acta Societatis Botanicorum Poloniae*, **83**(4), 349-362.

Bartnicki-Garcia, S. 1973. Fundamental aspects of hyphal morphogenesis. *Microbial Differentiation*, 245-267.

Baudelet, P.H., Ricochon, G., Linder, M., Muniglia, L. 2017. A new insight into cell walls of Chlorophyta. *Algal Research*, **25**, 333-371.

Baulina, O., Gorelova, O., Solovchenko, A., Chivkunova, O., Semenova, L., Selyakh, I., Scherbakov, P., Burakova, O., Lobakova, E. 2016. Diversity of the nitrogen starvation responses in subarctic Desmodesmus sp. (Chlorophyceae) strains isolated from symbioses with invertebrates. *FEMS Microbiology Ecology*, **92**(4).

Beacham, T.A., Bradley, C., White, D.A., Bond, P., Ali, S.T. 2014. Lipid productivity and cell wall ultrastructure of six strains of Nannochloropsis: Implications for biofuel production and downstream processing. *Algal Research*, **6**(PA), 64-69.

Beier, S., Bertilsson, S. 2013. Bacterial chitin degradation-mechanisms and ecophysiological strategies. *Frontiers in Microbiology*, **4**(JUN).

Bioenergy, I. 2017. State of Technology Review – Algae Bioenergy. An IEA Bioenergy Inter-Task Strategic Project

Bišová, K., Zachleder, V. 2014. Cell-cycle regulation in green algae dividing by multiple fission. *Journal of Experimental Botany*, **65**(10), 2585-2602.

Bobik, K., Dunlap, J.R., Burch-Smith, T.M. 2014. Tandem high-pressure freezing and quick freeze substitution of plant tissues for transmission electron microscopy. *Journal of Visualized Experiments*(92).

Bosma, R., de Vree, J.H., Slegers, P.M., Janssen, M., Wijffels, R.H., Barbosa, M.J. 2014. Design and construction of the microalgal pilot facility AlgaePARC. *Algal Research*, **6**(PB), 160-169.

Bourmaud, A., Beaugrand, J., Shah, D.U., Placet, V., Baley, C. 2018. Towards the design of high-performance plant fibre composites. *Progress in Materials Science*, **97**, 347-408.

Burczyk, J. 1986. Biogenetic relationships between ketocarotenoids and sporopollenins in green algae. *Phytochemistry*, **26**(1), 113-119.

Burczyk, J. 1973a. The chemical composition and ultrastructure of the cell wall of Scenedesmus obliquus. II. Amino acids, proteins and antigens. *Folia histochemica et cytochemica*, **11**(2), 135-154.

Burczyk, J. 1973b. The chemical composition of the cell wall of Scenedesmus obliquus. I. General chemical characteristics. *Folia histochemica et cytochemica*, **11**(2), 119-133.

Burczyk, J., Hesse, M. 1981. The ultrastructure of the outer cell wall-layer of Chlorella mutants with and without sporopollenin. *Plant Systematics and Evolution*, **138**(1-2), 121-137.

Burczyk, J., Śmietana, B., Termińska-Pabis, K., Zych, M., Kowalowski, P. 1999. Comparison of nitrogen content amino acid composition and glucosamine content of cell walls of various chlorococcalean algae. *Phytochemistry*, **51**(4), 491-497.

Burczyk, J., Zych, M., Ioannidis, N.E., Kotzabasis, K. 2014. Polyamines in cell walls of chlorococcalean microalgae. *Zeitschrift fur Naturforschung - Section C Journal of Biosciences*, **69 C**(1-2), 75-80.

Chantanachat, S., Bold, H.C. 1962. Some algae from arid soils. *Phycological Studies. II. University of Texas Publications*(No. 6218), 74 p.

Chen, B., Wan, C., Mehmood, M.A., Chang, J.S., Bai, F., Zhao, X. 2017. Manipulating environmental stresses and stress tolerance of microalgae for enhanced production of lipids and value-added products–A review. *Bioresource Technology*, **244**, 1198-1206.

Chen, Y., Xu, C., Vaidyanathan, S. 2018. Microalgae: a robust "green bio-bridge" between energy and environment. *Critical Reviews in Biotechnology*, **38**(3), 351-368.

Cheng, Y.S., Zheng, Y., Labavitch, J.M., Vandergheynst, J.S. 2011. The impact of cell wall carbohydrate composition on the chitosan flocculation of Chlorella. *Process Biochemistry*, **46**(10), 1927-1933.

Chu, W.L. 2017. Strategies to enhance production of microalgal biomass and lipids for biofuel feedstock. *European Journal of Phycology*, **52**(4), 419-437.

Chudzik, B., Zarzyka, B., Śniezko, R. 2005. Immunodetection of arabinogalactan proteins in different types of plant ovules. *Acta Biologica Cracoviensia Series Botanica*, **47**(1), 139-146.

Conesa, A., Götz, S., Garcia-Gomez, J.M., Terol, J., Talon, M., Robles, M. 2005. Blast2GO: a universal tool for annotation, visualization and analysis in functional genomics research. *Bioinformatics*, **21**.

Davis, R.W., Volponi, J.V., Jones, H.D.T., Carvalho, B.J., Wu, H., Singh, S. 2012. Multiplex fluorometric assessment of nutrient limitation as a strategy for enhanced lipid enrichment and harvesting of Neochloris oleoabundans. *Biotechnology and Bioengineering*, **109**(10), 2503-2512.

De Bhowmick, G., Sarmah, A.K., Sen, R. 2019. Zero-waste algal biorefinery for bioenergy and biochar: A green leap towards achieving energy and environmental sustainability. *Science of the Total Environment*, **650**, 2467-2482.

De Leeuw, J.W., Versteegh, G.J.M., Van Bergen, P.F. 2006. Biomacromolecules of algae and plants and their fossil analogues. *Plant Ecology*, **182**(1-2), 209-233.

De Winter, L., Cabanelas, I.T.D., Martens, D.E., Wijffels, R.H., Barbosa, M.J. 2017a. The influence of day/night cycles on biomass yield and composition of Neochloris oleoabundans. *Biotechnology for Biofuels*, **10**(1).

de Winter, L., Cabanelas, I.T.D., Órfão, A.N., Vaessen, E., Martens, D.E., Wijffels, R.H., Barbosa, M.J. 2017b. The influence of day length on circadian rhythms of Neochloris oleoabundans. *Algal Research*, **22**, 31-38.

de Winter, L., Klok, A.J., Cuaresma Franco, M., Barbosa, M.J., Wijffels, R.H. 2013. The synchronized cell cycle of Neochloris oleoabundans and its influence on biomass composition under constant light conditions. *Algal Research*, **2**(4), 313-320.

Dempsey, G.P., Lawrence, D., Cassie, V. 1980. The ultrastructure of Chlorella minutissima Fott et Nováková (Chlorophyceae, Chlorococcales). *Phycologia*, **19**(1), 13-19.

Demuez, M., Mahdy, A., Tomás-Pejó, E., González-Fernández, C., Ballesteros, M. 2015. Enzymatic cell disruption of microalgae biomass in biorefinery processes. *Biotechnology and Bioengineering*, **112**(10), 1955-1966.

Deprá, M.C., dos Santos, A.M., Severo, I.A., Santos, A.B., Zepka, L.Q., Jacob-Lopes, E. 2018. Microalgal Biorefineries for Bioenergy Production: Can We Move from Concept to Industrial Reality? *BioEnergy Research*.

Derenne, S., Largeau, C., Berkaloff, C., Rousseau, B., Wilhelm, C., Hatcher, P.G. 1992. Non-hydrolysable macromolecular constituents from outer walls of Chlorella fusca and Nanochlorum eucaryotum. *Phytochemistry*, **31**(6), 1923-1929.

Diévart, A., Gilbert, N., Droc, G., Attard, A., Gourgues, M., Guiderdoni, E., Périn, C. 2011. Leucine-Rich repeat receptor kinases are sporadically distributed in eukaryotic genomes. *BMC Evolutionary Biology*, **11**(1).

Dixon, C., Wilken, L.R. 2018. Green microalgae biomolecule separations and recovery. *Bioresources and Bioprocessing*, **5**(1).

Domozych, D.S., Ciancia, M., Fangel, J.U., Mikkelsen, M.D., Ulvskov, P., Willats, W.G.T. 2012. The cell walls of green algae: A journey through evolution and diversity. *Frontiers in Plant Science*, **3**(MAY).

Durkin, C.A., Mock, T., Armbrust, E.V. 2009. Chitin in diatoms and its association with the cell wall. *Eukaryotic Cell*, **8**(7), 1038-1050.

Eliáš, M., Němcová, Y., Škaloud, P., Neustupa, J., Kaufnerová, V., Šejnohová, L. 2010. Hylodesmus singaporensis gen. et sp. nov., a new autosporic subaerial green alga (Scenedesmaceae, Chlorophyta) from Singapore. *International Journal of Systematic and Evolutionary Microbiology*, **60**(5), 1224-1235.

Fangel, J.U., Pedersen, H.L., Vidal-Melgosa, S., Ahl, L.I., Salmean, A.A., Egelund, J., Rydahl, M.G., Clausen, M.H., Willats, W.G.T. 2012a. Carbohydrate microarrays in plant science. in: *Methods in Molecular Biology*, Vol. 918, pp. 351-362.

Fangel, J.U., Ulvskov, P., Knox, J.P., Mikkelsen, M.D., Harholt, J., Popper, Z.A., Willats, W.G.T. 2012b. Cell wall evolution and diversity. *Frontiers in Plant Science*, **3**(JUL).

Fernández, P.V., Arata, P.X., Ciancia, M. 2014. Polysaccharides from codium species: Chemical structure and biological activity. their role as components of the cell wall. in: *Advances in Botanical Research*, Vol. 71, pp. 253-278.

Fernández, P.V., Estevez, J.M., Cerezo, A.S., Ciancia, M. 2012. Sulfated β-d-mannan from green seaweed Codium vermilara. *Carbohydrate Polymers*, **87**(1), 916-919.

Fernández, P.V., Quintana, I., Cerezo, A.S., Caramelo, J.J., Pol-Fachin, L., Verli, H., Estevez, J.M., Ciancia, M. 2013. Anticoagulant activity of a unique sulfated pyranosic (1→3)-β-L- arabinan through direct interaction with thrombin. *Journal of Biological Chemistry*, **288**(1), 223-233.

Fry, S.C. 1986. Cross-Linking of Matrix Polymers in the Growing Cell Walls of Angiosperms. *Annual Review of Plant Physiology*, **37**(1), 165-186.

Fukada, K., Inoue, T., Shiraishi, H. 2006. A posttranslationally regulated protease, VheA, is involved in the liberation of juveniles from parental spheroids in Volvox carteri. *Plant Cell*, **18**(10), 2554-2566.

Garibay-Hernández, A., Vazquez-Duhalt, R., Serrano-Carreón, L., Martinez, A. 2013. Nitrogen Limitation in Neochloris oleoabundans: A Reassessment of Its Effect on Cell Growth and Biochemical Composition. *Applied Biochemistry and Biotechnology*, **171**(7), 1775-1791.

Gerken, H.G., Donohoe, B., Knoshaug, E.P. 2013. Enzymatic cell wall degradation of Chlorella vulgaris and other microalgae for biofuels production. *Planta*, **237**(1), 239-253.

Ghafari, M., Rashidi, B., Haznedaroglu, B.Z. 2018. Effects of macro and micronutrients on neutral lipid accumulation in oleaginous microalgae. *Biofuels*, **9**(2), 147-156.

Gimmler, H. 2000. Primary sodium plasma membrane ATPases in salt-tolerant algae: Facts and fictions. *Journal of Experimental Botany*, **51**(348), 1171-1178.

Goering HK, V.S.P. 1970. Forage fiber analyses (apparatus, reagents, procedures, and some applications). *Agric. Handbook No. 379. U.S. Agricultural Research Service, Washington, DC*.

Gorelova, O., Baulina, O., Solovchenko, A., Selyakh, I., Chivkunova, O., Semenova, L., Scherbakov, P., Burakova, O., Lobakova, E. 2014. Coordinated rearrangements of assimilatory and storage cell compartments in a nitrogen-starving symbiotic chlorophyte cultivated under high light. *Archives of Microbiology*, **197**(2), 181-195.

Grabherr, M.G., Haas, B.J., Yassour, M., Levin, J.Z., Thompson, D.A., Amit, I., Adiconis, X., Fan, L., Raychowdhury, R., Zeng, Q., Chen, Z., Mauceli, E., Hacohen, N., Gnirke, A., Rhind, N., Di Palma, F., Birren, B.W., Nusbaum, C., Lindblad-Toh, K., Friedman,

N., Regev, A. 2011. Full-length transcriptome assembly from RNA-Seq data without a reference genome. *Nature Biotechnology*, **29**(7), 644-652.

Graves, M.V., Burbank, D.E., Roth, R., Heuser, J., Deangelis, P.L., Van Etten, J.L. 1999. Hyaluronan synthesis in virus PBCV-1-infected chlorella-like green algae. *Virology*, **257**(1), 15-23.

Guzman-Murillo, M.A., Ascencio, F. 2000. Anti-adhesive activity of sulphated exopolysaccharides of microalgae on attachment of red sore disease-associated bacteria and Helicobacter pylori to tissue culture cells. *Letters in Applied Microbiology*, **30**(6), 473-478.

Harholt, J., Moestrup, O., Ulvskov, P. 2016. Why Plants Were Terrestrial from the Beginning. *Trends in Plant Science*, **21**(2), 96-101.

Harholt, J., Sørensen, I., Fangel, J., Roberts, A., Willats, W.G.T., Scheller, H.V., Petersen, B.L., Banks, J.A., Ulvskov, P. 2012. The glycosyltransferase repertoire of the spikemoss selaginella moellendorffii and a comparative study of its cell wall. *PLoS ONE*, **7**(5).

Herburger, K., Holzinger, A. 2015. Localization and Quantification of Callose in the Streptophyte Green Algae Zygnema and Klebsormidium: Correlation with Desiccation Tolerance. *Plant and Cell Physiology*, **56**(11), 2259-2270.

Huss, V.A.R., Ciniglia, C., Cennamo, P., Cozzolino, S., Pinto, G., Pollio, A. 2002. Phylogenetic relationships and taxonomic position of Chlorella-like isolates from low pH environments (pH < 3.0). *BMC Evolutionary Biology*, **2**.

Immerzeel, P. 2005. Characterization of carrot arabinogalactan proteins *PhD thesis, Wageningen University, The Netherlands*.

Jaeger, L.D., Carreres, B.M., Springer, J., Schaap, P.J., Eggink, G., Martins Dos Santos, V.A.P., Wijffels, R.H., Martens, D.E. 2018. Neochloris oleoabundans is worth its salt: Transcriptomic analysis under salt and nitrogen stress. *PLoS ONE*, **13**(4).

Jensen, J.K., Busse-Wicher, M., Poulsen, C.P., Fangel, J.U., Smith, P.J., Yang, J.Y., Peña, M.J., Dinesen, M.H., Martens, H.J., Melkonian, M., Wong, G.K.S., Moremen, K.W., Wilkerson, C.G., Scheller, H.V., Dupree, P., Ulvskov, P., Urbanowicz, B.R., Harholt, J. 2018. Identification of an algal xylan synthase indicates that there is functional orthology between algal and plant cell wall biosynthesis. *New Phytologist*, **218**(3), 1049-1060.

Jeong, S.W., Nam, S.W., Hwangbo, K., Jeong, W.J., Jeong, B.R., Chang, Y.K., Park, Y.I. 2017. Transcriptional Regulation of Cellulose Biosynthesis during the Early Phase of Nitrogen Deprivation in Nannochloropsis salina. *Scientific Reports*, **7**(1).

Jones, J., Manning, S., Montoya, M., Keller, K., Poenie, M. 2012. Extraction of algal lipids and their analysis by HPLC and mass spectrometry. *JAOCS, Journal of the American Oil Chemists' Society*, **89**(8), 1371-1381.

Kapaun, E., Reisser, W. 1995. A chitin-like glycan in the cell wall of a Chlorella sp. (Chlorococcales, Chlorophyceae). *Planta*, **197**(4), 577-582.

Khan, M.I., Shin, J.H., Kim, J.D. 2018. The promising future of microalgae: Current status, challenges, and optimization of a sustainable and renewable industry for biofuels, feed, and other products. *Microbial Cell Factories*, **17**(1).

Kinoshita, A., Niwa, Y., Onai, K., Yamano, T., Fukuzawa, H., Ishiura, M., Matsuo, T. 2017. CSL encodes a leucine-rich-repeat protein implicated in red/violet light signaling to the circadian clock in Chlamydomonas. *PLoS Genetics*, **13**(3).

Kliphuis, A.M.J., de Winter, L., Vejrazka, C., Martens, D.E., Janssen, M., Wijffels, R.H. 2010. Photosynthetic efficiency of Chlorella sorokiniana in a turbulently mixed short light-path photobioreactor. *Biotechnology Progress*, **26**(3), 687-696.

Klok, A.J., Martens, D.E., Wijffels, R.H., Lamers, P.P. 2013. Simultaneous growth and neutral lipid accumulation in microalgae. *Bioresource Technology*, **134**, 233-243.

Knox, J., Linstead, P., Cooper, J.P.C., Roberts, K. 1991. Developmentally regulated epitopes of cell surface arabinogalactan proteins and their relation to root tissue pattern formation. *The Plant Journal*, **1**(3), 317-326.

Kondo, S., Hori, K., Sasaki-Sekimoto, Y., Kobayashi, A., Kato, T., Yuno-Ohta, N., Nobusawa, T., Ohtaka, K., Shimojima, M., Ohta, H. 2016. Primitive extracellular lipid components on the surface of the charophytic alga Klebsormidium flaccidum and

their possible biosynthetic pathways as deduced from the genome sequence. *Frontiers in Plant Science*, **7**.

Kračun, S.K., Fangel, J.U., Rydahl, M.G., Pedersen, H.L., Vidal-Melgosa, S., Willats, W.G.T. 2017. Carbohydrate Microarray Technology Applied to High-Throughput Mapping of Plant Cell Wall Glycans Using Comprehensive Microarray Polymer Profiling (CoMPP). in: *High-Throughput Glycomics and Glycoproteomics: Methods and Protocols*, Springer New York. New York, NY, pp. 147-165.

Kubo, T., Kaida, S., Abe, J., Saito, T., Fukuzawa, H., Matsuda, Y. 2009. The chlamydomonas hatching enzyme, sporangin, is expressed in specific phases of the cell cycle and is localized to the flagella of daughter cells within the sporangial cell wall. *Plant and Cell Physiology*, **50**(3), 572-583.

Lalitha Sridhar, S., Ortega, J.K.E., Vernerey, F. 2018. A Statistical Model of Cell Wall Dynamics during Expansive Growth. *bioRxiv*.

Langmead, B., Salzberg, S.L. 2012. Fast gapped-read alignment with Bowtie 2. *Nature Methods*, **9**(4), 357-359.

León-Saiki, G.M., Cabrero Martí, T., van der Veen, D., Wijffels, R.H., Martens, D.E. 2018. The impact of day length on cell division and efficiency of light use in a starchless mutant of Tetradesmus obliquus. *Algal Research*, **31**, 387-394.

Leu, S., Boussiba, S. 2014. Advances in the Production of High-Value Products by Microalgae. *Industrial Biotechnology*, **10**(3), 169-183.

Liu, P.L., Du, L., Huang, Y., Gao, S.M., Yu, M. 2017. Origin and diversification of leucine-rich repeat receptor-like protein kinase (LRR-RLK) genes in plants. *BMC Evolutionary Biology*, **17**(1), 1-16.

Liu, X., Saydah, B., Eranki, P., Colosi, L.M., Greg Mitchell, B., Rhodes, J., Clarens, A.F. 2013. Pilot-scale data provide enhanced estimates of the life cycle energy and emissions profile of algae biofuels produced via hydrothermal liquefaction. *Bioresource Technology*, **148**, 163-171.

Lonsdale, J.E., McDonald, K.L., Jones, R.L. 1999. High pressure freezing and freeze substitution reveal new aspects of fine structure and maintain protein antigenicity in barley aleurone cells. *Plant Journal*, **17**(2), 221-229.

Loos, E., Meindl, D. 1982. Composition of the cell wall of Chlorella fusca. *Planta*, **156**(3), 270-273.

Matich, E.K., Ghafari, M., Camgoz, E., Caliskan, E., Pfeifer, B.A., Haznedaroglu, B.Z., Atilla-Gokcumen, G.E. 2018. Time-series lipidomic analysis of the oleaginous green microalga species Ettlia oleoabundans under nutrient stress. *Biotechnology for Biofuels*, **11**(1).

Matos, Â.P. 2017. The Impact of Microalgae in Food Science and Technology. *JAOCS, Journal of the American Oil Chemists' Society*, **94**(11), 1333-1350.

Matsuda, Y., Koseki, M., Shimada, T., Saito, T. 1995. Purification and characterization of a vegetative lytic enzyme responsible for liberation of daughter cells during the proliferation of Chlamydomonas reinhardtii. *Plant and Cell Physiology*, **36**(4), 681-689.

Moller, I., Sørensen, I., Bernal, A.J., Blaukopf, C., Lee, K., Øbro, J., Pettolino, F., Roberts, A., Mikkelsen, J.D., Knox, J.P., Bacic, A., Willats, W.G.T. 2007. High-throughput mapping of cell-wall polymers within and between plants using novel microarrays. *Plant Journal*, **50**(6), 1118-1128.

Muralidhar, A., Shabala, L., Broady, P., Shabala, S., Garrill, A. 2015. Mechanisms underlying turgor regulation in the estuarine alga Vaucheria erythrospora (Xanthophyceae) exposed to hyperosmotic shock. *Plant, Cell and Environment*, **38**(8), 1514-1527.

Mussgnug, J.H., Klassen, V., Schlüter, A., Kruse, O. 2010. Microalgae as substrates for fermentative biogas production in a combined biorefinery concept. *Journal of Biotechnology*, **150**(1), 51-56.

Nedukha, O.M. 2015. Callose: Localization, functions, and synthesis in plant cells. *Cytology and Genetics*, **49**(1), 49-57.

NREL. 2016. Nitrogen-to-Protein Factor Calculator.

Ortega, J.K. 2016. Dimensional Analysis of Expansive Growth of Cells with Walls. *Journal of Botanical Sciences*, **5**(3).

Pankiewicz, R., Łęska, B., Messyasz, B., Fabrowska, J., Sołoducha, M., Pikosz, M. 2016. First isolation of polysaccharidic ulvans from the cell walls of freshwater algae. *Algal Research*, **19**, 348-354.

Percival, E. 1979. The polysaccharides of green, red and brown seaweeds: Their basic structure, biosynthesis and function. *British Phycological Journal*, **14**(2), 103-117.

Pertea, G., Huang, X., Liang, F., Antonescu, V., Sultana, R., Karamycheva, S., Lee, Y., White, J., Cheung, F., Parvizi, B., Tsai, J., Quackenbush, J. 2003. TIGR gene indices clustering tools (TGICL): A software system for fast clustering of large EST datasets. *Bioinformatics*, **19**(5), 651-652.

Pettolino, F.A., Walsh, C., Fincher, G.B., Bacic, A. 2012. Determining the polysaccharide composition of plant cell walls. *Nature Protocols*, **7**(9), 1590-1607.

Phenomenex. EZfaast User's Guide for Protein Hydrolysates (GC/FID).

Pokora, W., Aksmann, A., Baścik-Remisiewicz, A., Dettlaff-Pokora, A., Rykaczewski, M., Gappa, M., Tukaj, Z. 2017. Changes in nitric oxide/hydrogen peroxide content and cell cycle progression: Study with synchronized cultures of green alga Chlamydomonas reinhardtii. *Journal of Plant Physiology*, **208**, 84-93.

Popovich, C.A., Damiani, C., Constenla, D., Martínez, A.M., Freije, H., Giovanardi, M., Pancaldi, S., Leonardi, P.I. 2012. Neochloris oleoabundans grown in enriched natural seawater for biodiesel feedstock: Evaluation of its growth and biochemical composition. *Bioresource Technology*, **114**, 287-293.

Quevillon, E., Silventoinen, V., Pillai, S., Harte, N., Mulder, N., Apweiler, R., Lopez, R. 2005. InterProScan: Protein domains identifier. *Nucleic Acids Research*, **33**(SUPPL. 2), W116-W120.

Rahman, M.A., Halfar, J. 2014. First evidence of chitin in calcified coralline algae: New insights into the calcification process of Clathromorphum compactum. *Scientific Reports*, **4**.

Rashidi, B., Trindade, L.M. 2018. Detailed biochemical and morphologic characteristics of the green microalga Neochloris oleoabundans cell wall. *Algal Research*, **35**, 152-159.

Riederer, M., Schreiber, L. 2001. Protecting against water loss: Analysis of the barrier properties of plant cuticles. *Journal of Experimental Botany*, **52**(363), 2023-2032.

Rismani-Yazdi, H., Haznedaroglu, B.Z., Hsin, C., Peccia, J. 2012. Transcriptomic analysis of the oleaginous microalga Neochloris oleoabundans reveals metabolic insights into triacylglyceride accumulation. *Biotechnology for Biofuels*, **5**.

Roberts, A.W., Roberts, E.M., Delmer, D.P. 2002. Cellulose synthase (CesA) genes in the green alga Mesotaenium caldariorum. *Eukaryotic Cell*, **1**(6), 847-855.

Rosenberg, I.M. 1996. Protein Structure. in: *Protein Analysis and Purification: Benchtop Techniques*, Birkhäuser Boston. Boston, MA, pp. 8-23.

Ruiz, J., Olivieri, G., De Vree, J., Bosma, R., Willems, P., Reith, J.H., Eppink, M.H.M., Kleinegris, D.M.M., Wijffels, R.H., Barbosa, M.J. 2016. Towards industrial products from microalgae. *Energy and Environmental Science*, **9**(10), 3036-3043.

Russell, B.L. 1995. Determination of factors limiting enzymatic hydrolysis of the "Chlorella sorokiniana" cell wall. *University of Florida, George A. Smathers Libraries*.

Rydahl, M.G., Kračun, S.K., Fangel, J.U., Michel, G., Guillouzo, A., Génicot, S., Mravec, J., Harholt, J., Wilkens, C., Motawia, M.S., Svensson, B., Tranquet, O., Ralet, M.C., Jørgensen, B., Domozych, D.S., Willats, W.G.T. 2017. Development of novel monoclonal antibodies against starch and ulvan - Implications for antibody production against polysaccharides with limited immunogenicity. *Scientific Reports*, **7**(1).

S. Chantanachat, Bold, H.C. 1962. Some algae from arid soils. *Phycological Studies. II, University of Texas Publications*, 74 p.

Sajjadi, B., Chen, W.Y., Raman, A.A.A., Ibrahim, S. 2018. Microalgae lipid and biomass for biofuel production: A comprehensive review on lipid enhancement strategies and their effects on fatty acid composition. *Renewable and Sustainable Energy Reviews*, **97**, 200-232.

Sarkar, P., Bosneaga, E., Auer, M. 2009. Plant cell walls throughout evolution: Towards a molecular understanding of their design principles. *Journal of Experimental Botany*, **60**(13), 3615-3635.

Satoh, H., Takeda, H. 1989. Detection and first characterization of a cell-wall lytic activity in Chlorella ellipsoidea C-27. *Physiologia Plantarum*, **77**(1), 20-26.

Scherp, P., Grotha, R., Kutschera, U. 2001. Occurrence and phylogenetic significance of cytokinesis-related callose in green algae, bryophytes, ferns and seed plants. *Plant Cell Reports*, **20**(2), 143-149.

Schlösser, U.G. 1981. Algal Wall-Degrading Enzymes — Autolysines. in: *Plant Carbohydrates II: Extracellular Carbohydrates*, (Eds.) W. Tanner, F.A. Loewus, Springer Berlin Heidelberg. Berlin, Heidelberg, pp. 333-351.

Scholz, M.J., Weiss, T.L., Jinkerson, R.E., Jing, J., Roth, R., Goodenough, U., Posewitz, M.C., Gerken, H.G. 2014. Ultrastructure and composition of the Nannochloropsis gaditana cell wall. *Eukaryotic Cell*, **13**(11), 1450-1464.

Selvaggini, S., Munro, C.A., Paschoud, S., Sanglard, D., Gow, N.A.R. 2004. Independent regulation of chitin synthase and chitinase activity in Candida albicans and Saccharomyces cerevisiae. *Microbiology*, **150**(4), 921-928.

Shao, Z., Thomas, Y., Hembach, L., Xing, X., Duan, D., Moerschbacher, B.M., Bulone, V., Tirichine, L., Bowler, C. 2018. Comparative characterization of putative chitin deacetylases from Phaeodactylum tricornutum and Thalassiosira pseudonana highlights the potential for distinct chitin-based metabolic processes in diatoms. *New Phytologist*.

Showalter, A.M. 2001. Arabinogalactan-proteins: Structure, expression and function. *Cellular and Molecular Life Sciences*, **58**(10), 1399-1417.

Showalter, A.M. 1993. Structure and function of plant cell wall proteins. *Plant Cell*, **5**(1), 9-23.

Solovchenko, A.E., Gorelova, O.A., Baulina, O.I., Selyakh, I.O., Semenova, L.R., Chivkunova, O.B., Scherbakov, P.N., Lobakova, E.S. 2015. Physiological plasticity of symbiotic Desmodesmus (Chlorophyceae) isolated from taxonomically distant white sea invertibrates. *Russian Journal of Plant Physiology*, **62**(5), 653-663.

Somogyi, B., Felföldi, T., Solymosi, K., Flieger, K., Márialigeti, K., Böddi, B., Vörös, L. 2013. One step closer to eliminating the nomenclatural problems of minute coccoid green algae: Pseudochloris wilhelmii, gen. et sp. nov. (Trebouxiophyceae, Chlorophyta). *European Journal of Phycology*, **48**(4), 427-436.

Sørensen, I., Domozych, D., Willats, W.G.T. 2010. How have plant cell walls evolved? *Plant Physiology*, **153**(2), 366-372.

Spolaore, P., Joannis-Cassan, C., Duran, E., Isambert, A. 2006. Commercial applications of microalgae. *Journal of Bioscience and Bioengineering*, **101**(2), 87-96.

Sticklen, M.B. 2010. Erratum: Plant genetic engineering for biofuel production: Towards affordable cellulosic ethanol (Nature Reviews Genetics (2008) 9 (433-443)). *Nature Reviews Genetics*, **11**(4), 308.

Suarez Ruiz, C.A., Emmery, D.P., Wijffels, R.H., Eppink, M.H.M., van den Berg, C. 2018. Selective and mild fractionation of microalgal proteins and pigments using aqueous two-phase systems. *Journal of Chemical Technology and Biotechnology*, **93**(9), 2774-2783.

Synytsya, A., Copíková, J., Kim, W.J., Park, Y.I. 2015. Cell wall polysaccharides of marine algae. in: *Springer Handbook of Marine Biotechnology*, pp. 543-590.

t Lam, G.P., Vermuë, M.H., Eppink, M.H.M., Wijffels, R.H., van den Berg, C. 2017. Multi-Product Microalgae Biorefineries: From Concept Towards Reality. *Trends in Biotechnology*.

Takeda, H. 1993. Chemical composition of cell walls as a taxonomical marker. *Journal of Plant Research*, **106**(3), 195-200.

Takeda, H. 1988a. Classification of Chlorella strains by cell wall sugar composition. *Phytochemistry*, **27**(12), 3823-3826.

Takeda, H. 1988b. Classification of Chlorella strains by means of the sugar components of the cell wall. *Biochemical Systematics and Ecology*, **16**(4), 367-371.

Takeda, H., Hirokawa, T. 1978. Studies on the cell wall of Chlorella I. Quantitative changes in cell wall polysaccharides during the cell cycle of Chlorella ellipsoidea. *Plant and Cell Physiology*, **19**(4), 591-598.

Takeda, H., Hirokawa, T. 1979. Studies on the cell wall of Chlorella II. Mode of increase of glucosamine in the cell wall during the synchronous growth of Chlorella ellipsoidea. *Plant and Cell Physiology*, **20**(5), 989-991.

Takeda, H., Hirokawa, T. 1982. Studies on the Cell Wall of Chlorella III. Incorporation of Photosynthetically Fixed Carbon into Cell Walls of Synchronously Growing Cells of Chlorella ellipsoidea. *Plant and Cell Physiology*, **23**(6), 1033-1040.

Tamiya, H., Iwamura, T., Shibata, K., Hase, E., Nihei, T. 1953. Correlation between photosynthesis and light-independent metabolism in the growth of Chlorella. *Biochimica et Biophysica Acta*, **12**(1), 23-40.

Tarazona, S., García-Alcalde, F., Dopazo, J., Ferrer, A., Conesa, A. 2011. Differential expression in RNA-seq: A matter of depth. *Genome Research*, **21**(12), 2213-2223.

Tenhaken, R. 2015. Cell wall remodeling under abiotic stress. *Frontiers in Plant Science*, **5**(JAN).

Tirichine, L., Bowler, C. 2011. Decoding algal genomes: tracing back the history of photosynthetic life on Earth. *The Plant Journal*, **66**(1), 45-57.

Van Donk, E., Lürling, M., Hessen, D.O., Lokhorst, G.M. 1997. Altered cell wall morphology in nutrient-deficient phytoplankton and its impact on grazers. *Limnology and Oceanography*, **42**(2), 357-364.

Van Etten, J.L., Agarkova, I., Dunigan, D.D., Tonetti, M., De Castro, C., Duncan, G.A. 2017. Chloroviruses have a sweet tooth. *Viruses*, **9**(4), 1-23.

Van Soest, P.J. 1967. Development of a Comprehensive System of Feed Analyses and its Application to Forages. *Journal of Animal Science*, **26**(1), 119-128.

Van Wychen, S., and Laurens, Lieve M. L. 2016. Determination of Total Carbohydrates in Algal Biomass. *Laboratory Analytical Procedure (LAP). United States: N. p.*

Voigt, J., Stolarczyk, A., Zych, M., Malec, P., Burczyk, J. 2014. The cell-wall glycoproteins of the green alga Scenedesmus obliquus. The predominant cell-wall polypeptide of Scenedesmus obliquus is related to the cell-wall glycoprotein gp3 of Chlamydomonas reinhardtii. *Plant Science*, **215–216**, 39-47.

Voigt, J., Wrann, D., Vogeler, H.P., König, W.A., Mix, M. 1994. Hydroxyproline-containing and glycine-rich cell wall polypeptides are widespread in the green algae. *Microbiological Research*, **149**(3), 223-229.

Wijffels, R.H., Barbosa, M.J. 2010. An outlook on microalgal biofuels. *Science*, **329**(5993), 796-799.

Wijffels, R.H., Kruse, O., Hellingwerf, K.J. 2013. Potential of industrial biotechnology with cyanobacteria and eukaryotic microalgae. *Current Opinion in Biotechnology*, **24**(3), 405-413.

Wychen, S.V., Laurens, L.M.L. 2013. Determination of Total Solids and Ash in Algal Biomass. *Laboratory Analytical Procedure. National Renewable Energy Laboratory, Golden, CO*.

Yamada, T., Sakaguchi, K. 1982. Comparative studies onChlorella cell walls: Induction of protoplast formation. *Archives of Microbiology*, **132**(1), 10-13.

Yamamoto, M., Fujishita, M., Hirata, A., Kawano, S. 2004. Regeneration and maturation of daughter cell walls in the autospore-forming green alga Chlorella vulgaris (Chlorophyta, Trebouxiophyceae). *Journal of Plant Research*, **117**(4), 257-264.

Yamamoto, M., Kurihara, I., Kawano, S. 2005. Late type of daughter cell wall synthesis in one of the Chlorellaceae, Parachlorella kessleri (Chlorophyta, Trebouxiophyceae). *Planta*, **221**(6), 766-775.

Yamamoto, M., Nishikawa, T., Kajitani, H., Kawano, S. 2007. Patterns of asexual reproduction in Nannochloris bacillaris and Marvania geminata (Chlorophyta, Trebouxiophyceae). *Planta*, **226**(4), 917-927.

Yamamoto, M., Nozaki, H., Miyazawa, Y., Koide, T., Kawano, S. 2003. Relationship between presence of a mother cell wall and speciation in the unicellular microalga Nannochloris (Chlorophyta). *Journal of Phycology*, **39**(1), 172-184.

Yates, E.A., Knox, J.P. 1994. Investigations into the occurrence of plant cell surface epitopes in exudate gums. *Carbohydrate Polymers*, **24**(4), 281-286.

Summary

An ever-increasing world population together with industrial development at an accelerated pace have push scientists to identify promising bio-resources to produce food, feed and fuel in the framework of carbon-neutral bio-economy. Amongst the bio-resources available, there has been a growing interest in the exploitation of microalgae biomass as an alternative green feedstock. However, at this moment, the microalgae-derived products are not economically feasible on account of a low return in investment.

One way to enhance the economic viability of microalgae production and utilization is to design effective and sustainable methods for the extraction of its components. To design such methods we need to understand the biology of the microalgae cell. *N. oleoabundans*, the studied green microalgae in this thesis, contains valuable components enclosed within a morphologically complex cell wall. Thus, before accessing the intracellular components the cell wall barrier needs to be deconstructed. The overall aim of this thesis was to generate in-depth insights into cell wall building blocks of *N. oleoabundans*. Fundamental knowledge on the physicochemical structure and the underlying molecular determinants of cell wall biosynthesis and modification are the main focus.

In **Chapter 1** of this thesis, we presented an introduction about the importance of microalgae as a promising renewable feedstock. Further, we described the enormous biodiversity among the cell walls of different life kingdoms and in particular Chlorophyta green microalgae.

In **Chapter 2**, we have made a comprehensive characterization of the *N. oleoabundans* cell walls. The results showed that *N. oleoabundans* cell walls are composed of about 2.4.3% carbohydrates, 31.5% proteins, 22.2% lipids and 7.8% inorganic compounds. A rather scarce amount of glucose in the *N. oleoabundans* suggested that non-cellulosic polysaccharides may underpin the cell wall rigidity. We concluded in this chapter that *N. oleoabundans* cell walls are very different from (higher) plant cell walls, and that similar functionalities can be achieved by (combinations of) different polymers.

In **Chapter 3**, we evaluated the wall composition and properties of *N. oleoabundans* cells grown under freshwater nitrogen-replete (optimum culture) and -depleted conditions, and seawater nitrogen-replete and -depleted conditions. Results from this chapter substantiated that variation in

cell wall composition was notably dependant on the growing conditions, supporting the importance of the cell wall as a dynamic structure to adapt to different environments.

In **Chapter 4,** microscopic approaches were applied to describe the morphologic characteristics of cell wall development throughout the cell cycle. We observed that throughout the cell cycle *N. oleoabundans* cell walls are mostly doubled. Electron microscopy images enabled us to propose a model for the daughter cell wall regeneration in *N. oleoabundans*. In this model, daughter cell wall deposition occurs at the beginning of the growth phase.

In **Chapter 5**, we performed a comparative transcriptomics study followed by biochemical characterisation to identify the molecular mechanisms underlying the cell wall development throughout the cell cycle. We disclosed that glucosamine, glucose, galactose and rhamnose were the main carbohydrates of *N. oleoabundans* cell wall that undergo controlled variations through the cell cycle. An important factor identified in cell wall dynamic process throughout the cell cycle was an increase in the bulk of uridine diphosphate glucose (UDP-D-Glu) during the growth phase, which was mainly related to chitin and galactose degradation.

In **Chapter 6**, we integrated the entire knowledge and new insights generated within this research. We discussed the uniqueness of *N. oleoabundans* cell wall, considering its constitutive components, its morphological properties, and changes in response to the environment and developmental phase. Furthermore, we proposed a new approach, based on the fundamental knowledge generated on cell wall-degrading enzymes, that could facilitate a valorisation of the whole microalgae biomass.

Acknowledgements

After almost five years of PhD-journey filled with excitement, challenges, growth, both professionally and personally and, if truth be told, sometimes panic, it is time to write the most readable (as they said the non-boring) section of any PhD thesis. I would like to take this opportunity to express my gratitude towards many of you who help and accompanied me during my PhD, and hope not to forget anyone.

First and foremost I would like to thank my promotor, **Prof. Luisa Trindade**. In all honesty, I need to write another thesis entitled “Definition of an amazing supervisor” to be able to some extent acknowledge you! I remember our first emails exchanged on February 2013, when I asked you to be my supervisor during my internship at Buffalo University, and how warm, kind and fast you replied my email and showed your willingness. Undoubtedly, that was a milestone in my life that filled me with motivation and inspiration. Dear Luisa, thank you for this lifetime opportunity of being able to learn from your extensive knowledge for more than 6 years. Thank you for all the time of proofreading and correcting my manuscripts. Thank you for all the patience and sorry for stealing some of your time commenting my manuscripts when you were in the airplane traveling to different destinations! Thank you for your endless kindness, permanent smile, positive encouragement and guidance throughout this exciting and very much challenging project.

Prof. Richard Visser, thank you for accepting me into the Plant Breeding department. Although we have not had a scientific discussion, you encouraged me permanently with your smile, greetings in the coffee corner and your permanent attendance at the social event.

A huge thank you has to go to **Dr. Maria Barbosa**! Officially in my PhD proposal you are my external supervisor, but in reality you were very internally involved in my PhD project and provided me lots of help and contributions. Thank you for all your help, advice and support on the synchronization experiment. Besides your scientific input, your endless laugh, friendly personality and shining smile always provided me an enormous amount of energy. In the last stage of my PhD, I always reached to you for advice for the next phase of my future career and you were always willing to help! Thank you for everything!

I would like to give my special thanks to all the members of **Biobased Economy Group**. I learned a lot from all of you. Thank you for all the fun moments we spent together on the BBE activity days and on our Tuesday BBE lunch meetings! I would like to thanks **Dr. Robert van Loo**, having a conversation with you is always very interesting. You inspire so many people at PBR with your knowledge and your smart way of thinking. In particular, I would like to thanks all the BBE staff in the Biochemical and Molecular Laboratory. Nobody gets through a PhD without support from the lab colleagues. My sincere appreciation is extended to **Annemarie**

Dechesne. Thank you for your support, introduction to the biochemical Laboratory, supervisions and your amazing organization. Thank you very much for your trust and for providing me (enough) self-confidence to work with all the equipment in the Lab. Without any doubt, you make the life of BBE PhD students so much easier. I also want to thank **Marcel Visser** for all the help and fruitful discussions in the biochemical Laboratory.

Heleen Furrer, thank you for all the amazing help and your happy spirit. I always enjoyed speaking Dutch with you and learn from you. Dear **Dianka Dees**, you were my first daily supervisor during my master thesis. I learned a lot from you and never forget your patience and help.

I would like to thank **Dr. Marcel Giesbers** and **Dr. Jan van Lent** from Wageningen Electron Microscopy Centre for the support with electron microscopy imaging and fruitful discussions and valuable input during the experiments. Special thanks to **Dr. Arjen Bader** for the training, help and support during the confocal microscopy experiments.

I also want to express my gratitude to **Rick Wieggers** and **Ruud Veloo**. Thank you so much for your help at AlgaePARC facilities along with your input during the AlgaePARC Biorefinery meetings. Without your effort and hard work was nearly impossible to have sufficient biomass for the different experiments. Thanks for all the fun and joy moments that we had together in Nergena!

Special thanks to the PBR secretary ladies, dear **Nicole, Letty and Danielle**. Thank you for all the help during my PhD journey.

Dear **Enid**, thank you very much for your help editing some of my manuscripts. I learned a lot from you!

I further would like to express my appreciation to the BBE colleagues, amazing officemate and indeed lifetime friends:

Andres! Bro, is impossible to put our 7 years of friendship in few words! I can write about our early drinking adventures at De zaaier, our (almost) everyday lunch and deep-funny discussions, our special Lombardos diet, our trip to Berlin, your scientific inputs and notes with your special microscopic handwritings, and...! I sincerely believe that we are one step ahead of being just friends! We are truly brothers! I am glad that you are one of my paranymphs and I sincerely appreciate your time!

Mi Vivicito, like they said, home is where the heart is. I feel home much more in Wageningen three years ago when I met you. Under different circumstances and in other times, I would never had a chance to meet you. My English vocabulary is not

large enough to find the proper words and express my love to you! More than girlfriend you are my best friend. I owe a lot of gratitude to you for all your love. Besides, your clear thinking has been such a valuable contribution to all stages of my PhD research. Thank you so much for everything!! I am very happy that you will be my second paranymph and be close to me in the stage!

Jordi, my super hyperactive friend! We spent more than four years in the same office. We share so many fun moments together. Thank you for all the positive energy and happiness. We had so many deep discussion together, from cell wall-related topics to the independency of the Catalonia!

Ramon, thanks for all the fun and happy moments. We shared amazing and unforgettable days at Spain. Thank you!

Agata, you are a very kind and happy person. I was so lucky to meet you at the last part of my PhD journey. We have become good friends and I am sure we will remain friends forever.

Tim, I still remember the first time we met. You are a very friendly person, willing to listen and help. I enjoyed very much our time at office, coffee break, playing soccer, We-day and....! Thanks for everything.

Next, I'd like to thank my fellow (ex) PhD colleagues that I have met during my research. It is impossible to mention everybody by name, kindly accept my sincere apology if your name is not mentioned. Manos, Ernest, Ying, Peter Dinh, Anne, Jarst, Pauline, Charlie, Francesco, Kim, Peter Bourke, Mehdi, Naser, Narges, Ehsan and Raana.

Charlotte, Marine and Mas, thanks for the amazing trip to Paris and all the fun and laugh! Charlotte, thanks for your (almost) permanent presence at any gathering. Mas, your sweet personality and delicious cakes are unforgettable! Marine, you are a very determined lady! I am sure that our road trip to Iran will happen soon!

Mathilde, you are such a sportive and powerful lady! We shared a lot together and created unforgettable moments and memories. Thank you and I wish you a bright future!

Special thanks to my special friends, **Farnoosh, Hesam, Farzad, Delaram, Sanaz, Mohammadreza and Mehdi**. I cannot thank you guys enough for all the fun moments that we shared together. Farnoosh and Hesam, I am so happy that I met you in 2012 in Wageningen. I cannot forget our crazy gathering, our drinking, amazing Iranian foods, trip to Porto and...! We made a lifetime friendship and I am grateful for that! Farzad, my partner in crime friend! My best friend! You are an

example of a positive, kind, happy and generous person. Thank you so much for all the fun moments! Sanaz, Mohammadreza and Delaram, we shared a lot during the last step of my PhD! Thanks for all the fun moments and all the delicious food! Mehdi, I would never forget the first time I met you. You happiness is always an example for me! Thank you for your help reading some my manuscripts.

Hamed and **Shahrzad**, my lovely cousins! In all sincerity, you inspired me to come to Holland and study at Wageningen University. You welcomed me with all your sympathy and help me with all the details at the early days at Wageningen. Thank you so much!

Finally yet importantly, I would like to thank all the project partners for their contribution and critical comments during the consortium meetings. Your valuable input motivated me to improve my research. Special thanks to **Hans Reith**, **Dr. Lolke Sijtsma and Dr. Ben van den Broek** for their scientific advice and discussions. I also want to thanks the financial support from the Netherlands' Ministry of Economic Affairs in the framework of the TKI BioBased Economy**.**

در پایان این پایان نامه را تقدیم می‌کنم به مهربانترین همراهان زندگیم، به مقدس ترین واژه ها در لغت نامه دلم، مادر و پدر مهربانم و رضا و بهار غزیزتر از جانم . تمام زندگیم را مدیون مهر و عطوفت شما هستم. بابا و مامان هنور بغض شما را در فرودگاه تهران فراموش نکردم، ممنون برای آن همه بزرگواری ، مردانگی، سخاوت، سکوت و مهربانی. ممنون از اعتماد و حمایت شما که به من اجازه دادید برای ادامه تحصیل به هلند مهاجرت کنم. برای تمام حمایت‌ها و زحمات بی دریغشان سپاسگزاری می‌کنم. محمد ، نازنین و بردیا و دینا عزیز تر از جانم، ممنون برای همه انرژی مثبت و حمایت شما.

The friends and memories I have collected during this journey will stay with me forever.

Thank you!
Behzad
April 2019

About the author

Behzad Rashidi was born on 21-09-1987 in Esfahan, Iran. After completing high school he started with a Bachelor in agricultural engineering-agronomy and plant breeding at the Esfahan University of Technology. In last year of the Bachelor study, he focused on biofuel production with a central goal to reduce poverty and promote sustainability. In 2013 he was nominated for a full scholarship offered by NUFFIC and that provided the opportunity to deepen his knowledge abroad. In 2014 Behzad started with an MSc study in Plant Biotechnology at the Wageningen University and Research centre. During the master study, he had the opportunity to join a research group at the University of Buffalo, NY, USA. During this internship, he expanded his knowledge on system biology-driven research. In 2015 an MSc thesis resulted in the completion of the degree. During MSc thesis, he studied the cell wall composition of several green microalgae and diatoms at Plant Breeding Department of Wageningen University.

After completing the master study, he continued as a PhD at Plant Breeding group of Wageningen University on the project AlgaePARC Biorefinery and under the supervision of Prof. Dr Luisa Trindade. The results of his PhD research are described in this thesis.

Education certificate

Education Statement of the Graduate School
Experimental Plant Sciences

Issued to: Behzad Rashidi
Date: 29 May 2019
Group: Laboratory of Plant Breeding
University: Wageningen University & Research

1) Start-Up Phase	date	cp
► **First presentation of your project**		
Cell wall characterization of Microalgae	07 Dec 2014	1.5
► **Writing or rewriting a project proposal**		
Cell wall of Microalgae- Development of Enabling Tools – Basic Knowledge	17 Mar 2015	6.0
► **Writing a review or book chapter**		
► **MSc courses**		
Subtotal Start-Up Phase		7.5

2) Scientific Exposure	date	cp
► **EPS PhD student days**		
EPS Get2Gether	29-30 Jan 2015	0.6
EPS Get2Gether	28-29 Jan 2016	0.6
EPS Get2Gether	09-10 Feb 2017	0.6
► **EPS theme symposia**		
EPS theme 4: Genome biology, Wageningen, NL	03 Dec 2014	0.3
EPS theme 3: Metabolism and Adaptation, Amsterdam, NL	23 Feb 2016	0.3
EPS theme 2: Interactions between Plants and Biotic Agents, Leiden, NL	22 Jan 2016	0.3
► **National meetings (e.g. Lunteren days) and other National Platforms**		
Annual meeting 'Experimental Plant Sciences', Lunteren, NL	13-14 Apr 2015	0.6
Annual meeting 'Experimental Plant Sciences', Lunteren, NL	11-12 Apr 2016	0.6
Annual meeting 'Experimental Plant Sciences', Lunteren, NL	10-11 Apr 2017	0.6
Annual meeting 'Experimental Plant Sciences', Lunteren,NL	09-10 Apr 2018	0.6

► **Seminars (series), workshops and symposia**		
Plant Breeding Research Day	23 Sep 2014	0.2
All-inclusive Breeding: Integrating high-throughput science	16 Oct 2014	0.3
2nd PhD students meeting on Fibre Crops	20 Nov 2014	0.2
2nd AlgaePARC Biorefinery consortium meeting	06 Jun 2014	0.3
3rd AlgaePARC Biorefinery consortium meeting	11 Dec 2014	0.3
4th AlgaePARC Biorefinery consortium meeting	17-18 Jun 2015	0.5
5th AlgaePARC Biorefinery consortium meeting	9-10 Dec 2015	0.5
6th AlgaePARC Biorefinery consortium meeting	15-16 Jun 2016	0.6
7th AlgaePARC Biorefinery consortium meeting	7-8 Dec 2016	0.6
8th AlgaePARC Biorefinery consortium meeting	7-8 Jun 2017	0.5
9th AlgaePARC Biorefinery consortium meeting	13-14 Dec 2017	0.6
10th AlgaePARC Biorefinery consortium meeting	19-20 Jun 2018	0.6
Plant Breeding Research Day	29 Sep 2015	0.3
Seminar 'An introduction to sorghum breeding',Wilfred Vermerris	16 Nov 2016	0.1
Seminar 'Genetic and genomic resources for sorghum',Wilfred Vermerris	17 Nov 2016	0.1
Breeding for sustainability: Perspectives from a company and academic plant breeder	20 Nov 2018	0.3
► **Seminar plus**		
► **International symposia and congresses**		
8th European Plant Science Retreat (EPSR), Barcelona, Spain	20-23 Jun 2016	1.2
The AlgaEurope 2017 Conference, Berlin, Germany	5-7 Dec 2017	0.9
► **Presentations**		
Annual meeting 'Experimental Plant Sciences', Lunteren,NL (Talk)	10-11 Apr 2017	1.0
2nd PhD students Meeting on Fibre Crops (Talk)	20 Nov 2014	1.0
8th European Plant Science Retreat (EPSR), Barcelona, Spain (Poster)	20-23 Jun 2016	1.0
2nd AlgaePARC Biorefinery consortium meeting (Talk)	06 Jun 2014	1.0
The AlgaEurope 2017 Conference, Berlin, Germany (Poster)	5-7 Dec 2017	1.0
10th AlgaePARC Biorefinery consortium meeting (Talk)	19-20 Jun 2018	1.0
Annual meeting 'Experimental Plant Sciences', Lunteren,NL (Poster)	9-10 Apr 2018	1.0
► **IAB interview**		

► **Excursions**		
Company visit (In2care & genetwister)	19 Sep 2014	0.2
Subtotal Scientific Exposure		20.4

3) In-Depth Studies	**date**	**cp**
► **EPS courses or other PhD courses**		
Glycosciences- 13th European Training Course on Carbohydrates	13-17 Apr 2014	1.5
Postgraduate course "Bio-energy Production from Crop Plants and Algae"	17-19 Nov 2014	0.9
VLAG : Biorefinery for Biomolecules	15-16 Apr 2015	0.6
VLAG : Microalgae Process Design: from cells to photobioreactors (3rd edition)	10-17 Jul 2015	2.3
WEMC: Basic Transmission Electron Microscopy (TEM)	Oct 2015	1.7
The Power of RNA-seq	10-12 Feb 2016	0.9
PE&RC-SENSE course "Introduction to R for statistical analysis"	12-13 May 2016	0.6
► **Journal club**		
► **Individual research training**		
Subtotal In-Depth Studies		8.5

4) Personal Development	**date**	**cp**
► **Skill training courses**		
EPS Introduction course	20 Jan 2015	0.2
Presenting with impact	28 Nov-12 Dec 2016	1.0
Scientific Writing	13 Sep-15 Nov 2016	1.8
Nederlandse taal: van A2 naar B1	Feb-Jun 2017	1.6
► **Organisation of PhD students day, course or conference**		
► **Membership of Board, Committee or PhD council**		
Subtotal Personal Development		4.6
TOTAL NUMBER OF CREDIT POINTS*		**41.0**

Herewith the Graduate School declares that the PhD candidate has complied with the educational requirements set by the Educational Committee of EPS with a minimum total of 30 ECTS credits.
* A credit represents a normative study load of 28 hours of study.

This work is performed within the TKI AlgaePARC Biorefinery program with financial support from the Netherlands' Ministry of Economic Affairs in the framework of the TKI BioBased Economy under contract nr. TKIBE01009. Financial support from Wageningen University for printing this thesis is greatly appreciated.

Cover & layout design: Behzad Rashidi
Printed by: proefschriftmaken || www.proefschriftmaken.nl